VOLUME 31 | SUPPLEMENT 2 | MARCH 2018

MODERN PATHOLOGY

USCAP 2018

ABSTRACTS

BONE & SOFT TISSUE PATHOLOGY

(45-120)

107TH ANNUAL MEETING

GEARED TO LEARN

MARCH 17-23, 2018

Vancouver Convention Centre
Vancouver, BC, Canada

Published by
SPRINGER NATURE
www.ModernPathology.org

USCAP
Creating a Better Pathologist
AN OFFICIAL JOURNAL OF THE UNITED STATES AND CANADIAN ACADEMY OF PATHOLOGY

EDUCATION COMMITTEE

Jason L. Hornick, Chair
Rhonda Yantiss, Chair, Abstract Review Board and Assignment Committee
Laura W. Lamps, Chair, CME Subcommittee
Steven D. Billings, Chair, Interactive Microscopy
Shree G. Sharma, Chair, Informatics Subcommittee
Raja R. Seethala, Short Course Coordinator
Ilan Weinreb, Chair, Subcommittee for Unique Live Course Offerings
David B. Kaminsky, Executive Vice President (Ex-Officio)
Aleodor (Doru) Andea
Zubair Baloch
Olca Basturk
Gregory R. Bean, Pathologist-in-Training
Daniel J. Brat
Amy Chadburn
Ashley M. Cimino-Mathews
James R. Cook
Carol F. Farver
Meera R. Hameed
Michelle S. Hirsch
Anna Marie Mulligan
Rish Pai
Vinita Parkash
Anil Parwani
Deepa Patil
Lakshmi Priya Kunju
John D. Reith
Raja R. Seethala
Kwun Wah Wen, Pathologist-in-Training

ABSTRACT REVIEW BOARD

Narasimhan Agaram
Christina Arnold
Dan Berney
Ritu Bhalla
Parul Bhargava
Justin Bishop
Jennifer Black
Thomas Brenn
Fadi Brimo
Natalia Buza
Yingbei Chen
Benjamin Chen
Rebecca Chernock
Andres Chiesa-Vottero
James Conner
Claudiu Cotta
Tim D'Alfonso
Leona Doyle
Daniel Dye
Andrew Evans
Alton Farris
Dennis Firchau
Ann Folkins
Karen Fritchie
Karuna Garg
James Gill
Anthony Gill
Ryan Gill
Tamara Giorgadze
Raul Gonzalez
Anuradha Gopalan
Jennifer Gordetsky
Ilyssa Gordon
Alejandro Gru
Mamta Gupta
Omar Habeeb
Marc Halushka
Krisztina Hanley
Douglas Hartman
Yael Heher
Walter Henricks
John Higgins
Jason Hornick
Mojgan Hosseini
David Hwang
Michael Idowu
Peter Illei
Kristin Jensen
Vickie Jo
Kirk Jones
Chia-Sui Kao
Ashraf Khan
Michael Kluk
Kristine Konopka
Gregor Krings
Asangi Kumarapeli
Frank Kuo
Alvaro Laga
Robin LeGallo
Melinda Lerwill
Rebecca Levy
Zaibo Li
Yen-Chun Liu
Tamara Lotan
Joe Maleszewski
Adrian Marino-Enriquez
Jonathan Marotti
Jerri McLemore
David Meredith
Dylan Miller
Roberto Miranda
Elizabeth Morgan
Juan-Miguel Mosquera
Atis Muehlenbachs
Raouf Nakhleh
Ericka Olgaard
Horatiu Olteanu
Kay Park
Rajiv Patel
Yan Peng
David Pisapia
Jenny Pogoriler
Alexi Polydorides
Sonam Prakash
Manju Prasad
Bobbi Pritt
Peter Pytel
Charles Quick
Joseph Rabban
Raga Ramachandran
Preetha Ramalingam
Priya Rao
Vijaya Reddy
Robyn Reed
Michelle Reid
Natasha Rekhtman
Michael Rivera
Mike Roh
Marianna Ruzinova
Peter Sadow
Safia Salaria
Steven Salvatore
Souzan Sanati
Sandro Santagata
Anjali Saqi
Frank Schneider
Michael Seidman
Shree Sharma
Jeanne Shen
Steven Shen
Jiaqi Shi
Wun-Ju Shieh
Konstantin Shilo
Steven Smith
Lauren Smith
Aliyah Sohani
Heather Stevenson-Lerner
Khin Thway
Evi Vakiani
Sonal Varma
Marina Vivero
Yihong Wang
Christopher Weber
Olga Weinberg
Astrid Weins
Maria Westerhoff
Sean Williamson
Laura Wood
Wei Xin
Mina Xu
Rhonda Yantiss
Akihiko Yoshida
Xuefeng Zhang
Debra Zynger

To cite abstracts in this publication, please use the following format: **Author A, Author B, Author C, et al. Abstract title (abs#).** ***Modern Pathology*** **2018; 31 (suppl 2): page#**

45 Hibernoma Mimicking Atypical Lipomatous Tumor: A Morphologically Distinct Variant Studied in a Series of 64 Cases

Youssef Al Hmada[1], *Inga-Marie Schaefer*[2], *Christopher D Fletcher*[2]. [1]Brigham and Women's Hospital, [2]Brigham and Women's Hospital, Boston, MA

Background: Hibernoma is a benign adipocytic tumor with predilection for subcutaneous tissue of the thigh, upper trunk, and neck of middle-aged adults with equal gender distribution. 11q13 rearrangement resulting in *MEN1* and *AIP* co-deletion is a characteristic finding. Hibernomas are composed, in varying proportions, of brown fat cells, mature adipocytes and microvacuolated lipoblast-like cells. Local recurrence or malignant transformation has not been reported. Examples containing predominantly multivacuolated lipoblast-like cells are uncommon. Distinction from atypical lipomatous tumor (ALT) is important for clinical management.

Design: Sixty-four cases of hibernoma histologically mimicking ALT were identified in consult files between 2000 and 2017. H&E stained slides were reviewed in all cases. Immunohistochemical stains for MDM2 and CDK4 as well as *MDM2* FISH were performed in a subset of cases. Clinical and follow-up information was obtained from referring pathologists.

Results: Thirty-four patients were male and 30 female, with a median age of 43 yrs (range, 20-78 yrs). The tumors were well-circumscribed and mostly deeply located (N=53) or superficial (N=11). Tumor sizes ranged from 3.5-23 cm (median, 12.9 cm). Most tumors arose in the thigh (N=42), followed by buttock/inguinal region (N=14), trunk (N=3). Histologically, the hibernomas showed predominantly large cells with prominent lipoblast-like fatty vacuoles and small central nuclei, and less prominent mature univacuolated adipocytes, along with small numbers of large, finely vacuolated cells with eosinophilic granular cytoplasm (brown fat cells). Mitoses were scant; nuclear atypia or necrosis were not identified. None of the tumors tested expressed MDM2 (0/10) or CDK4 (0/11). *MDM2* FISH, performed in 6 cases, did not reveal amplification. Forty-two tumors were excised with a suspected diagnosis of ALT. Following a benign diagnosis, many patients received no follow-up. Follow-up data, available for 16/64 cases with a median follow-up time of 45 mo (range, 1-170 mo), revealed that none of the patients developed local recurrence or metastases. All patients were alive without evidence of disease.

Conclusions: Hibernoma consisting predominantly of multivacuolated lipoblast-like cells shows predilection for the thigh but the same epidemiologic and clinical features as conventional hibernoma. Histologically, these tumors may be mistaken for ALT but behave in a benign fashion and MDM2/CDK4 negativity may be useful in excluding ALT.

46 Lipofibromatosis (LPF): A Clinicopathological and Molecular Genetic Study of 16 Cases Suggesting a Link to Calcifying Aponeurotic Fibroma (CAF) and LPF-like Neural Tumor (LPFLNT)

Alyaa Al-Ibraheemi[1], *Antonio Perez-Atayde*[2], *Kyle D Perry*[3], *Jakob Hofvander*[4], *Linda Magnusson*[4], *Andrew Folpe*[5], *Fredrik Mertens*[6]. [1]Boston Children's Hospital, Boston, MA, [2]Boston Children's Hospital, Boston, MA, [3]Mayo Clinic, Rochester MN, [4]Lund University, Lund, Sweden, [5]Mayo Clinic, Rochester, MN, [6]University Hospital Lund

Background: LPF is a rare pediatric soft tissue tumor with predilection for the hands and feet. Previously considered to represent "infantile fibromatosis", LPF has distinctive morphological features, with mature adipose tissue, short fascicles of bland fibroblastic cells and lipoblast-like cells. Very little is known about the genetic underpinnings of LPF. Prompted by a recent case of LPF that recurred showing features of CAF, we studied 16 LPF for the CAF-associated *FN1-EGF* fusion and other genetic events

Design: 30 cases previously classified as "LPF" were retrieved and re-reviewed by 2 experienced soft tissue pathologists. On re-review,14 cases were felt to represent something other than LPF and were excluded. The final study group comprised 16 cases. For this group, blocks or unstained slides were available for 13 primary tumors and 3 local recurrences. Cases were analyzed for *FN1* gene rearrangement and *FN1-EGF* gene fusion by FISH; FFPE sections from negative cases were further analyzed by RNA sequencing and RT-PCR.

Results: The tumors occurred in 10M and 6F (median 3 yrs; range 1 mo-14 yrs) and involved the forearm (n=3), arm (n=2), finger (n=2), hand (n=1), foot (n=2), leg (n=1), abdomen (n=2), hip/buttock (n=2), and "unknown" (n=1). All primary tumors showed classical LPF morphology, lacking features suggestive of CAF or LPFLNT. In 2 patients, local recurrences contained CAF-like nodular calcifications in addition to areas of classic LPF. The recurrent tumor in the third patient showed only typical LPF. By FISH, 3 of 14 informative cases were positive for *FN1-EGF* fusion, including one recurrent lesion with CAF morphology. RNA sequencing detected the novel fusions *EGR1-GRIA1, TPR-ROS1, SPARC-PDGFRB, FN1-TGFA*, and *HBEGF-RBM27* in 5 cases (all validated by RT-PCR and 3 also by FISH). Six cases with FISH or RNA seq data lacked identifiable genetic events. No case showed *NTRK1* rearrangement.

Conclusions: LPF appears to be a genetically heterogeneous tumor, despite stereotypical morphologic features. A subset of LPF harbors the CAF-related *FN1-EGF* fusion, or the related *FN1-TGFA* fusion, suggesting that some "LPF" may represent instead CAF lacking hallmark calcifications. Other LPF showed alterations involving a kinase-encoding gene (*TPR-ROS1 and SPARC-PDGFRB*), suggesting a possible link to LPFLNT. A third subset of LPF showed novel gene fusions (*HBEGF-RBM27* and *EGR1-GRIA1*). Ongoing study of other strictly defined LPF should help to clarify the relationships between LPF, CAF and LPFLNT.

47 Clinical genomic sequencing of 72 pediatric and adult osteosarcomas reveals distinct molecular subsets with potentially targetable alterations

Deepu Alex[1], *Yoshiyuki Suehara*[2], *Anita Bowman*[3], *Sumit Middha*[3], *Ahmet Zehir*[4], *Lu Wang*[5], *George Jour*[6], *Khedoudja Nafa*[3], *Paul Meyers*[3], *John Healey*[3], *Meera Hameed*[7], *Marc Ladanyi*[7]. [1]Memorial Sloan Kettering Cancer Center, New York, NY, [2]Juntendo University School of Medicine, Tokyo, Japan, [3]Memorial Sloan Kettering Cancer Center, [4]MSKCC, [5]St Jude Children's Research Hospital, Memphis, TN, [6]MDAnderson Cancer Center at Cooper, Camden, NJ, [7]Memorial Sloan-Kettering CC, New York, NY

Background: Osteosarcoma (OS), the most common primary malignant bone tumor shows a bimodal age distribution with one peak during childhood/adolescence and a second smaller peak in adults over 50. While multimodal chemotherapy has shown substantial benefit, the prognosis for patients who present with metastatic and/or recurrent disease remains poor. We performed clinical sequencing of 72 high grade OS (HGOS) samples using our NGS platform, MSK-IMPACT to identify potentially actionable alterations that may point to novel therapeutic options.

Design: Tumor/germline DNA in 72 HGOS (35 primary, 4 recurrent and 33 metastases samples) were sequenced using MSK-IMPACT, a hybridization capture-based NGS panel that detects mutations and copy number alterations (CNAs) in 341 to 468 cancer-associated genes. These genomic alterations were analyzed using the MSK-cBioPortal for Cancer Genomics. Potentially actionable genetic events were categorized into one of 4 levels (L 1-4) according to the MSK-Precision Oncology Knowledge base (OncoKB).

Results: In 72 HGOS samples from 67 patients, 240 somatic mutations in 137 genes and 503 CNAs in 157 genes were identified by the MSK-IMPACT panel. Genomic alterations that can help guide clinical treatment were found in 15 of 67 cases (22.4%). 12 of 67 cases (17.9%; OncoKB: L1-3) had at least one potentially actionable alteration (AA). This included *CDK4* amplification (AMP) (n=9, 13.4%: L 2B), *MDM2* AMP (n=8, 11.9%: L 3B), *BRCA2* truncating mutation (n=1, 1.5%: L 2B), *GULP1-PTCH1* fusion (n=1, 1.5%: L 3B) and *PTEN* deletion/truncating mutation (n=3, 4.5%: L 4) as defined by OncoKB. Additionally, concurrent gene AMPs of the 4q12 locus involving *KIT, KDR* and *PDGFRA* were identified in 13 of 67 cases (19.4%). These gene AMPs are potentially targetable by multi-kinase inhibitors such as pazopanib, imatinib and sorafenib. Co-occuring *VEGFA* and *CCND3* AMPs at 6p12-21 was identified as another potential target (e.g. by angiogenesis inhibitors) in 14 of 67 OS cases (20.9%) and was mutually exclusive with 4q12 AMPs. 8q24 amplifications harboring *MYC* were found in 6 cases (8.3%).

Conclusions: The implementation of precision medicine for rare tumors is a challenging task. In our study, MSK-IMPACT and OncoKB identified potentially AAs in approximately 18% of HGOS. Additionally, concurrent gene AMPs of *KIT, KDR* and *PDGFRA* at the 4q12 locus and, concurrent AMPs of *VEGFA* and *CCND3* at the 6p12-21 locus are of particular interest as they might represent future therapeutic targets in 40% of cases.

48 MTAP Expression in Osteosarcoma

Samer Baba[1], *John A Livingston*[2], *Cheuk Hong Leung*[3], *Heather Lin*[2], *Yu Liang*[4], *Alexander Lazar*[5], *Wei-Lien Billy Wang*[6]. [1]The University of Texas MD Anderson Cancer Center, Houston, TX, [2]The University of Texas MD Anderson Cancer Center, [3]The University of Texas MD Anderson Cancer Center, Houston, Texas, [4]City of Hope National Medical Center, Duarte, CA, [5]M. D. Anderson Cancer Center, Houston, TX, [6]UT MD Anderson Cancer Center, Houston, TX

Background: Osteosarcoma is the most common primary bone malignancy and is currently treated with a combination of neoadjuvant chemotherapy and surgery. However, improvements in patient outcome has stalled and new biomarkers and therapeutic targets to assist in prognostication and treatment are lacking. One potential therapeutic target is methylthioadenosine phosphorylase (MTAP; 9p21) and its encoding gene is often co-deleted with C*DKN2A*, a tumor suppressor located at 9p21.3 that encodes P16. MTAP is important for salvage pathways of both adenosine and methionine and solid tumors with *MTAP* mutations can be susceptible to anti-folate agents. Since C*DKN2A* can be mutated in osteosarcomas and is a known biomarker, we examined the prevalence and prognostic significance of MTAP expression in a large series of osteosarcomas and correlated its expression with P16.

Design: A tissue microarray (TMA) of osteosarcomas consisting of 260 patients including 184 primary tumors and 94 metastatic tumors was created. Immunohistochemical studies were performed using an anti-MTAP (Proteintech, 1:1200) and CINtec/p16 (Ventana/Roche, 1:3). Both extent and intensity were recorded. Loss of expression was defined as <10% labeling. Clinical information was obtained by retrospective chart review. The correlation was measured by Spearmen correlation coefficient. Log-rank test was used to compare survival distributions of the two groups.

Results: Loss of P16 was seen in 49/193 (25%) and loss of MTAP in 70/196 (36%) of specimens. Overall, MTAP expression was correlated with p16 expression (Spearman correlation 0.165, p=0.025) with the correlation strongest in metastatic specimens (Spearman correlation 0.322, p=0.011). Patients who had localized tumors with MTAP intensity of none to weak expression had inferior overall (Log-rank test, p=0.008), while those with localized tumors with P16 intensity of none or weak trended toward inferior overall survival, though this did not reach statistical significance (Log-rank test, p 0.092).

Conclusions: Osteosarcomas can lose MTAP expression and its loss may be marker for aggressive disease. Given the correlation with P16 loss of expression, this loss may be related to alternations involving the 9q21 region. These findings suggest a subset of osteosarcomas may be benefit from anti-folate therapies.

49 Epithelioid Myxofibrosarcoma: A Clinicopathologic Re-Appraisal in a Series of 48 Cases

Ryan Berry[1], *Karen Fritchie*[2], *John Goldblum*[3], *Scott Kilpatrick*[3], *Steven Billings*[3], *Brian P Rubin*[3]. [1]Danville, PA, [2]Mayo Clinic, Rochester, MN, [3]Cleveland Clinic, Cleveland, OH

Background: Epithelioid myxofibrosarcoma (MFS) is a recently characterized variant of MFS that appears to behave in a more aggressive manner than typical high-grade MFS. We sought to expand the current literature by evaluating a large series of epithelioid MFS.

Design: Fourth-eight cases diagnosed as epithelioid MFS were identified from our databases.

Results: Thirty-two patients were male and 16 were female. Age ranged from 16 to 90 years old with an average age of 67. Tumor size ranged from 2.5 to 35 cm. The majority of tumors (85%) were located superficial (subcutaneous) and a minority (15%) were deep (sub-fascial). The extremities (22 lower, 13 upper) were most often involved, followed by trunk (8), inguina (2), scalp (2), and cheek (1). The majority of cases were classified as intermediate to high grade per FNCLCC, typically having necrosis and increased mitotic activity (3-41 per 10 hpf, average 17). Histologically, tumors typically exhibited a multinodular growth pattern consisting of epithelioid cells within a prominent myxoid stroma, characteristic curvilinear vessels, and a variable mixed inflammatory infiltrate. The epithelioid component ranged from focal (5-10%) to diffuse (100%) and was characterized by plump, round to oval cells with eosinophilic cytoplasm, round nuclei, and often with prominent nucleoli. Immunohistochemical stains showed variable positivity with actins in a portion of cases, occasional expression of CD34, and no reactivity with melanocytic markers, S100, desmin, and cytokeratin. Clinical follow-up was available for 15 patients (2 to 96 mo). Five developed local recurrence (33%). Metastasis occurred in 7 patients (47%), mostly to lymph nodes, but also to lung. Five patients died of disease (6 to 72 mo; mean 21.8 mo), 4 who died within 12 months of initial diagnosis. Six patients are alive without disease (40%), two are alive with disease (13%), and two are dead of unknown cause (13%).

Conclusions: In summary, our findings are congruent with the reported literature regarding epithelioid MFS. It represents a rare but aggressive variant of MFS that appears to have a higher risk of metastases and often a rapidly progressive course. Although MFS typically affects older adults, our study shows that it may occur in adolescents and young adults, as eight (17%) were less than 50 years old and the youngest just 16. Epithelioid MFS is an aggressive variant of MFS that one should keep in the differential when evaluating epithelioid malignancies with prominent myxoid stroma.

50 Clinical Utility of Comprehensive Molecular Profiling of Sarcomas for Diagnosis and Target Identification: an institutional experience

Marilyn Bui[1], *Evita Henderson-Jackson*[2], *Spandana Boddu*[3], *Stephanie M Bienasz*[4], *Christine M Walko*[5], *Damon R Reed*[5], *Michaela Druta*[5], *Andrew S Brohl*[6]. [1]H. Lee Moffitt Cancer Ctr, Tampa, FL, [2]Riverview, FL, [3]University of South Florida, [4]University of South Florida, Lutz, FL, [5]Moffitt Cancer Center, [6]H. Lee Moffitt Cancer Center & Research Institute, Tampa, FL

Background: Sarcoma is a heterogeneous disease encompasses a variety of tumors that present a significant challenge to diagnose and treatment. Given the rarity and histologic overlap of sarcoma subtypes, some entities are extremely challenging to classify, even in the hands of the experienced and specialized sarcoma pathologists. Next-generation sequencing (NGS) based molecular profiling might augment standard pathological techniques as well as provide potential therapeutic target identification. This study reviews our institutional experience of the utility of NGS profiling for advanced sarcomas.

Design: We reviewed all sarcoma cases at our institution between 2014 and early 2017 that underwent evaluation by NGS based molecular profiling using a commercial platform. Clinical and pathological characteristics of the patients were collected in addition to the genetic information.

Results: One hundred and fifteen sarcoma patients were identified for which their tumor underwent molecular profiling (age 16-86 years, median 55; male: female 51:64). A median of 3 (range 0-19) putatively oncogenic mutations were identified per tumor. The most commonly affected genes include *TP53* (37.4%), *CDKN2A* (22.6%), *CDK4/MDM2* (19.1%), *ATRX* (13.0%), and *RB1* (13.0%). In six patients (5.2%) the diagnosis was modified as a result of molecular findings, typically from one sarcoma subtype to another. One monophasic synovial sarcoma was correctly diagnosed in the presence of a SS18-SSX2 fusion despite the apparent intraneural origin which was initially considered as malignant peripheral nerve sheath tumor. This opened up much more treatment options including clinical trials for this patient. Fifty five of 115 (47.8%) tumors contained at least one mutation potentially targetable by a commercially available therapy. Several novel or semi-novel likely oncogenic fusion events were discovered including *EWSR1-PATZ1*, *PHF1-TFE3*, and *BCOR-ZC3H7B*.

Conclusions: Comprehensive molecular profiling augments standard pathological techniques for the classification of sarcomas in a subset of cases and identifies potential targets for therapeutic intervention. Novel, potentially disease-defining fusion events can also be identified by this method. Further study is encouraged to define the feasibility and clinical benefit of molecularly guided therapeutic intervention in this disease.

51 Fusion Gene Detection in Sarcomas by Next-Generation Sequencing-Based Anchored Multiplex PCR

Kenneth CHANG[1], *Chik Hong Kuick*[2]. [1]KKH, Singapore, [2]KKH

Background: Molecular testing for fusion transcripts is important for diagnosis and management of many sarcoma types characterized by specific gene translocations. The aim of this study was to evaluate a next-generation sequencing (NGS)-based assay for identification of gene fusion transcripts in archival formalin-fixed paraffin-embedded (FFPE) soft tissue tumor samples.

Design: Archival FFPE samples of soft tissue tumors were obtained for an NGS-based fusion transcript detection assay (Archer FusionPlex Sarcoma Assay) that identifies gene fusions involving any of 26 genes commonly involved in sarcoma gene fusions, with the identity of the other gene partner obtained through NGS in a manner agnostic of the identity and breakpoint of this other gene. The results were compared (where previously performed) or verified with RT-PCR findings (if not previously performed).

Results: The study cohort comprised 67 cases. 24 cases had canonical sarcoma gene fusions identified, of which 15 cases had previously performed matching molecular results and the other 9 had subsequent confirmatory RT-PCR findings. 3 cases had gene fusions involving novel gene partners, namely *COL1A2-ALK* in an ALK-positive histiocytosis, *MAGED2-PLAG1* and *MEAF6-PHF1* in an endometrial sarcoma, and *FOXO1-TSC22D1* in a rhabdomyosarcoma. 9 cases had novel breakpoints in gene fusions involving previously described gene pairs, including 2 cases of *CIC-DUX4* sarcoma, *EWSR1-FLI1* in one Ewing sarcoma, *KFI5B-ALK* in two ALK-positive histiocytosis cases, *NAB2-STAT6* in a solitary fibrous tumor, *JAZF1-PHF1* in an endometrial stromal sarcoma, *FUS-CREB3L2* in a low-grade fibromyxoid sarcoma, and *EWSR1-NR4A3* in a soft tissue myoepithelioma. There were no false positive results. There were 6 false negative results, relating to suboptimal nucleic acid input quantity (one case), low trimmed read counts (two cases), low frequency fusion event as revealed by whole transcriptome sequencing (one case) and currently unknown reasons (two cases).

Conclusions: Our results demonstrate the ability of this NGS-based sarcoma gene fusion assay to identify fusion gene transcripts in sarcomas, including transcripts from gene translocations involving novel gene partners, and translocations with novel gene breakpoints. However, false negative results may occur because of nucleic acid input quantity, sequencing trimmed read counts and the gene fusion frequency.

52 Use of Multiplex Next Generation Sequencing for Detection of Fusion Products in Soft Tissue Tumors

Ivan Chebib[1], *Jochen Lennerz*[2], *G. Petur Nielsen*[3], *Vikram Deshpande*[3]. [1]Massachusetts General Hospital and Harvard Medical School, Boston, MA, [2]Massachusetts General Hospital and Harvard Medical, Boston, MA, [3]Massachusetts General Hospital, Boston, MA

Background: There is growing demand for identification of molecular targets in the diagnosis of soft tissue tumors (STT). Use of multiplex next generation sequencing (NGS) platforms for the targeted detection of fusion genes in translocation-associated STT has been increasingly adopted. We report our experience with the use of this technology for fusion detection in STT.

Design: The laboratory information system was searched for all reports of NGS fusion transcript detection in STT from 2015-2017. Nucleic acid from FFPE (with >15% tumor purity) was subjected to anchored multiplex PCR for targeted NGS, allowing the detection of gene rearrangement without prior knowledge of fusion partners. Surgical pathology diagnoses were compared to fusion results.

Results: A total of 2594 cases of NGS for fusion transcript detection were performed. Of those, 99 (3.8%) were reported for STT. Twelve cases were positive for a fusion transcript. There were 3 angiomatoid fibrous histiocytoma (for confirmation of EWSR1-CREB1), 2 inflammatory myofibroblastic tumor (ALK fusion), 1 EWSR1 FISH-negative Ewing sarcoma (variant ERG-FUS), and 1 soft tissue malignant myoepithelioma (EWSR1-PBX3). There were 3 cases with unexpected results: uterine leiomyoma harboring ALK fusion, inflammatory myofibroblastic tumor with ETV6-NTRK3 mutation originally interpreted as IgG4-related disease, and a mediastinal spindle cell tumor of uncertain differentiation found to have EWSR1-CREB1, consistent with angiomatoid fibrous histiocytoma. There were also 3 positive cases of uncertain significance: 1 case diagnosed as spindle cell variant of liposarcoma contained TRIO-TERT, 1 case of STT of uncertain differentiation harbored MIR143-NOTCH2 fusion suggesting malignant glomus tumor, and 1 malignant peripheral nerve sheath tumor harbored an EWSR1-PATZ1 fusion.

Conclusions: Multiplex NGS platforms that target multiple possible fusion products are a powerful method for identification and confirmation of translocation-associated STT. We consider the discovery potential for novel STT fusion partners in a NGS fusion panel a useful clinical diagnostic tool.

53 Nodular Fasciitis and Soft Tissue Aneurysmal Bone Cyst: Expanding the Spectrum of USP6 Fusion Partners

Catherine T Chung[1], *Mary Shago*[2], *Elizabeth Demicco*[3], *Rita Kandel*[4], *George S Charames*[5], *Gino R Somers*[2], *David Swanson*[6], *Brendan C Dickson*[5]. [1]Hospital for Sick Children, [2]The Hospital for Sick Children, Toronto, ON, Canada, [3]Mount Sinai Hospital, [4]Mount Sinai Hospital, Toronto, ON, [5]Mount Sinai Hospital, Toronto, ON, [6]Mount Sinai Hospital, Toronto, ON

Background: Nodular fasciitis (NF) is a common mesenchymal neoplasm with broad age and anatomic distributions. Aneurysmal bone cyst (ABC) is less common and generally occurs in younger patients; even rarer is its soft tissue counterpart (ST-ABC). Both NF and ABC are characterized by translocations involving the ubiquitin specific peptidase 6 (*USP6)* gene; this encodes a de-ubiquitinating enzyme with diverse roles, including cell transformation. Most cases of NF contain *MYH9-USP6* fusion products, with the number of potential *USP6* partners recently expanding. Similarly, initial reports suggested *CDH11-USP6* and *COL1A1-USP6* were common fusion partners in ABC, but here the diversity of *USP6* partners has likewise increased. Despite few reports of molecular testing in ST-ABC, translocations in this tumor are presumed to parallel conventional ABC. Herein, we describe a series of NF and ST-ABC interrogated by targeted next generation sequencing (NGS) to further delineate the diversity of *USP6* fusion partners in these neoplasms.

Design: A retrospective review was performed for NF and ST-ABC cases. The morphologic diagnosis was confirmed in each. Targeted next-generation sequencing (NGS) was performed on RNA extracted from fresh frozen or formalin-fixed paraffin-embedded tissue. The results were analyzed using Manta and JAFFA fusion callers, and validated by whole transcriptome sequencing, RT-PCR, or FISH.

Results: NF (N=26): mean age was 31 years (range: 2-68); 11 females and 15 males; tumors most commonly arose in the head (N=9) and extremities (N=8). *USP6* fusion partners included: *MYH9* (N=14), *SPARC* (N=3), *CTNNB1* (N=2) and individual cases of *CALD1*, *CNBP*, *COL1A1*, *FILIP1L*, *MiR22HG*, *PALLD* and *PRICKLE1*. ST-ABC (N=4): mean age was 42 years (range: 37-46); 2 females and 2 males; tumors involved the extremities (N=2), chest (N=1) and shoulder (N=1). *USP6* fusion partners included: *COL1A1* (N=3) and *C9orf3* (N=1).

Conclusions: We confirm *MYH9-USP6* to be the most common fusion product in NF (54%); moreover, we identified multiple novel *USP6* partner genes, including: *CALD1*, *CNBP*, *COL1A1*, *FILIP1L*, *PALLD* and *PRICKLE1*, highlighting the genetic diversity of *USP6* fusion partners. Similar to its bone counterpart, *COL1A1* was a common *USP6* partner in ST-ABC; *C9orf3* appears to be a novel fusion product. Finally, the presence of *COL1A1-USP6* and *CNBP-USP6* in NF – fusion products that, to this point, have only been observed in ABC – suggests similar fusion gene pairs may be capable of driving both NF and ABC.

54 Immunohistochemistry of H3F3A G34W and H3F3 K36M as a diagnostic tool for giant cell tumor of bone and chondroblastoma

Arjen Cleven, *Frank Reinink*[1], *Inge I.H. Briaire-de Bruijn*[2], *Anne-Marie Cleton-Jansen*[2], *Judith Bovee*[3]. [1]Leiden University Medical Center, Leiden, Zuid-Holland, [2]Leiden University Medical Center, [3]Leiden Univ. Med. Ctr., Leiden

Background: Specific *H3F3A* driver mutations were detected in giant cell tumor of bone (GCTB) and *H3F3B* mutations in chondroblastoma (CB). We investigated the sensitivity and specificity of anti-histone H3F3A G34W and H3F3 K36M antibodies as a diagnostic tool for respectively GCTB and CB.

Design: Using immunohistochemistry on tissue microarrays, in total 60 GCTBs, 8 CBs and 24 other giant cell containing tumors (including aneurysmal bone cyst (n=6), chondromyxoid fibroma (n=12) and telangiectatic osteosarcoma (n=6)) were tested.

Results: In total 77% (46/60) of GCTBs showed nuclear H3F3A p.G34W positive staining including all GCTBs which harboured an H3F3A G34W mutation by Sanger sequencing or NGS targeted sequencing. GCTBs with rare H3F3A mutation variant p.G34V,R and all other tested tumors were negative for H3F3A G34W. Positive staining for H3F3 K36M was observed in 100% of CBs including all cases of CBs that harboured the H3F3B K36M mutation detected by using Sanger sequencing. All other tumors were negative for H3F3 K36M immunohistochemistry.

Conclusions: Our results show that H3F3A G34W and H3F3 K36M immunohistochemistry appears to be a highly specific diagnostic tool for the distinction of GCTB and CB from other giant-cell containing lesions. Furthermore it is an easy applicable and less expensive diagnostic tool compared to Sanger sequencing or NGS especially in case of decalcification.

55 EWSR1-NFATC2 Gene Fusions Define A Group of Undifferentiated Tumors in Bone and Soft Tissue with Round and Epithelioid Morphology

Jarish Cohen[1], *Amit J Sabnis*[2], *James Grenert*[3], *Gregor Krings*[4], *Soo-Jin Cho*[5], *Andrew Horvai*[6], *Jessica L Davis*[7]. [1]UCSF, San Francisco, CA, [2]UCSF, [3]University of California, San Francisco, CA, [4]UCSF, San Francisco, CA, [5]University of California San Francisco, San Francisco, CA, [6]Univ of Caliornia San Francisco, San Francisco, CA, [7]University of California, San Francisco, San Francisco, CA

Background: Mesenchymal small round cell tumors are a diverse group of neoplasms defined by primitive, often high-grade cytomorphology. The most common molecular alterations detected in these tumors are gene rearrangements involving Ewing sarcoma RNA binding protein 1 (*EWSR1*) to one of many fusion partners. Rare tumors harboring a t(20;22) gene translocation corresponding to fusion of *EWSR1* to nuclear factor of activated T cells 2 (*NFATC2*) have been described in mesenchymal tumors with clear round cell morphology and a predilection for the skeleton.

Design: Two mesenchymal tumors with small round cell morphology and abundant stroma were identified. The clinicopathologic features of these tumors, including response to treatment, were described and evaluated (Table 1). To identify the genetic rearrangements, DNA was purified from tumor tissue and next-generation sequencing of a panel of 480 cancer-associated genes was performed.

Results: One tumor arose in the subcutaneous tissue of the lower extremity of a young woman and the other in the intramedullary proximal radius of a middle-aged man. The tumor in the subcutis was well-circumscribed, arranged in cords and thin trabeculae of epithelioid clear cells within abundant myxoid and fibrous stroma and the intraosseous tumor showed small nests of epithelioid clear cells clustered around central osteoclast-like giant cells in copious fibrous stroma. The soft tissue tumor showed immunoreactivity for NKX2.2, CD99, keratin, and EMA, but was weak to negative for S100 and negative other myoepithelial markers. The intraosseous tumor exhibited minimal patchy positivity for CD99 and EMA only (Figure 1). Chromosomal copy number analysis revealed amplification of the *EWSR1-NFATC2* fusion gene with loss of chromosomes 20q and 22q distal to the breakpoints in both tumors (Figure 2). The subcutaneous tumor had an otherwise simple genome with only a few additional gains and losses on 20q. The intraosseous tumor showed partial gain of 17p and 20p, and partial loss of 19p. The clinical courses were indolent/protracted and the subcutaneous mass showed a negligible response to traditional Ewing sarcoma chemotherapy.

Age/Sex	Site	Cytomorphology	Stroma	CD99	EMA	Keratin	S100	Radiology	Initial Treatment	Clinical Follow-up
24/F	Left calf	Small round cells, cords, trabecule	Abundant fibromyxoid	Patchy +	Dot-like +	Dot-like +	-	Well-circumscribed, lobulated lesion	Neo-adjuvant chemotherapy (alternating doxorubicin, vincristine, and cyclophosphamide with ifosfamide and etoposide, 5 cycles), then resection	NED, 6 month follow up
42/M	Right radius	Epithelioid clear cells, nests	Abundant fibrous	Patchy +	Patchy +	-	-	Expansile lytic lesion	Neo-adjuvant chemotherapy, ongoing (vincristine, adriamycin, and cyclophosphamide alternating with ifosfamide and etoposide)	AWD, 4 month follow up

NED- no evidence of disease, AWD- alive with disease

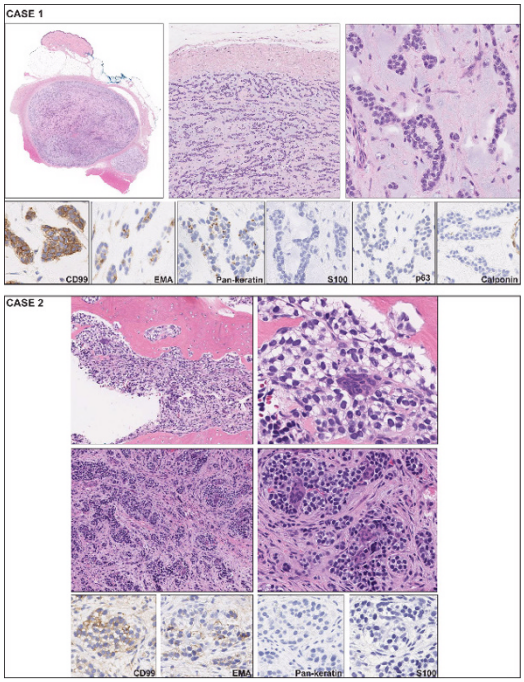

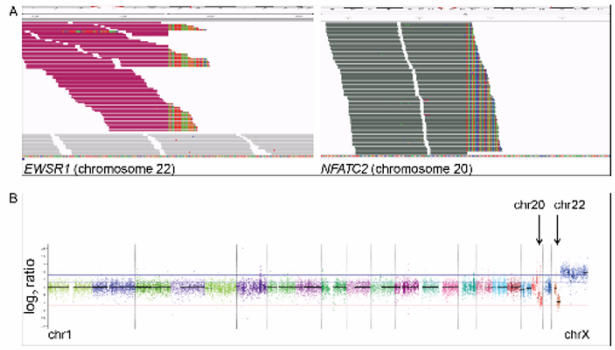

56 The Morphologic Spectrum of Benign Notochordal Cell Tumors

Rory Crotty[1], *Vikram Deshpande*[1], *Ivan Chebib*[2], *G. Petur Nielsen*[1]. [1]Massachusetts General Hospital, Boston, MA, [2]Massachusetts General Hospital and Harvard Medical School, Boston, MA

Background: Benign notochordal cell tumors (BNCTs) are proliferations of cells with notochordal differentiation that behave in an indolent fashion. The typical morphology consists of an intraosseous proliferation of bland adipocyte-like clear cells with sclerotic bone and without myxoid matrix. These findings help to distinguish BNCT from chordoma. However, features typical of chordoma have been reported in BNCTs, which may complicate the diagnosis, especially on core biopsy. We sought to further evaluate the morphologic spectrum of BNCTs, especially in cases associated with chordomas.

Design: The laboratory information system was searched for cases of BNCT that arose in association with and without chordoma. Histologic slides were reviewed and clinical, radiologic and pathologic features were evaluated.

Results: We identified 19 sacral resections for chordoma which also contained BNCTs. Nine of the chordoma resections demonstrated intimate association of BNCT with chordoma, with the other ten showing isolated foci of BNCT unassociated with chordoma. Of the 19 cases identified, 15 had at least one atypical BNCT feature: 12/19 had marked nuclear atypia, 5/19 had epithelioid change, and 4/19 showed eosinophilic cytoplasm. Ten cases of BNCT had focal areas of extracellular myxoid matrix. Two cases also demonstrated extraosseous extension of the BNCT.

Conclusions: The morphologic spectrum of BNCT is wide, and may show atypical features that overlap with chordoma. There is no single feature which reliably distinguish these two tumors, and differentiation must be made with combined correlation of clinical, radiologic and histologic features.

57 Identification of Novel Genomic Alterations in Myoepithelial Carcinoma of Soft Tissue

Joanna Cyrta[1], *Marcin Imielinski*[2], *Rohan Bareja*[3], *Samaneh Motanagh*[4], *Susan Mathew*[6], *Kenneth Eng*[3], *Tuo Zhang*[6], *Andrea Sboner*[7], *Olivier Elemento*[5], *Mark Rubin*[8], *Brian P Rubin*[9], *Juan Miguel Mosquera*[8] [1]Weill Cornell Medicine, New York, NY, [2]Weill Cornell Medicine, New York, NY, [3]Englander Institute for Precision Medicine, New York, NY, [4]Weill Cornell Medicine, New York, NY, [5] New York, NY, [6]Elmhurst, NY, [7]Weill Cornell Medicine, [8]Weill Cornell Medical College, New York, NY, [9]Cleveland Clinic, Cleveland, OH

Background: Myoepithelial carcinoma of soft tissue (MCST) is a rare, aggressive tumor that affects young adults and children. Recurrent gene fusions (involving *EWSR1* in ~50% of cases) and deletions (*SMARCB1*) have been described. However, genome-wide characterization of MCST has not been reported to date.

Design: We analyzed 6 fresh-frozen and 7 formalin-fixed paraffin-embedded MCST samples from 3 patients aged 8 weeks, 27 years and 37 years. Whole exome sequencing (WES) was performed on all samples and RNA-seq was done on a subset of samples from the 3 patients. Whole genome sequencing (WGS) was performed on 2 fresh-frozen samples from 2 patients. Additional studies included fluorescence *in situ* hybridization, immunohistochemistry and RT-PCR with Sanger sequencing.

Results: WES showed a very low point mutation rate [mean per patient (pt): 0.48 mutations/Mb, range: 0.18-1.77]. No actionable alterations in known cancer genes were detected. *SMARCB1* displayed complete

homozygous loss (1pt); partial loss on one allele and complete loss on the other (1pt); and no alteration (1pt). Other copy number alterations included deletions of *SPECC1L* and *NF1* (1pt), *MSN* and *CAMTA1* (1pt) and *MDM4* amplification (1pt). RNA-seq revealed a novel *ASCC2-GGNBP2* fusion transcript (1pt) and a *EWSR1-KLF15* fusion (1pt). WGS identified rearrangements recurrently involving 22q: inversion (1pt) and a complex rearrangement between 22q and 17q combined with chromothripsis (1pt). Clinical follow up showed that two patients died of disease and one developed metastases.

Conclusions: Our results suggest that MCST do not harbor recurrent point mutations, but instead show genomic rearrangements invariably involving 22q. Incidence of *ASCC2-GGNBP2* and *EWSR1-KLF15* fusions will be assessed on a larger cohort. Partial homozygous deletion of *SMARCB1* can explain discrepancies between FISH (heterozygous status) and IHC (complete loss of expression) in some MCST.

58 Histologic Spectrum of Low Grade Fibromyxoid Sarcoma in Patients ≤21 Years of Age: A Study of 28 Cases

Nooshin Dashti[1], *Jorge Torres-Mora*[2]. [1]Mayo Clinic, Rochester, MN, [2]Mayo Clinic, MN

Background: Low Grade FibroMyxoid Sarcoma (LGFMS) is a bland spindle cell tumor with aggressive behavior and tendency to recur and metastasize. LGFMS is thought to occur in young to middle-aged adults. Although a few pediatric cases have been described, full histologic spectrum is unclear. We gathered a large number of LGFMS in children to elaborate on clinicopathologic features in this group.

Design: Cases of primary LGFMS in patients ≤ 21 years old were retrieved from our archive. H&E slides were reviewed with focus on: growth pattern, cellularity, collagen rosettes, vascular pattern, atypia, mitotic count and necrosis. FISH studies for FUS rearrangement were performed on cases with available material.

Results: Of total 274 histologically confirmed LGFMS cases 42 (15.3%) occurred in patients ≤21 years old. Pathology material was available in 28 cases: 12 (43%) male and 16 (57%) female. The age range was (4-21 years, mean 14.2). Tumor size was known in 25 cases (range 0.5-8 cm, mean 4.2 cm). Tumors occurred in lower extremity (9), upper extremity (7), trunk (6), head/neck (3), retroperitoneum (1), paraspinous (1), and vulva (1). Depth of tumor in soft tissue was known in 23 cases: 13 deep, 10 superficial. Most tumors were obviously infiltrative (17). Half of the tumors showed whorls. The other half showed a combination of whorls and nodules. Transition between hyper and hypocellular areas was gradual in majority of cases (23), with 3 cases showing abrupt transition and 1 case with both patterns. Moderate cellularity was the predominant pattern (21). Giant collagen rosettes were identified in 46%. All cases showed thin walled delicate branching vessels. In addition 5 cases also had thick walled vessels. All cases showed perivascular condensation which was striking in 86% (24). Mitotic rate range was 0-35 per 50 high power field (mean 5). The level of atypia was mild or moderate in all cases. Necrosis was only present in 5 cases (18%). Material for FISH was available in 27 cases. Majority showed FUS rearrangement (19), 1 case had EWSR1-CREB3L2 rearrangement and 7 cases were negative for both.

Conclusions: Pediatric LGFMS may be more frequent than previously thought, constituting 15% of LGFMS cases in our institution. The morphologic spectrum is broad and pediatric cases show similar morphology to adult tumors. Half of our cases occurred in superficial soft tissue. Due to risk of recurrence or metastasis many years after the primary tumor, their recognition in children and indefinite follow up is essential.

59 Prognostic Evaluation of Localized Primary Gastrointestinal Stromal Tumors (GIST): Comparison between Risk Classification Systems and Role of Mutational Analysis in a Single Unit Experience

Antonio De Leo[1], *Jacopo Lenzi*[2], *Margherita Nannini*[3], *Melissa A Monica*[4], *Costantino Ricci*[5], *Barbara Corti*[5], *Maria Pia Fantini*[2], *Maria Abbondanza Pantaleo*[3], *Donatella Santini*[1]. [1]S. Orsola-Malpighi Hospital, University of Bologna, [2]Alma Mater Studiorum-University of Bologna, Bologna, Emilia-Romagna, [3]Sant'Orsola-Malpighi Hospital, University of Bologna, [4]S.Orsola-Malpighi Hospital, University of Bologna, Bologna, [5]Sant'Orsola-Malpighi Hospital, University of Bologna, Bologna, Italy, Bologna, Emilia Romagna, [6]S. Orsola-Malpighi Hospitale, University of Bologna

Background: An accurate risk assessment of primary GIST is crucial for the decision-making on imatinib adjuvant treatment.

Design: The aim of the study was to determine the most accurate and reliable risk stratification system for primary GIST comparing: the National Institute of Health (NIH), the modified NIH (m-NIH), the Armed Forces Institute of Pathology (AFIP) schemes, the Memorial Sloan Kettering Cancer Center (MSKCC) GIST Nomogram, and the 8th American Joint Committee on Cancer (AJCC) staging system. Recurrence-free survival (RFS) was estimated by using the Kaplan-Meier method; discrimination ability of each system was assessed using the Harrell's *C* statistic; the association of clinicopathological findings with RFS was assessed using univariate and multivariate Cox proportional hazard models; the prognostic power of covariates was expressed by hazard ratios (HRs).

Results: We retrospectively analyzed 291 surgically treated GIST-patients (median age 59 yrs). Tumor sites were stomach 53.3%, small bowel 40.5%, colon-rectum 4.1% and others 2.1%. 94.8% of the patients had R0 resection, and the incidence of tumor rupture was 7.6%. RFS was 95.5% at 1 yr, 79.0% at 3 yrs, and 70.1% at 5 yrs. On univariate analysis, factors significantly associated with shorter RFS were: small intestine site (HR 2.20), tumor size >5 cm (HR 2.57) or >10 cm (HR 4.64), age of 50-59 yrs (HR 1.82) and 60-69 yrs (HR 2.10). Non-deleted *KIT* exon 11 (HR 0.45) and *PDGFRA* D842V exon 18 mutations (HR 0.16) were associated with longer RFS. On multivariate analysis, tumor rupture (HR 2.35) was independently associated with shorter RFS, in addition to site, size, age, and mutational status. The association between RFS and each prognostic score was statistically significant (NIH: HR 2.75; m-NIH: HR 2.78; AFIP: HR 2.51; MSKCC: HR 2.13; gastric AJCC: HR 2.40; non-gastric AJCC: HR 1.53, P<0.001). The MSKCC GIST Nomogram was superior for discrimination of RFS (*C* statistic 0.73) for non-gastric tumors, whereas the AJCC system had the best discrimination (*C* statistic 0.78) for gastric tumors.

Conclusions: All applied risk-stratification systems have shown a fair discriminative ability in our study population. However, the AJCC system was able to better stratify gastric tumors, while the MSKCC GIST Nomogram resulted to be the most reliable tool for assessing prognosis of non-gastric GIST. Furthermore, our analysis has confirmed the prognostic value of mutational status in the clinical decision making on duration of adjuvant therapy.

60 Comparative Analysis of Competing Risk Models for Solitary Fibrous Tumors

Elizabeth Demicco[1], *Alexander Lazar*[2], *Wei-Lien Billy Wang*[3]. [1]Mount Sinai Hospital, Toronto, ON, [2]M. D. Anderson Cancer Center, Houston, TX, [3]UT MD Anderson Cancer Ctr, Houston, TX

Background: Several clinicopathologic risk-stratification models for solitary fibrous tumors (SFT) have recently been published (Pasquali et al, 2016, Salas et al. 2017). In order to characterize their performance characteristics, we evaluated these models on our SFT dataset.

Design: We applied the risk model of Pasquali et al. (2016) for recurrence free survival (RFS) and those of Salas et al. (2017) for risk of metastasis and overall survival (OS) to 157 SFT which had been previously used to model and validate a model for metastasis (Demicco et al., 2017). Kaplan-Meier curves were used to assess risk of metastasis, risk of recurrence (distant or local), and overall survival (OS) for all 4 models. We did not assess the Salas model for local recurrence risk due to incomplete data on radiotherapy in our dataset. For the purposes of outcome analyses, Salas metastasis risk score 2-3 were combined as there was only one case with a score of 3.

Results: All four models used mitotic activity (≥ or > 4 mitotic figures/10 HPF). Pasquali et al. included cellularity and atypia, Salas et al. included age in both risk models and location in the model for metastatic risk, and Demicco et al. included age, size and necrosis. The Pasquali model identified 16 very low risk SFT, 53 low risk, 64 intermediate, and 24 high risk SFT, the Salas model for metastasis identified 63 very low risk SFT, 65 low risk, 28 intermediate, and 1 high risk SFT, and the Demicco model identified 89 low risk SFT, 46 intermediate, and 22 high risk SFT. There was very poor concordance between the models, with 10 cases identified as very low risk across all 3 models, and 6 as high risk by both the Demicco and Pasquali models. OS and risk of recurrence or metastasis at 5 and 10 years for each model are shown in Table 1. All models were able to significantly discriminate risk of recurrence or metastasis in Kaplan-Meier analyses (log-rank p<0.005), though only the Salas and Demicco models predicted OS.

Table1. Outcomes at 5 and 10 Years

Risk group	OS (%)			Metastasis-free (%)			Recur-rence-free (%)		
	5-year	10-year	n	5-year	10-year		5-year	10-year	n
Demicco Low Intermediate High	92 88 58	70 74 0	p<0.0001 74 47 23	100 77 7	100 64 -	P<0.0001	98 77 7	98 64 -	P<0.0001 65 45 22
Pasquali Very low Low Intermediate High	86 94 80 83	64 59 65 50	P=0.6211 12 48 58 22	100 96 68 51	100 90 68 26	P=0.0043	100 93 68 52	100 87 68 26	P<0.0001 10 42 55 21
Salas Very low Low Intermedi-ate-high	89 85 79	83 52 0	P=0.016 63 58 23	92 77 40	92 63 40	P=0.0003	90 77 42	90 64 42	P=0.0002 51 51 30

Conclusions: Risk stratification models proposed by Salas et al. and Pasquali et al. were able to predict SFT behavior, but correctly stratified fewer cases as non-metastasizing or at very high risk of metastasis than the model of Demicco et al, though these results may be biased due to the nature of the available dataset. The 3 models also produced different patient membership within risk categories when applied to the same set of SFT, likely reflecting the different parameters used in each model. Evaluation in an independent dataset is needed.

61 NUT Carcinoma: a Midline Shift – Identification of a Subset of Undifferentiated Soft Tissue and Visceral Tumors Defined by NUTM1 Gene Fusions

Brendan C Dickson[1], *Marc Rosenblum*[2], *David Swanson*[3], *Jay S Wunder*, *Cristina R Antonescu*[4]. [1]Mount Sinai Hospital, Toronto, ON, [2]Memorial Sloan-Kettering CC, New York, NY, [3]Mount Sinai Hospital, Toronto, ON, [4]Memorial Sloan Kettering Cancer Center, New York, NY

Background: NUT midline carcinoma is a rare, aggressive and undifferentiated neoplasm that typically occurs in the head and neck. Tumors occasionally arise in the mediastinum/lung, with isolated reports of primary renal involvement. Prompted by an index case of an undifferentiated soft tissue tumor bearing a *NUTM1* gene fusion, we examined additional undifferentiated soft tissue and visceral tumors for *NUTM1* rearrangement.

Design: A retrospective archival review was performed of undifferentiated soft tissue and visceral tumors characterized by relative nuclear isomorphism (2007-2017). Targeted next-generation sequencing (NGS) was performed on RNA extracted from formalin-fixed paraffin-embedded tissue. The results were analyzed using both Manta and JAFFA fusion callers, and validated by fluorescence *in situ* hybridization (FISH) using custom BAC probes.

Results: Five patients were identified (mean age: 44 years [range: 3-71]; 3 males, 2 females); two tumors occurred in the extremities (arm, thigh), with one case each of brain (parietal lobe), kidney and stomach. On systemic work-up all patients lacked any other sites of disease. The tumors were morphologically heterogeneous. They contained sheets, and/or cords of primitive round-epithelioid-rhabdoid-spindle cells; however, most cases contained only focal nuclear pleomorphism. Mitotic activity was frequently brisk. Squamous differentiation was not identified. Three cases expressed pancytokeratin, only one of which was diffuse. NGS demonstrated the following *NUTM1* fusion partners: *BRD4-NUTM1* (two cases), *BRD3-NUTM1*, *MDX1-NUTM1*, and *BCORL1-NUTM1*. Independent testing by FISH confirmed the presence of *NUTM1* and partner gene rearrangement.

Conclusions: This study establishes that a subset of primary soft tissue and visceral undifferentiated neoplasms – occurring beyond an archetypal midline head/neck and mediastinum/lung distribution – are defined by recurrent *NUTM1* gene rearrangement. In addition, we report two novel *NUTM1* fusion partners in neoplasia. It is unclear whether *MDX1* and *BCORL1* account for any of the previous reports of *BRD4/3* negative *NUT* midline carcinoma. Moreover, the relationship, if any, between *NUT*-associated tumors in soft tissue and/or viscera, and conventional NUT carcinoma, remains to be elucidated.

62 Mismatch Repair Deficiency in Sarcomas is Extremely Rare

Leona A Doyle[1], *Jonathan A Nowak*[2], *Michael J Nathenson*[3], *Jason Johnson*[3], *Adem Albrayak*[3], *Suzanne George*[3], *Lynette Sholl*[4] [1]Brigham and Women's Hospital, Brookline, MA, [2]Brigham and Women's Hospital, [3]Dana Farber Cancer Institute, [4]Brigham & Women's Hospital, Boston, MA

Background: Due to the efficacy of immune checkpoint inhibitor therapy in tumors with deficient mismatch repair (MMR), there has been a surge in demand for MMR deficiency testing in various different tumor types. MMR deficiency is not known to play a role in the pathogenesis of sarcomas, and the utility of testing in these tumor types is not well established. This study aimed to determine the frequency, pattern, and clinicopathologic correlates of MMR deficiency in sarcomas.

Design: Tumors were profiled using a genomic platform that employs massively parallel sequencing to interrogate 447 cancer-associated genes. MMR status was evaluated by determining the number of small insertion/deletion events occurring in homopolymer regions per megabase of exonic sequence data across all genes. A threshold of > 1.5 such events per Mb was used to classify cases as MMR-deficient (MMR-D, "MSI-H") based upon a previously validated method in our laboratory. Separately, tumor mutational burden (TMB) was calculated as the number of non-synonymous somatic mutations per megabase of exonic sequence data. MMR immunohistochemistry (IHC) was performed on all MMR-D cases.

Results: 213 sarcomas (37 unclassified sarcomas or unclassified malignant neoplasms, likely sarcoma) were analyzed, from 93 males and 120 females, with a median patient age of 58 (range 20-88 yrs). Four cases (1.8%) were classified as MMR-D (see Table); all occurred in men. One patient was known to have Lynch syndrome. For the 3 non-Lynch syndrome patients, the allele fraction of the identified MMR gene mutation was consistent with somatic origin. MMR IHC confirmed the MMR-D status of all cases.

Diagnosis	Location	Age	Sex	Tumor Mutational Burden/ Megabase	MMR Gene Mutation	Immu-nohisto-chem-istry
Pleomorphic rhabdomyo-sarcoma (known Lynch syndrome)	Lower limb	39	M	21.293	**MSH2** c.2034T>A (p.Y678*)	MSH2 and MSH6 loss
Pleomorphic malignant neoplasm, most sug-gestive of unclassified sarcoma	Mediasti-num	79	M	25.856	**MSH2** c1165C>T (p.R389*)	MSH2 and MSH6 loss
Malignant ep-ithelioid and spindle cell neoplasm	Kidney	69	M	13.688	**PMS2** c943C>T (p.R315*)	PMS2 loss
Unclassified sarcoma with epithelioid features	Deltoid muscle	64	M	20.532	**MSH6** c.3254delC (p.F1088Sfs*2)	MSH6 loss

Conclusions: MMR deficiency in classifiable sarcomas is exceptionally rare and may be limited to patients with Lynch syndrome who also develop sarcoma. Of the three non-Lynch syndrome associated cases identified as MMR-D only one was definitively considered unclassified sarcoma, while the remaining two were diagnosed as malignant neoplasms possibly representing sarcomas. Focusing MMR testing on unclassified sarcomas or unclassified malignant neoplasms appears to be higher yield than screening all sarcomas. For those unclassified malignancies with MMR deficiency, immune checkpoint therapy may be a viable treatment option.

63 H3F3 K36M Immunohistochemistry is a Useful Diagnostic Marker for Chondroblastoma in Small Biopsy Specimens

Joseph S Frye[1], *Wonwoo Shon*[2], *Vastal Patel*[3], *John D Reith*[4], *Earl W Brien*[5], *Bonnie Balzer*[6]. [1]Cedars Sinai Medical Center, Los Angeles, CA, [2]Cedars-Sinai Medical Center, Studio City, CA, [3]University of Texas, [4]Cleveland Clinic, Cleveland, OH, [5]Cedars-Sinai Medical Center, [6]Cedars-Sinai Medical Center, Los Angeles, CA

Background: Chondroblastoma is a benign tumor predominantly occurring in the epiphysis of skeletally immature individuals. In most cases the diagnosis of chondroblastoma is often straightforward, but rendering a definitive diagnosis can be difficult, particularly in

limited small specimens. Moreover, distinguishing chondroblastoma from other malignant bone tumors such as chondroblastoma-like osteosarcoma carries significant clinical implications. Previous studies have shown recurrent mutations of *H3F3* genes in the majority of chondroblastomas and detection of this characteristic genetic event is potentially valuable in diagnostically challenging cases, but molecular diagnostics are not routinely available. In this study, we investigated the expression of recently developed anti-H3F3 K36M antibody from a series of chondroblastomas and other histologic mimics including chondroblastoma-like osteosarcoma.

Design: Formalin-fixed, paraffin-embedded sections from 26 chondroblastomas (including small biopsy/curettage specimens) and 46 control cases including conventional chondrosarcoma (6), chondromyxoid fibroma (5), giant cell tumor (5), enchondroma (5), chondroblastic osteosarcoma (4), extraskeletal myxoid chondrosarcoma (4), aneurysmal bone cyst (4), mixed tumor (3), clear cell chondrosarcoma (2), dedifferentiated chondrosarcoma with well-differentiated component (2), mesenchymal chondrosarcoma (2), chondroblastoma-like osteosarcoma (2), and chordoma (2) were retrieved from our surgical pathology archives. An automated immunohistochemistry system (Ventana BenchMark XT, Ventana Medical Systems, Inc., Tucson, AZ) was used for the detection of H3F3 K36M, using a commercially available antibody (clone RM193; RevMAb Biosciences, San Francisco, CA).

Results: H3F3 K36M was diffusely and strongly expressed in 23/26 cases of chondroblastoma. In those positive cases, distinct nuclear expression was present only in the lesional mononuclear chondroblasts; however, multinucleated osteoclast-like giant cells and other non-lesional cells were consistently negative. All other tumor types examined were completely negative for H3F3 K36M.

Conclusions: In keeping with the previously reported frequency of *H3F3* mutation in chondroblastomas, strong H3F3 K36M expression was identified in the majority of chondroblastoma cases, whereas other morphologic mimics including chondroblastoma-like osteosarcomas were negative. Detection of H3F3 K36M expression is a very useful diagnositc tool, especially in limited small specimens.

64 Grading, Histology, Loss of INI1 and Type of Translocation as Prognostic Factors in Synovial Sarcoma: a Single Institution Experience

Marco Gambarotti[1], *Alberto Righi*[2], *Marta Sbaraglia*[3], *Piero Picci*[2], *Angelo Dei Tos*[4]. [1]Bologna, [2]Rizzoli Institute, Bologna, Italy, [3]Ospedale Regionale di Treviso, Treviso, [4]Hospital of Treviso, Treviso, Italy

Background: Synovial sarcoma accounts for 5-10% all soft tissue sarcomas, classically affecting the extremities of young adults. The diagnosis is confirmed by the identification of tumor-specific fusion-genes, the most frequent being SS18-SSX1 and SS18-SSX2. Several morphologic features have been proposed as prognostic factors. The aim of this study was to verify whether grading, histology (monophasic vs biphasic), immunohistochemical loss of INI1 expression and type of translocation influence the prognosis of the disease.

Design: One-hundred and ninety-six patients affected by synovial sarcoma treated consecutively at our institution were retrospective evaluated. Tumor grade was assessed according to the FNLCC system (considering that as synovial sarcoma has a differentiation score of 3 it is therefore always either grade 2 or 3 depending on the presence and amount of necrosis and mitotic count). Loss of expression of INI1 and *SS18-SSX* fusion type (*SS18-SSX1* vs *SS18-SSX2*) were also evaluated in all cases.

Results: Seventy-two percent of cases were monophasic and 41% were grade 3. Fifty-one percent maintained the expression of INI1. Sixty percent harbored a SSX1 translocation. Sarcoma specific survival was 56.6% at 5 years and 46.9% at 10 years. The monophasic morphology was related to a worse prognosis (p=0.011) in terms of overall survival. No correlation was found neither between survival and *SSX* fusion types nor INI1 loss. Local recurrence-free survival was 78.9% at 5 years and 75.9% at 10 years. Grade 3 tumors and those with *SSX2* translocation showed a higher local recurrence rate (p=0.028 and p=0.049 respectively). Moreover, a higher rate of metastasis was found in patients older than 65 years (p=0.014) and in synovial sarcoma larger than 5 cm (p=0.007).

Conclusions: Our data confirm that not all cases of SS present the same severe outcome. High-risk patients identified on the basis of morphology and grading may qualify for an aggressive treatment approach.

65 Intraosseous Hibernoma: A Multi-Institutional Retrospective Case Series

Chiraag Gangahar[1], *David P Wang*[2], *Christopher J O'Conor*[3], *Behrang Amini*[4], *Kathleen Byrnes*[5], *Elizabeth Montgomery*[6], *Wei-Lien Billy Wang*[7], *John S Chrisinger*[8]. [1]Washington University, [2]MD Anderson Cancer Center, Houston, Texas, [3]Washington University, St. Louis, Missouri, [4]MD Anderson, [5]Johns Hopkins Hospital, Baltimore, MD, [6]Johns Hopkins Medical Institutions, Baltimore, MD, [7]UT MD Anderson Cancer Ctr, Houston, TX, [8]Washington University School of Medicine, St. Louis, MO

Background: Hibernomas are benign lipomatous tumors comprised of cells resembling brown fat. Hibernomas most commonly occur in the soft tissues of the thigh, head and neck, upper trunk and retroperitoneum. Intraosseous hibernomas (IH) are exceedingly rare. The clinical, radiologic and pathologic features of IH are thus not well understood.

Design: A multi-institutional retrospective search of the pathology archives was performed to identify intraosseous hibernomas. The clinical, radiographic and pathologic findings were analyzed.

Results: Five cases of IH were identified (one previously published). Four of five patients were female and one was male, with an average age of 44 years (range: 7-69 years). Three IH were asymptomatic and were identified on surveillance imaging, while two presented with pain. By imaging, lesions were small (mean 1.4 cm, range: 0.8-2.0 cm), sclerotic and situated in the pelvis (3 sacrum, 2 ilium). By imaging, two were considered at least suspicious for metastasis, one was thought to be osteomyelitis or leukemia, and one was deemed likely benign. Microscopically, large cells with small central nuclei and abundant finely vacuolated cytoplasm were noted between bony trabeculae. Immunohistochemical studies (IHC) were performed in four cases and showed tumor cells to be positive for S100 protein and adipophilin (4/4), and negative for cytokeratins (0/4), brachyury (0/2) and CD163 (0/2). Clinical follow-up was available in 4/5 cases with a mean follow-up of 14 months (range: 3-40 months). None of the patients received further treatment and no aggressive behavior was observed. In one case the lesion appeared to regress.

Conclusions: We confirm that IH tend to be small, sclerotic and occur in the axial skeleton, particularly the pelvis. These tumors are often clinically or radiographically thought to represent metastatic disease. This highlights the importance of histologic evaluation in these cases, as IH are benign. In histologically ambiguous cases, an immunohistochemical panel including S100 protein, adipophilin, cytokeratin and brachyury can help distinguish this tumor from benign notochordal cell tumors, metastatic carcinoma and histiocytic proliferations.

66 Pan-TRK Immunohistochemistry is a Sensitive Diagnostic Marker for Infantile Fibrosarcoma

Yin P. (Rex) Hung[1], *Christopher D Fletcher*[2], *Jason L Hornick*[2]. [1]Brigham & Women's Hospital, Boston, MA, [2]Brigham and Women's Hospital, Boston, MA

Background: Infantile fibrosarcoma, a rare mesenchymal neoplasm of intermediate biologic potential, is characterized by intersecting fascicles of spindle cells and *ETV6-NTRK3* fusion. Given histologic overlap with other pediatric spindle-cell tumors, the diagnosis of infantile fibrosarcoma can be challenging and often requires molecular confirmation. A recently developed pan-TRK antibody (which recognizes a conserved sequence near the C-terminus of TRK proteins) shows promise for identifying tumors with *NTRK* fusions. The purpose of this study was to evaluate the potential diagnostic utility of immunohistochemistry (IHC) using this pan-TRK antibody for infantile fibrosarcoma.

Design: We evaluated whole-tissue sections from 210 cases including 15 infantile fibrosarcomas (all confirmed to harbor *ETV6* gene rearrangement); 20 each low-grade fibromyxoid sarcoma, synovial sarcoma, spindle-cell rhabdomyosarcoma, malignant peripheral nerve sheath tumor, fibrosarcomatous dermatofibrosarcoma protuberans (DFSP), and nodular fasciitis; 15 each fibrous hamartoma of infancy (FHI), myofibroma/myofibromatosis, and desmoid-type fibromatosis; 10 each low-grade myofibroblastic sarcoma and primitive myxoid mesenchymal tumor of infancy (PMMTI); and 5 each lipofibromatosis and lipofibromatosis-like neural tumor. IHC for pan-TRK was performed following heat-induced antigen retrieval using a pan-TRK rabbit monoclonal antibody (clone EPR17341; Abcam).

Results: Immunoreactivity for pan-TRK was observed in all 15 (100%) infantile fibrosarcomas, including diffuse immunoreactivity (>50% of cells) in 14 (94%) cases, with staining patterns ranging from nuclear and cytoplasmic (11 cases) to membranous or granular cytoplasmic (4 cases). Of the 195 histologic mimics, diffuse pan-TRK immunoreactivity

was noted in 21 (11%) cases, including all 5 (100%) lipofibromatosis-like neural tumors, 5 (50%) PMMTI, 5 (33%) FHI (highlighting only the primitive myxoid spindle cell components), 3 (15%) fibrosarcomatous DFSP, 1 (10%) low-grade myofibroblastic sarcoma, 1 (7%) myofibroma, and 1 (5%) spindle-cell rhabdomyosarcoma.

Conclusions: Diffuse pan-TRK immunoreactivity is a highly sensitive but not entirely specific diagnostic marker for infantile fibrosarcoma and may be helpful in selecting patients for TRK-targeted therapy. As expected, lipofibromatosis-like neural tumors (which harbor *NTRK1* fusions) also show diffuse pan-TRK immunoreactivity. Considerable TRK expression in PMMTI and FHI suggests TRK signaling may play a pathogenetic role.

67 Low-Frequency CTNNB1 Mutations in "Wild-Type" Sporadic Desmoid-Type Fibromatosis Detected by Droplet Digital PCR

Davis Ingram[1], *Khalida Wani*[1], *Fernando Carapeto*[1], *Dzifa Duose*[2], *Eveline Chen*[3], *Danielle Braggio*[4], *Jonathan Trent*[6], *Breelyn Wilky*[6], *Wei-Lien Billy Wang*[7], *Alexander Lazar*[8]. [1]M D Anderson Cancer Center, [2]UT MD Anderson Cancer Center, [3]UT MD Anderson Cancer Center, Houston, TX, [4]OSU Comprehensive Cancer Center, [5]University of Miami Sylvester Comprehensive Cancer Center, [6]University of Miami Sylvester Comprehensive Cancer Center, Miami, FL, [7]UT MD Anderson Cancer Ctr, Houston, TX, [8]M. D. Anderson Cancer Center, Houston, TX

Background: Desmoid-type fibromatosis is a locally aggressive fibroblastic tumor that can arise either sporadically or in association with familial adenomatous polyposis (FAP). Sanger sequencing reveals that ~85% of sporadic desmoid tumors harbor one of 3 recurrent point mutations in exon 3 of *CTNNB1*, the gene encoding -catenin. Recent studies reveal that next-generation sequencing can recover *CTNNB1* mutations in additional tumors initially deemed wild-type (non-mutated) by Sanger sequencing. We tested desmoid tumors previously determined to be wild-type by Sanger or pyrosequencing with droplet digital PCR, a highly sensitive and quantitative PCR-based assay.

Design: DNA was extracted from formalin-fixed, paraffin-embedded (FFPE) desmoid tumor samples (40 samples from 31 patients), which were previously called wild-type by Sanger and/or pyrosequencing. Samples from multiple tumor recurrences were available for 7 patients (6 patients with 2 recurrences and 1 with 4). Digital droplet PCR was performed using a Bio-Rad automated droplet generator and QX200 droplet reader with primer-probe mixes for the *CTNNB1* S45F and T41A point mutations.

Results: *CTNNB1* mutations were detected in 15/40(38%) samples from 10/31(32%) patients, 7 in codon 45 and 3 in codon 41. All FFPE samples were estimated to contain 60% or greater tumor nuclei content. In all but one of the patients for whom multiple tumor recurrences were tested, the genotype remained consistent across all samples. Allele frequencies of recovered mutations varied from 0.3% to 56.5% (median, 16.1%). Some samples (8/15) exhibited allele frequencies (>20%), which would be expected to be detectable by Sanger sequencing.

Conclusions: Pure "wild-type" desmoid-type fibromatosis is rare, as low allelic frequency *CTNNB1* mutations can be identified using highly sensitive approaches such as droplet digital PCR. Desmoid tumors show subclonal heterogeneity possibly due to genomic subclonality or perhaps lower neoplastic content than suggested by histologic examination. The effects of low mutant allelic fractions on tumor behavior are the subject of current study.

68 Ewing Sarcoma in Adults: A Study of 48 Cases

Khadijeh Jahanseir[1], *Andrew Folpe*[2], *Caterina Giannini*[2], *Karen Fritchie*[2]. [1]Mayo Clinic, Rochester, MN, [2]Mayo Clinic, Rochester, MN

Background: Ewing sarcoma (ES) overwhelming affects children and young adults, reaching peak incidence in the 2nd decade. We explore the clinicopathologic features of ES presenting in adulthood.

Design: ES arising in patients ≥ 40 years of age were retrieved from our institutional/consultation archives (1990-2017). Only cases confirmed by FISH for *EWSR1* rearrangement or RT-PCR for *EWSR1-FLI1* and *EWSR1-ERG* were included. H&E slides were evaluated for low power architecture, fibrous septa, cytology, rosettes and necrosis. Clinical data was reviewed.

Results: 48 cases (15 institutional; 33 consultation) of ES were identified (31M, 17F) with patients ranging in age from 41 to 86 years (median 54 years). 36 tumors (75%) arose in soft tissue (extremities=15, paraspinal=7, abdomen/pelvis/retroperitoneum=7, chest wall=3, head/neck=3, back=1), 7 (15%) in bone (vertebra=3, rib=1, tibia=1, scapula=1, metatarsal=1) and 4 (8%) in viscera (liver=1, kidney=1, lung=1, duodenum/pancreas=1). The remaining case involved bone and soft tissue equally. In cases with adequate tissue for low power assessment (n=46), the majority exhibited a nested architecture (n=26), while the remaining cases (n=20) showed sheet-like growth. In cases with nested architecture, the fibrous septa were classified as thin (n=14), thick (n=11) or both (n=1). Tumor cytology was categorized as typical (n=39), crushed (n=5), clear cell (n=3), epithelioid (n=23) and rhabdoid (n=2) with 3 cases harboring more than one appearance. 50% (24/48) of cases had necrosis, while rosettes were noted in only 1 case. Follow-up (n=41, 1-147 months, mean 35.5 months) revealed that 7 patients (17%) presented with metastasis and 6 (15%) developed metastasis after their initial presentation (time to metastasis 12-39 months, median=20 months). The lung (n=6) was the most common site of metastasis followed by bone (n=4). At last follow up, 18 died of disease, 12 are alive with disease, 10 are alive without disease, and 1 died of other causes.

Conclusions: ES may arise in patients 40 years and older, often triggering expert consultation when it presents in this population. Although most cases exhibit classic cytologic features, a subset have crushed, clear cell, epithelioid or rhabdoid morphologies, potentially mimicking entities such as carcinomas and lymphomas that are more common in this age group. ES in adults is an aggressive disease with high rates of distant metastasis and mortality.

69 Amplification of FRS2 in Atypical Lipomatous Tumor/Well -Differentiated Liposarcoma and Dedifferentiated Liposarcoma Clinicopathological and Genetic Study of 146 Cases

Wenyi Jing[1], *Ting Lan*[1], *Huijiao Chen*[2], *ZHANG ZHANG*[3], *Min Chen*[4], *Ran Peng*, *Xin He*[5], *Hongying Zhang*[6]. [1]Department of Pathology, West China Hospital, Sichuan University, Chengdu, Sichuan, [2], Chengdu, SC, [3]West China Hospital, Sichuan University, Chengdu, Sichuan, [4]West China Hospital, Sichuan University, Chengdu, Sichuan, [5]West China Hospital, Sichuan University, [6]West China Hospital, Sichuan University, China, Chengdu, Sichuan

Background: Atypical lipomatous tumor/well-differentiated liposarcoma (ALT/WDL)/dedifferentiated liposarcoma (DDL) represents the most common subtype of liposarcomas. Fibroblast growth factor receptor substrate 2 (*FRS2)* gene is located close to *MDM2* and *CDK4* within the 12q13-15 band. FRS2 plays a critical role in the fibroblast growth factor receptor (FGFR) pathway. The aim of this study was to better evaluate the frequency of *FRS2* amplification and its relationship with the clinicopathological features of ALT/WDL/DDL.

Design: *FRS2* and *MDM2* fluorescence *in situ* hybridization (FISH) was performed on 146 tumors (70 ALT/WDLs and 76 DDLs). Seventy-nine control samples were obtained for *FRS2* analysis, including 25 ordinary lipomas, 7 spindle cell lipomas, 8 pleomorphic liposarcomas, 3 spindle cell liposarcomas, 6 myxoid liposarcomas, 7 undifferentiated pleomorphic sarcomas, 5 myxofibrosarcomas, 5 leiomyosarcomas, 5 conventional osteosarcomas, 3 low-grade myofibroblastic sarcomas and 5 normal fat samples. we evaluated the frequency of *FRS2* amplification of ALT/WDL/DDL and its relationship with the clinicopathological features of ALT/WDL/DDLs.We also compared the frequency between *FRS2* and *MDM2* amplification in this tumor group.

Results: Amplification of *FRS2* was detected in 136/146 (93.2%) ALT/WDLs/DDLs, including 63 ALT/WDLs and 73 DDLs. None of the control samples demonstrated amplification of *FRS2*. A higher *FRS2*/CEP12 ratio was observed in DDLs than in ALT/WDLs (mean: 9.5 vs. 7.1, p=0.0005). The *FRS2*/CEP12 ratio of peripheral tumors was lower than that of central tumors (mean: 6.2 vs. 9.3, p=0.00004). All of the 146 ALT/WDLs/DDLs showed *MDM2* amplification (100%). Compared to the 136 *MDM2*+/*FRS2*+ tumors, the 10 *MDM2*+/*FRS2*- tumors were more likely to occur in peripheral sites (70.0% vs. 27.9%, p=0.015). A high percentage of sclerosing ALT/WDLs (4/7) and homologous pleomorphic liposarcoma-like DDLs (2/3) were observed in the *MDM2*+/*FRS2*- group. None of these tumors showed heterologous differentiation.

Conclusions: These findings suggest that *FRS2* is consistently amplified in ALT/WDLs/DDLs and offer another avenue for the investigation of the biology of this tumor group. FRS2 has the potential to be a therapeutic target in the future. *MDM2*+/*FRS2*- cases seem to be associated with unusual clinicopathological features, and further investigation is needed. Analysis *FRS2* gene, in combination with *MDM2* and other genes located at 12q13-15, may more precisely characterize ALT/WDL/DDLs.

70 PAX7 is a Robust Marker for Adult-Type Rhabdomyosarcomas

Ivy John[1], *Uma Rao*[2], *Karen Schoedel*[3], *Lori Schmitt*[4], *S. Ranganathan*[5], *Rita Alaggio*[6]. [1]University of Pittsburgh Medical Center, Pittsburgh, PA, [2]UPMC, Shadyside Campus, Pittsburgh, PA, [3]UPMC Presbyterian, Pittsburgh, PA, [4]Children's Hospital of Pittsburgh, [5]Children's Hospital of Pittsburgh, Pittsburgh, PA, [6]Pittsburgh, PA

Background: Rhabdomyosarcoma (RMS) is the most common soft tissue sarcoma in children but accounts for only 2-5% of all adult sarcomas. RMS can be broadly divided into pediatric-type (alveolar [ARMS] and embryonal [ERMS]) and adult-type (pleomorphic [PRMS] and spindle/sclerosing [Sp/ScRMS]). The diagnosis of RMS, particularly adult-type, is often challenging due to limited expression of myogenic markers. We investigated the potential diagnostic utility of PAX family transcription factors including PAX7 (required in the developmental specification of satellite cells and recently shown to be specific for skeletal muscle differentiation and Ewing sarcoma) and PAX5 (often expressed in translocated pediatric cases of ARMS) in RMS arising in adults.

Design: RMS in patients over 20 years were retrieved from our archives and reviewed to confirm the diagnosis. The cases were classified into ARMS, ERMS, PRMS, Sp/ScRMS or EpRMS (epithelioid RMS). IHC for myogenin (MYOG), PAX7 and PAX5 were performed on all cases with available material. Only nuclear staining (weak to strong) was considered positive and scored as follows: negative <1%, focal 1-20%, intermediate 20-70% and diffuse >70%.

Results: 34 RMS were identified (27M, 7F; range 22 to 85 years, median 57.5). The tumors involved extremities (n=17), trunk (n=8), head and neck (n=5), retroperitoneum (n=2), liver and bladder (1 each) and included 16 PRMS, 8 ARMS, 4 ERMS (including 1 with anaplasia), 3 ScRMS, 2 SpRMS and 1 EpRMS. FISH or RT-PCR studies were available in 15 cases and 7 ARMS demonstrated FOXO1A translocation. The results of the MYOG, PAX7 and PAX5 IHC are summarized in Table 1. MYOG was expressed in 33/34 (97%) cases and MYOG negative ScRMS demonstrated diffuse (98%) PAX7 expression. PAX7 was expressed in 32/34 (94%) cases; 2 PAX7 negative PRMS demonstrated focal to intermediate MYOG expression. PAX5 was expressed in a single FOXO1A translocated ARMS.

SUBTYPE (n)	SCORE	MYOG	PAX-7	PAX-5
PRMS (16)	Diffuse		13	
	Intermediate	2		
	Focal	14	1	
	Negative		2	16
Sp/ScRMS (5)	Diffuse		5	
	Intermediate	2		
	Focal	2		
	Negative	1		5
ARMS (8)	Diffuse	4		1
	Intermediate	4	8	
	Focal			
	Negative			7
ERMS (4)	Diffuse		3	
	Intermediate	4	1	
	Focal			
	Negative			4
EpRMS (1)	Diffuse			
	Intermediate		1	
	Focal	1		
	Negative			1

Conclusions: PAX7 is a reliable marker for the diagnosis of RMS in adults. PAX7 expression is often diffuse (n=18, 86%) in adult-type RMS compared to MYOG which typically shows focal to intermediate staining making it particularly useful for tumors sampled with limited needle biopsies. Intriguingly, ARMS arising in adults differ from their pediatric counterparts, showing only intermediate expression of MYOG in half the cases and infrequent expression of PAX5 (10% vs reported 67% in children), suggesting different underlying biologic profiles in these two groups.

71 TERT Promoter Mutations in Granular Cell Tumors

Ivy John[1], *Karen Fritchie*[2], *Peter Lucas*[3], *Abigail I Wald*[1], *Karen Schoedel*[4]. [1]University of Pittsburgh Medical Center, Pittsburgh, PA, [2]Mayo Clinic, Rochester, MN, [3]University of Pittsburgh School of Medicine, Pittsburgh, PA, [4]UPMC Presbyterian, Pittsburgh, PA

Background: Most granular cell tumors (GCT) are benign but rare examples are malignant with a 50% rate of metastasis. The molecular determinants of malignancy in GCT are yet to be determined. We investigated telomerase reverse transcriptase (TERT) reactivation induced by promoter mutations as a potential molecular mechanism for malignant phenotype and aggressive behavior in GCTs.

Design: TERT promoter mutation analysis was performed by Sanger sequencing in samples from 17 patients with GCT. The tumors were classified as benign, atypical or malignant based on the proposed criteria by Fanburg-Smith *et al*. Clinical information was obtained as available.

Results: The 17 tumors occurred in 14 females and 3 male patients, ranging from 7 to 74 years. The majority of the cases involved skin and superficial soft tissues (12). Other locations included tongue, esophagus, ulnar nerve, gastrocnemius muscle and lung (1 each). The tumors ranged from 0.4 to 5 cm (median, 2 cm). Using a constellation of findings including necrosis, spindling, vesicular nuclei with prominent nucleoli, increased mitotic activity (> 2/10HPF), high nuclear to cytoplasmic ratio and pleomorphism, the tumors were classified as benign (8), atypical (7) and malignant (2). Ten samples were successfully analyzed by Sanger sequencing; TERT promoter mutation (C228T) was identified in 1 of 2 (50%) malignant GCTs but in none of the atypical and benign tumors. The TERT mutated malignant GCT involved the ulnar nerve, measured 4.5 cm and fulfilled 5/6 criteria proposed by Fanburg-Smith *et al* including necrosis and mitotic count of 8/10HPF. All cases were treated by excision while 1 case (TERT mutated malignant GCT) also received adjuvant radiation. Follow up information was obtained in 15/17 patients (range 2 to 155 months, median 29 months) revealed 1 patient (benign GCT with unknown TERT status) with local recurrance (96 months). 14 patients are alive without disease and 1 patient (TERT mutated malignant GCT) died of unrelated cause.

Conclusions: TERT promoter mutations can be seen in a subset of granular cell tumors and appears to be associated with a malignant histologic phenotype, although study of additional cases is needed. Patients with GCTs harboring this mutation may benefit from targeted telomerase inhibitor therapy.

72 Chondroblastomas Presenting in Adulthood: A Study of 26 Patients with Emphasis on Histologic Features and Skeletal Distribution

Ivy John[1], *Carrie Inwards*[2], *Don Williams*[3], *Doris Wenger*[2], *Karen Fritchie*[2]. [1]University of Pittsburgh Medical Center, Pittsburgh, PA, [2]Mayo Clinic, Rochester, MN, [3]University of Pittsburgh Medical Center

Background: Chondroblastomas (CB) are rare bone tumors that typically arise in the epiphyses/apophysis of long bones in skeletally immature patients (< 18 years of age). We explore the clinicopathologic features of CB presenting in adults.

Design: CB in patients ≥20 years of age were retrieved from our archives. H&E slides were examined to confirm the diagnosis and to evaluate histologic features including: giant cell distribution, pattern of calcification, presence/type of matrix, hemosiderin deposition, foamy macrophages and secondary aneurysmal bone cyst. Clinical data/radiologic findings were reviewed.

Results: 26 CB were identified (19M, 7F; range 20-50 years, median 28 years). Pain was the presenting symptom in 12 patients (46%). Fifteen (58%) cases occurred in long tubular bones (femur (9); humerus (4); tibia (1); ulna (1)), 6 (23%) in small bones of the hands/feet (talus (3); calcaneus (2); cuboid (1)), 3 (12%) in flat bones (rib (2); acromion (1)), and 2 (8%) in the patella. All cases showed classic cytologic features of chondroblastoma. Chondroid matrix was universally present. While the majority of cases exhibited an even distribution of giant cells (n=18, 69%), the remaining 8 cases showed giant cells predominantly centered around chondroid matrix. Calcification was identified in 9 cases (35%), including various combinations of punctate (n=6), serpiginous (n=5), classic chicken-wire (n=4) and psammomatous (n=2) patterns. Hemosiderin deposition (n=15), woven bone (n=9), foamy macrophages (n=3) and secondary aneurysmal bone cyst formation (n=5) were also noted. Imaging findings were compatible with CB in all cases reviewed (n=17). Lesions involving bones with an epiphysis/apophysis (n=9) more frequently involved the apophysis (n=7) compared to the epiphysis (n=2). 25 patients underwent simple curettage and one was followed after biopsy. Follow up information (n=22, 1 to 299 months; median 42.5 months) revealed 1 patient with local recurrence (270 months).

Conclusions: CB presenting in patients >20 years more frequently involve the small bones of the hands/feet and flat bones compared to those arising in their younger counterparts. While the morphological spectrum is similar to what is seen in skeletally immature patients, a subset may harbor extensive serpiginous calcification rather than the classic chicken-wire pattern. Simple curettage is typically curative with a local recurrence rate less than 10%.

73 True Neoplastic Cells in Giant Cell Tumor of Bone Potentially Have Osteogenic Nature and Reveal their Osteogenic Histology After Denosumab Therapy: Integrated Analyses Including Immunofluorescent Double Staining

Ikuma Kato[1], *Mitsuko Furuya*[2], *Yusuke Kawabata*[3], *Reiko Tanaka*[4], *Kenichi Ohashi*[5]. [1]Yokohama City University Graduate School of Medicine, Yokohama, Kanagawa, [2]Yokohama City University Graduate School of Medicine, Yokohama, Kanagawa, [3]Yokohama City University Hospital, Yokohama, Kanagawa, [4]Chiba University, [5]Yokohama City University Hospital

Background: Giant cell tumor of bone (GCTB) is characterized by very large osteoclast-like multinucleated giant cells. Denosumab, which is a human monoclonal antibody directed against RANKL, has recently been introduced into the therapy of GCTB. The histology after denosumab shows dramatic changes including disappearance of osteoclast-like giant cells and formation of woven bone, whereas the actual mechanism remains unclear. We attempted integrated analyses including immunofluorescent double staining in GCTBs before and after denosumab therapy.

Design: Eight patients with GCTB that were diagnosed via biopsy and underwent curettage after denosumab therapy were reviewed. Immunohistochemistry for NFATc1 (an osteoclast marker, mouse monoclonal), RUNX2 (an osteoblast marker, mouse monoclonal), and Histone H3.3 G34W (G34W, a GCTB marker, rabbit monoclonal) was performed. Nuclear staining was considered as positive. Immunofluorescent double staining (G34W/NFATc1 and G34W/RUNX2) was also performed. Mutation status of *H3F3A* was examined by direct sequencing on FFPE samples.

Results: All cases showed the similar immunostaining pattern. Before denosumab therapy, half of mononuclear cells were G34W+, and co-expressed RUNX2. Osteoclast-like giant cells were G34W-NFATc1+. After the therapy, no NFATc1+ cells were observed. However, G34W+RUNX2+ cells still existed, and some of them surrounded woven bones. All cases before and after the therapy harbored *H3F3A* (G34W) mutation.

Conclusions: True tumor cells in GCTBs, i.e. G34W+ cells, do not seem to be osteoclastic but osteoblastic lineage cells. The G34W+ tumor cells survive denosumab therapy and reveal their osteogenic nature which is hidden before denosumab therapy. Although osteoclast-like giant cells are not neoplastic, they may have some influences to suppress osteogenic nature of the tumor cells, and help expand the lesion with the osteolytic function.

74 Immunohistochemical Characterization of Giant Cell Tumor of Bone Treated with Denosumab: Support for Osteoblastic Differentiation

Darcy Arendt Kerr[1], *Angela R Shih*[2], *G. Petur Nielsen*[2], *Andrew Rosenberg*[3]. [1]University of Miami Miller School of Medicine, Sylvester Cancer Center, [2]Massachusetts General Hospital, Boston, MA, [3]University of Miami Miller School of Medicine, Miami, FL

Background: Giant cell tumor of bone (GCT) is a neoplasm of intermediate biologic potential with frequent local recurrence and rare metastasis. While the cell of origin is uncertain, evidence suggests the neoplastic cells resemble osteoblast precursors. Surgical therapy is standard treatment, but medical therapy with denosumab, an inhibitor of RANKL, has proven successful. The mechanism of denosumab's effect on GCT is unknown; however, treated tumors show characteristic morphological changes including loss of giant cells, bone matrix deposition, and replacement with spindle cells. Denosumab-treated GCT (DT-GCT) bears little resemblance to GCT. Immunohistochemical studies may provide insight into the phenotype of the cells in DT-GCT.

Design: Surgical pathology files were reviewed for DT-GCT. Twenty-one cases were found from 2013-2017: 6 cases of from Massachusetts General Hospital, 4 cases from Miami, and 1 case from the consultation files of one of the authors (AER). Clinical and demographic information was reviewed along with available slides, and immunohistochemistry for H3.3 (mutation-specific antibody useful for GCT diagnosis), SATB2 (marker of osteoblastic differentiation), and p63 (marker expressed by GCT tumor cells) was performed.

Results: The cohort included 21 tumors from 20 patients (3:2 M:F), ages 23-73 years (median 33.5). Morphology ranged from tumors composed of abundant reactive bone matrix with few inter-trabecular spindle cells to tumors comprised predominantly of spindle cells. Four tumors had focal residual classic CGT, and 2 tumors had mild nuclear atypia. Nineteen cases (90.5%) expressed H3.3 and 20 cases (95.2%) SATB2; all expressed p63. All markers stained the various tumor components including spindle cells and the cells on the surface of and within the treated tumor bone matrix. Most markers were also positive in reactive-appearing woven bone adjacent to tumor: 100% for SATB2, 88% for H3.3, and 69% for p63.

Conclusions: The majority of DT-GCT cases strongly co-express H3.3, SATB2, and p63. These markers are also expressed in the reactive woven bone within and at the periphery of the tumor. This suggests that treatment of GCT with denosumab stimulates the neoplastic mononuclear cells to differentiate along the lines of mature osteoblasts, an idea that fits well with the observation that DT-GCT frequently demonstrates abundant new bone formation. The biologic potential of the residual tumor cells is unknown; specifically, do they harbor the potential to form recurrent GCT?

75 Primary Fibrosarcoma of Bone with Cytokeratin Expression

Mahsa Khanlari[1], *Darcy Arendt Kerr*[2], *Andrew Rosenberg*[3]. [1]Jackson Memorial Hospital, Miami, FL, [2]University of Miami Miller School of Medicine, Sylvester Cancer Center, [3]University of Miami Miller School of Medicine, Miami, FL

Background: Fibrosarcoma (FS) of bone is an uncommon primary malignant tumor of the skeleton composed of malignant cells, usually spindled, and associated with a collagenous stroma secreted by the tumor cells without evidence of other lines of differentiation. The degree of cellularity, cytologic atypia, mitotic activity, and necrosis varies according to grade and correlates with prognosis. FS often arises during middle or late adulthood, age groups in which other forms of malignancies (especially carcinomas) are more common. We present FS of bone that exhibits cytokeratin (CK) staining by immunohistochemistry (IHC) and discuss the diagnostic challenges.

Design: Pathology files of the consultations of one author (AER) and University of Miami/Jackson Memorial Hospitals were searched for the diagnosis of FS of bone between the years 2004-2017. Cases containing CK-positive cells that lacked the cytomorphology of epithelial cells were identified and formed the study cohort. The original pathology reports, H&E-stained and IHC slides were reviewed.

Results: Of 58 cases of FS of bone, IHC was performed on 44, and 9 (20%) showed CK+ staining. The patients ranged in age from 28-71 years, and the M: F ratio was 7:2. Tumors originated in the femur (4), proximal tibia (3) and distal tibia (1). The tumors were composed of malignant spindle cells intimately associated with collagen fibers of various quantities. Abundant collagen, hypocellularity and storiform pattern were present in some cases. The degree of atypia ranged from subtle to marked pleomorphism. The tumors grew with an infiltrative pattern encasing preexisting cancellous bone, sometimes associated with a peculiar form of bone resorption in the center of the trabeculae and intact surface (frame-like pattern). The percentage of CK+ tumor cells ranged from 10 - 95%, and the staining was intense in all cases. Five (5) cases also expressed markers of myogenic differentiation (SMA/Desmin), in focal (3) and diffuse (2) patterns.

Conclusions: FS of bone is a heterogeneous group of tumors, and 20% of cases are positive for CK, a finding not previously well described. The expression of CK often raises the differential diagnosis of metastatic sarcomatoid carcinoma - a diagnosis more common in older patients and histologically hard to exclude. We recommend careful staging of the patients to exclude a primary carcinoma elsewhere in the body. Lastly, the co-expression of CK and Desmin by tumor cells is helpful as it is very uncommon in epithelial malignancies.

76 Dedifferentiated Chondrosarcoma of Bone with Cytokeratin (CK) Staining: A Diagnostic Pitfall.

Mahsa Khanlari[1], *Darcy Arendt Kerr*[2], *Andrew Rosenberg*[3]. [1]Jackson Memorial Hospital, Miami, FL, [2]University of Miami Miller School of Medicine, Sylvester Cancer Center, [3]University of Miami Miller School of Medicine, Miami, FL

Background: Dedifferentiated chondrosarcoma (DDCS) is defined as a biphasic tumor composed of two distinct components: enchondroma or well-differentiated chondrosarcoma and a non-cartilaginous sarcoma. The non-cartilaginous portion or dedifferentiated component (DDC) is usually poorly differentiated, aggressive, and often exhibits the features of pleomorphic fibroblastic spindle cell sarcoma. It may also show osteoblastic, myogenic, endothelial and rarely epithelial differentiation. DDCS is often diagnosed by needle biopsy which may capture only the DDC. Immunohistochemistry (IHC) is generally performed to identify the phenotype of the dedifferentiated cells and the results may be confounding. We present 10 cases of DDCS in which the DDC exhibited keratin (CK) staining without cytomorphologic evidence of epithelial differentiation. This finding is a diagnostic pitfall for other CK+ neoplasms, especially metastatic sarcomatoid carcinoma.

Design: The surgical pathology files of the consultations of one author (AER), and University of Miami hospital between 2004-2017 were searched for the diagnosis of DDCS. Cases containing a dedifferentiated cytokeratin-positive non-epithelial component were identified and formed the study cohort. The pathology reports, H&E-stained and IHC slides were reviewed.

Results: Of 47 cases of DDCS, IHC was performed on 16 and 10 tumors (62%) showed CK+ staining of the DDC. Patient age ranged from 39-75 yrs and M:F ratio was 6:4. Tumors were located in the femur (3), sternum (1), rib (1), scapula (1), and vertebra (1). All contained enchondroma and/or well differentiated chondrosarcoma and the DDC was composed of malignant spindle/polyhedral cells arranged in varying architectural patterns. Three (3) showed an additional osteosacomatous component and 2 contained rhabdomyosarcoma. Percent of CK+ cells ranged from 10 - 95% and the staining was intense. Seven (7) cases also expressed myogenic markers (SMA/Desmin).

Conclusions: DDCS is heterogeneous and may be strongly CK positive. In our experience, CK expression of DDC is common (62%) and can be extensive, but it is not well described. Specimens lacking the cartilaginous element can be confused with other CK-positive neoplasms. Important amongst these is metastatic sarcomatoid carcinoma which is more common, occurs in a similar age group and is treated differently. Identification of the cartilaginous component (histologically or radiologically) and molecular analysis for IDH mutation are helpful in making the accurate diagnosis.

77 Atypical "sclerosing" osteoblastic lesions: do they represent aggressive osteoblastomas, malignant osteoblastomas, or low grade osteosarcomas?

Scott Kilpatrick[1], *John D Reith*[1]. [1]Cleveland Clinic, Cleveland, OH

Background: The existence of aggressive osteoblastoma or malignant transformation of osteoblastoma is controversial. Over the years, we have encountered a group of "sclerosing" osteoblastic lesions which have been difficult to classify. We considered most of these tumors forms of osteoblastoma, but they were associated with a high rate of local recurrence, and there sometimes was disagreement regarding their diagnosis.

Design: The consultative files from the 2 co-authors over the last 20 years, were reviewed for diagnoses of atypical osteoblastoma, malignant transformation of osteoblastoma, well differentiated osteosarcoma, and osteoblastoma-like osteosarcoma. Six cases were identified, and their clinicoradiologic and pathologic features re-reviewed. Five of these tumors were initially diagnosed as osteoblastoma, and 1 was interpreted as well differentiated intraosseous osteosarcoma. Three cases were evaluated initially by more than 1 subspecialty expert, often with differing opinions.

Results: There were 4 males and 2 females, ages ranging from 13-55 years (mean, 28 years). Two cases arose in the foot metatarsal, 2 in the fibula, and 1 each in the humerus and femur. Histologically, all cases showed a dominant and compact sclerosing osteoblastic pattern always associated with more conventional osteoblastoma-like areas but without sheets of osteoblasts without intervening stroma. No permeation of surrounding bone was present on the initial biopsy/curettage.

Follow-up ranged from 1 to 11 years. (mean, 4.4 years). 4 patients underwent initial curettage, and 2 were treated with local excision/resection. 1 patient had a below the knee amputation following a local recurrence. Overall, 5 (of 6) patients locally recurred, within 4 months to 3 years after the initial diagnosis. Two tumors were re-classified as osteosarcomas following evaluation of the local recurrence. To date, no patient has developed metastases or died from their disease.

Conclusions: There exists a group of atypical "sclerosing" osteoblastic lesions which appear to behave in a low grade fashion with frequent local recurrences but are difficult to precisely classify. Whether such lesions represent low grade osteosarcomas or aggressive forms of osteoblastoma is unclear. Larger study groups with more prolonged follow-up are needed to better understand the biology and behavior of these lesions. At the present time, we believe such tumors are best classified as "atypical sclerosing osteoblastic lesions", and complete resection is recommended.

78 Brachyury expression in SMARCB1/INI1-deficient tumors

Kenichi Kohashi[1], *Hidetaka Yamamoto*[2], *Yuichi Yamada*[3], *Yoshinao Oda*[2]. [1]Kyushu University, Fukuoka, Fukuoka, [2]Kyushu University, Fukuoka, [3]Kyushu University, Fukuoka-shi Fukuoka-, Japan

Background: Brachyury is a transcription factor within the T-box family typically expressed in notochord and chordoma. Some studies report brachyury as highly specific and sensitive for chordoma. SMRRCB1/INI1 (SMARCB1) is one of the evolutionarily conserved core subunits in SWI/SNF chromatin remodeling complex and is ubiquitously expressed in the nuclei of all normal cells. Loss of SMARCB1 protein expression has recently been identified in a variety of tumors such as malignant rhabdoid tumor (MRT) including atypical teratoid/rhabdoid tumor (AT/RT) and epithelioid sarcoma (ES). In addition, pediatric chordoma with SMARCB1-deficiendy has been reported. Especially, poorly differentiated chordoma shows poorly differentiated epithelioid tumor cell, sheet arrangement and coexpression of vimentin and epithelial markers, and sometimes have rhabdoid cells. Therefore, differential diagnosis of these tumors is often difficult. In the present study, we analyzed immunohistochemical brachyury expressions in SMARCB1-deficient tumors and discuss the clinicopatologic and diagnostic point in cases of SMARCB1-deficient tumors with brachyury expression.

Design: Brachyury immunoexpression status in 85 formalin-fixed paraffin-embedded SMARCB1-deficient tumor specimens (extra-central nervous system MRT, 27 cases; AT/RT, 12 cases; proximal-type ES, 20 cases; conventional-type ES, 26 cases) was examined. Immunoreactivity was graded semiquantitatively as follows: 0, no staining; 1+, <5% of tumor cells reactive; 2+, 5–25% of tumor cells reactive; 3+, 26–50% of tumor cells reactive; and 4+, >50% of tumor cells of reactive.

Results: Brachyury expression was observed in 3 of 27 (11%) extra-central nervous system MRTs, 7 of 12 (58%) AT/RTs, 1 of 20 (5%) proximal-type ESs and 0 of 26 (0%) conventional-type ESs. Brachyury immunoreactivity was found significantly more frequently in AT/RT than in extra-central nervous system MRT (P = .004). There was no statistically significant difference between the prognosis of MRT with brachyury expression group and that without brachyury expression group (P = .47).

Conclusions: Seven of the 12 cases of AT/RT show brachyury immunoexpression, whereas almost all the other SMARCB1-deficient tumors cases are negative for brachyury. Our findings support that poorly differentiated chordoma with SMARCB1-deficiency cases may be part of the spectrum of the AT/RT entity.

79 Fibroma-like PEComas: A Tuberous Sclerosis Complex Related Lesion

Ana Larque Daza[1], *Richard Kradin*[2], *Ivan Chebib*[3], *G. Petur Nielsen*[4], *Martin Selig*[5], *Anat Stemmer-Rachamimov*[4], *Elizabeth Thiele*[2], *Miriam A Bredella*[2], *Paweł Kurzawa*[6], *Vikram Deshpande*[4]. [1]Dorchester, MA, [2]Massachusetts General Hospital, [3]Massachusetts General Hospital and Harvard Medical School, Boston, MA, [4]Massachusetts General Hospital, Boston, MA, [5]Medford, MA, [6]Poznan University of Medical Sciences

Background: Perivascular epithelioid tumor (PEComa), mesenchymal tumors morphologically characterized by epithelioid cells, co-express melanocytic and muscle markers. Herein, we describe a heretofore-undescribed tuberous sclerosis complex (TSC)-related neoplasm morphologically resembling a soft tissue fibroma-like lesion but showing an immunophenotypic resembling PEComa.

Design: We identified three soft tissue fibroma-like lesions in individuals with TSC. We also evaluated 6 TSC- related periungual fibromas as well as a range of non-TSC fibroma-like lesions (n=19). Immunohistochemistry for HMB45, desmin, smooth muscle actin, TFE3 and S100 was performed on the TSC-related fibromas. Periungual fibromas and non-TSC fibroma-like lesions were also stained for HMB45.

Results: All 3 TSC patients were female, ranging in age from 4 to 51 years (mean 26.7). Two tumors were located in extremities and the other one on the chest. On histologic examination, the tumors showed elongated to stellate spindle shape cells, lacked mitotic activity and cytologic atypia, and prominent collagenous background. Immunohistochemically, all 3 tumors were positive for HMB45; SMA or desmin was positive in both tumors tested. TFE3 was negative. All patients are alive with no evidence of disease with median follow-up of 55 months (range 6-131). Non-TSC fibroma-like lesion and periungual fibromas were negative for HMB45.

Conclusions: Fibroma-like PEComa, a newly recognized soft tissue tumor with a strong association with TSC, mimics soft tissue fibroma but shows reactivity with melanocytic markers.

80 NanoString Technology Validation of the Complexity Index in SARComas (CINSARC) Prognostic Signature on Formalin-Fixed, Paraffin-Embedded (FFPE) Soft Tissue Sarcomas

Sophie Le Guellec[1], *Tom Lesluyes*[2], *Emeline Sarot*[3], *Carine Valle*[4], *Philippe Rochaix*[5], *Gaëlle Pérot*[6], *Jean-Michel Coindre*[7], *Frédéric Chibon*[6]. [1]Institut Claudius Regaud, Toulouse, Midi-Pyrrn, France, [2]Inserm U1218, Institut Bergonié, Bordeaux, [3]Inserm-U1037, Institut Claudius Regaud/CRCT, Toulouse, France, [4]Inserm-U1037, CRCT, Toulouse, France, [5]Institut Claudius Regaud, IUCTO, Toulouse, France, [6]Inserm U1218, Institut Bergonié, Bordeaux, France, [7]Institut Bergonie, Bordeaux, France

Background: Prediction of metastatic outcome in soft tissue sarcomas is an important clinical challenge since these tumors can be very aggressive (up to 50% of recurring events). A gene expression signature (composed of 67 genes), Complexity INdex in SARComas (CINSARC), has been identified as a better prognostic factor as compared to the current international grading system defined by the Fédération Nationale des Centres de Lutte Contre le Cancer. Since CINSARC has been established on frozen tumors analyzed by microarrays and next generation sequencing (NGS), we were interested in evaluating its prognostic capacity using NanoString technology on formalin-fixed, paraffin-embedded (FFPE) blocks to better fit laboratory practices.

Design: To compare the performance of RNA-seq and NanoString technology, we used expressions (from both technologies) of various sarcomas (n=127, frozen samples) and compared predictive values based on CINSARC risk groups and clinical annotations from the Conticabase (European sarcoma database). We also performed Nanostring technology on FFPE blocks (n=48) and matching frozen and FFPE samples (RNA-seq technology) to compare the level of agreement between these two material supports. Metastatic-free survivals and agreement values in classification groups were evaluated.

Results: CINSARC remains a strong predictive factor for metastatic outcome in both RNA-seq and NanoString technologies on frozen samples ($P < 0.05$; Figure 1), with similar risk-group classifications (92%). We also measured similar (risk-group) classifications with frozen tumors (RNA-seq) compared to FFPE (NanoString) blocks (88% agreement), while more than 50% of the same samples (FFPE blocks) were not analyzable by RNA-seq technology due to poor RNA quality consecutively to their degradation.

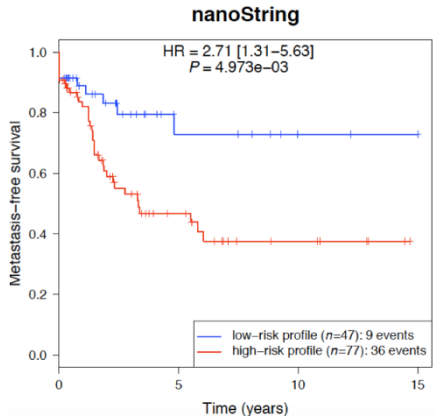

Conclusions: CINSARC is a platform and material independent prognostic signature for metastatic outcome in various sarcomas. Since Nanostring technology (unlike RNA-seq) is not influenced by the poor quality of RNA extracted from FFPE blocks, this result opens access to metastatic prediction sarcomas through Nanostring technology on FFPE tumors via the CINSARC signature. Application of the signature will permit more selective use of adjuvant therapies for patients with sarcomas.

81 Detection of Fusion Genes in Formalin-Fixed Paraffin-Embedded Phosphaturic Mesenchymal Tumors by Anchored Multiplex PCR-Based RNA Sequencing

Jen-Chieh Lee[1], *Andrew Folpe*[2], *Cheng-Han Lee*[3] [1]National Taiwan University Hospital, Taipei City, [2]Mayo Clinic, Rochester, MN, [3]British Columbia Cancer Agency, Vancouver, British Columbia

Background: Phosphaturic mesenchymal tumors (PMT) are uncommon tumors that cause hypophosphatemia/osteomalacia by secreting phosphatonins such as FGF23. We have identified *FN1-FGFR1* **or** *FN1-FGF1* fusion genes in about half of PMT, suggesting roles of the FGF1-FGFR1 axis and fibronectin-extracellular matrix interaction in the pathogenesis of PMT. Tumorigenic drivers are unknown for remaining cases where neither fusion gene was detected, including most bone tumors where FISH failed because of decalcification-induced DNA degradation. Recently, anchored multiplex PCR (AMP)-based NGS techniques (AMP-NGS) have proved efficient in identifying novel fusion partners using FFPE RNA. The goals of this study were to 1) determine the utility of AMP-NGS in fusion detection in decalcified FFPE RNA and 2) identify alternative fusions in PMT involving FN1 and/or cognate genes in the FGFR and FGF families.

Design: FFPE samples of 23 PMT (1997-2016) were collected, including 8 with *FN1-FGFR1* fusion shown by FISH (Group A), 2 with FN1-FGF1 fusion (Group B), 5 with neither fusion (Group C), and 8 with unknown fusion status (Group D, mostly decalcified bone tumors where FISH analysis had failed). RNA was subjected to an AMP-NGS platform (ArcherDx) using custom primers to target and enrich genes encoding FN1, FGF1-23, and FGFR1-4.

Results: The actually sequenced RNA read numbers ranged from 4K to 1,171K (median 807K). 3 cases had < 220K reads (arbitrary quality threshold) and were considered to have significantly worse RNA quality, including the 2 oldest specimens (19 and 17 years old, respectively) and 2 Group D bone tumors. Group D as a whole had significantly lower RNA reads vs. the other groups ($P = .005$). The sample age negatively correlated with RNA reads ($r = -0.68$; $P < .001$). In 6 of the 8 Group A and both Group B cases, the results of AMP-NGS were consistent with FISH and/or RNA-sequencing data. One case had a novel FGFR1 exon 9 breakpoint, confirmed by genomic DNA sequencing. The 2 specimens with discrepant inter-platform results either were old or had a borderline FISH result. No fusion genes were detected in Group C or D, except for 1 Group D bone tumor found to harbor FN1-FGF1.

Conclusions: AMP-NGS may succeed in decalcified specimens and may prove valuable complements to other molecular diagnostic tools. However, the utility of this technique is compromised by prior tissue decalcification. PMT without identifiable fusions probably harbor driver mutations other than fusions involving FN1, FGFR, or FGF genes.

82 High P16 Expression Is Associated with Malignancy and Shorter Disease-Free Survival in Solitary Fibrous Tumor / Hemangiopericytoma

Yuanxin Liang[1], *Robert Heller*[2], *Knarik Arkun*[2]. [1]Boston, MA, [2]Tufts Medical Center

Background: Solitary fibrous tumor (SFT) /hemangiopericytoma (HPC) is considered to belong in the spectrum of fibroblastic mesenchymal tumor with NAB2-STAT6 fusion. This fusion/driver mutation is known to constitutively activate EGR 1. It is reported that p16 overexpression results from the activation of the transcription factor EGR1 in the malignant transformation of skin cells. Overexpression of p16 is associated with malignancy and worse prognosis in multiple mesenchymal tumors. Therefore we investigated p16 expression and its clinical significance in SFT/HPC tumors.

Design: Twenty-six SFT/HPC tumors (14 in central nervous system, 12 in other sites) diagnosed at Tufts Medical Center from 2002-2016 were assigned into 3 grades. Data from microarray immunohistochemistry for STAT6, Synaptophysin, EGR1 and p16, grade and survival was analyzed.

Results: Overexpression of p16 (immunopositivity ≥50% tumor cells) is associated with malignancy (Grade 3) tumors (Figure 1A-C), and has a sensitivity of 70% (7/10) and a specificity of 81% (13/16) as a predictive marker for malignancy. SFT/HPC patients with low p16 expression demonstrated significantly longer disease-free survival time (median survival >113 months) than those with high p16 expression (median survival = 30 months, p= 0.0449) (Figure 1D). Interestingly, EGR1 protein is not detected by double immunohistochemistry in p16 positive tumor cells (Figure 2A), despite of the presence of STAT-6.

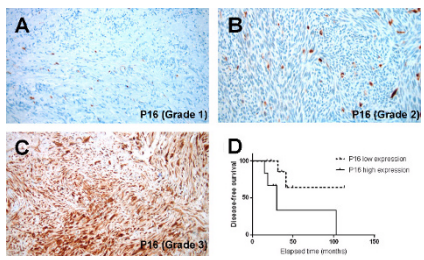

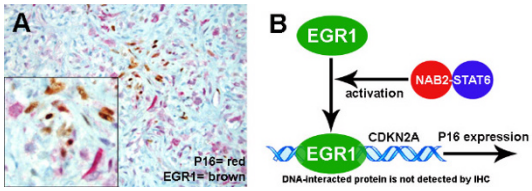

Conclusions: SFT/HPCs in central nervous system are more likely to be malignant and to express neuroendocrine marker than the tumors in other sites. High p16 expression is associated with malignancy and shorter disease-free survival time in SFT/HPC tumors in our study cohort. We propose a novel model of p16 overexpression (Figure 2B). Clinically, p16 overexpression can be used as predictive marker for malignancy and possibly could be a therapeutic target.

83 Loss of Expression of a Novel Chromatin Remodeler SMARCA1 in Soft Tissue Sarcoma

Pallavi A Patil[1], *Kara A Lombardol*[2], *Ashlee Sturtevant*[3], *Shamlal Mangray*[1], *Evgeny Yakirevich*[1] [1]Brown University Lifespan Academic Medical Center, Providence, RI, [2]Rhode Island Hospital, Providence, RI, [3]Brown University

Background: Chromatin remodelling complexes are involved in the regulation of vital cellular processes such as proliferation and differentiation. Genomic alterations (GAs) and loss of immunohistochemical (IHC) expression of chromatin remodelers ARID1A (BAF250A), SMARCA2 (BRM), SMARCA4 (BRG1), and SMARCB1 (INI1) have been described in a variety of neoplasms and tend to be associated with specific morphologies. The role of SMARCA1 (SNF2L), another member of the chromatin remodelers, in neoplasia is largely unknown. As *SMARCA1* is located on chromosome X, it may be a "risky" gene that may be potentially inactivated by a single hit. The aim of this study was to evaluate GAs and protein expression of SMARCA1 in soft tissue tumors.

Design: We queried the publically available cBioPortal.32e34 platform to analyze data from The Cancer Genome Atlas project (TCGA) related to *SMARCA1* GAs in soft tissue tumors. Twenty-six cases of soft tissue tumors were retrieved from our institutional archives including 10 undifferentiated sarcomas, 5 leiomyosarcomas, 6 liposarcomas, and 5 malignant peripheral sheath tumors (MPNST). Paraffin embedded whole tissue sections were analyzed for IHC expression of SMARCA1 with an SNF 2C4 monoclonal antibody. Normal testis tissue was used as a positive control.

Results: Analysis of TCGA dataset revealed *SMARCA1* GAs in eight of 261 soft tissue sarcomas (3%). The most common *SMARCA1* GAs were in 6 of 99 leiomyosarcomas (3 cases with deletions, 1 with missense mutation, and 2 with amplifications). One of 56 dedifferentiated liposarcomas and 1 of 48 undifferentiated sarcomas had SMARCA1 deletions. No *SMARCA1* GAs were identified in other sarcoma subtypes. The sarcoma subtypes with potential *SMARCA1* alterations were further analyzed for SMARCA1 IHC expression in cases selected from our archives. SMARCA1 nuclear expression was lost in 3 of 10 cases (30%) of undifferentiated sarcoma (Figure1) [Figure 1], and 2 of 5 cases of MPNST (40%). SMARCA1 expression was intact in all cases of leiomyosarcoma (Figure 2) [Figure 2], dedifferentiated, pleomorphic, and myxoid liposarcoma.

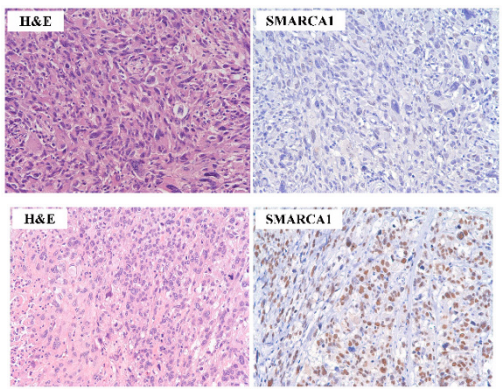

Conclusions: This study shows for the first time that expression of SMARCA1 may be lost in subtypes of soft tissue sarcomas, including undifferentiated sarcoma. The role of SMARCA1 in the differentiation process and molecular mechanisms of SMARCA1 inactivation merit further investigation.

84 Histone H3K36M Mutation and Trimethylation Patterns in Chondroblastoma

Chuanyong Lu[1], *Meera Hameed*[2], *Daniel Ramirez*[3]. [1]Memorial Sloan Kettering Cancer Center, New York, NY, [2]Memorial Sloan-Kettering CC, New York, NY, [3]Jersey City, NJ

Background: Histones are important protein components of chromatin and their mutations and methylation play an important role in tumorigenesis. Recent studies have shown that chondroblastomas harbor histone H3 lysine 36 to methionine mutation (H3K36M), and is associated with increased H3K27 methylation and decreased H3K36 methylation. The goal of this study is to determine the presence of H3K36M mutation and to correlate H3K36M mutation status with methylation status of H3K27 and H3K36 in a series of chondroblastoma cases.

Design: Thirty-two patients treated at our institution with a pathological diagnosis of chondroblastoma during the period from 2000 to 2013 were included in this study. H&E staining and immunohistochemical stains using antibodies for H3K36M, H3K27me3 and H3K36me3, and osteoblastic marker (SATB2) were performed. The results were reviewed by two pathologists, and scored as positive (diffuse or focal), heterogeneous and negative. Medical records were reviewed for the patients' age, gender, site of involvement, treatment, follow-up, and recurrence of tumor.

Results: Patients include 23 males and 9 females with ages ranging from 5 to 52 years (median 20 years). The locations of tumors include acromion (2), femur (8), fibula (1), humerus (8), ischium (2), scapula (1), spine and ribs (1), talus (5), and tibia (4). All tumors were treated by curettage. The patients were followed for 1 to 129 months after surgery (median 25.5 months) and 2 had local recurrence. 21 cases showed classic morphology of chondroblastoma and 20 of them (95%) were positive for H3K36M mutation. The other 11 cases exhibited additional histologic features including prominent aneurysmal bone cyst-like changes, myxoid changes, hyaline cartilage, or giant cell tumor-like areas. Only 6 of these 11 tumors (55%) showed positivity for H3K36M mutation. Methylation status as determined by H3K27me3 and H3K36me3 revealed heterogeneous staining pattern in both mutation positive and negative tumors. SATB2, a marker for osteoblastic differentiation was positive in the chondroblasts of 23 out of 31 tumors (75%), including both mutation positive and negative cases.

Conclusions: Our results confirm the presence of H3K36M mutation in a vast majority of chondroblastomas with typical morphology. H3K36M mutation does not abrogate H3K36me3 methylation status, however the expression of H3K27me3 and H3K36me3 are heterogeneous in these tumors and may reflect aberrant methylation patterns. SATB2 is positive in a subset of chondroblastomas.

85 Dedifferentiated/Well-Differentiated Liposarcoma with DDIT3 Amplification: a Distinct Subtype or Morphological Variant?

Jose Mantilla[1], *Robert Ricciott*[2], *Eleanor Chen*[1], *Yajuan Liu*[1], *Benjamin Hoch*[3]. [1]University of Washington, Seattle, WA, [2] Seattle, WA, [3]Seattle, WA

Background: Dedifferentiated liposarcoma (DDLS) is defined as progression of atypical lipomatous tumor/well-differentiated liposarcoma (ALT) to a higher grade usually non-lipogenic sarcoma with amplification of 12q13-15. Prognostic factors include site, FNCLCC grade 3 features and high amplification of *MDM2, CDK4* and *JUN*. *DDIT3* may be amplified in ALT and DDLS and is rearranged in myxoid/round cell liposarcoma (M/RCLS). *DDIT3* is necessary for adipogenesis and can induce a liposarcoma phenotype in vitro. Its overexpression along with *MDM2* and *CDK4* may contribute to the pathogenesis of DDLS and ALT by interfering with adipocytic differentiation. DDLS/ALT with *DDIT3* amplification has not been well characterized.

Design: We reviewed 47 cases of DDLS and 2 cases of ALT with co-amplification of *MDM2* and *DDIT3* by FISH. For all DDLS genomic DNA isolated from tissue blocks was evaluated for gene amplifications of multiple loci including *CDK4* (12q14.1), *MDM2* (12q15), and *DDIT3* (12q13.3) by array CGH. Slides were evaluated for distinct morphological features including features of M/RCLS and grade. Clinical follow-up for each case was reviewed including death of disease (DOD), distant metastasis (DM) and local recurrence (LR).

Results: Of 47 cases of DDLS, 15 (33%) had amplification of *DDIT3* (≥6 copies/cell). Of these, 8 (53%) had LR, and 6 (40%) DOD. None had DM. Of the 32 (67%) cases without *DDIT3* amplification, 13 had LRs (41%), 7 DOD (22%), and 2 (6%) had DM. There was no difference in recurrence-free survival, age, grade, or number of copies of *MDM2* and *CDK4*. *DDIT3* amplified DDLS more commonly had M/RCLS-like morphology, classic lipoblasts in low and higher grade components, and lipoma-

like ALT areas. Both cases of ALT with DDIT3 amplification had low grade M/RCLS-like features and one developed bone metastases with identical morphology.

Conclusions: DDIT3 amplified DDLS commonly has M/RCLS-like morphology and lipoblastic differentiation indicative of a role in morphogenesis and demonstrates a tendency for local recurrence and poorer survival. ALT with M/RCLS-like features and DDIT3 amplification can have metastatic behavior. Additional study is necessary to fully understand the significance of DDIT3 amplification in DDLS and ALT.

86 Diagnostic Utility of AMACR (P504S) Immunohistochemistry in Distinguishing Myxofibrosarcoma from Other Sarcoma Types

Jose Mantilla[1], *Anshu Bandhlish*[2], *Yajuan Liu*[1], *Robert Ricciotti*[3], *Benjamin Hoch*[4], *Eleanor Chen*[1]. [1]University of Washington, Seattle, WA, [2]Washington, DC, [3]Seattle, WA, [4]Seattle, WA

Background: Alpha Methyl Acyl Coenzyme A Racemase (AMACR) immunohistochemistry (IHC) is useful in prostate carcinoma diagnosis and is expressed in colorectal, gastric, renal and other carcinomas. AMACR expression has not been widely studied in sarcomas. *AMACR* gene amplification was recently described in a large subset of myxofibrosarcoma (MFS). MFS is one of the more aggressive types of soft tissue sarcoma and can have a wide morphologic differential diagnosis. In this study we evaluate the diagnostic utility of AMACR IHC in MFS compared to other similar-appearing sarcomas.

Design: After institutional review board approval we reviewed 32 cases of MFS, 21 leiomyosarcomas (LMS), 6 low grade fibromyxoid sarcomas (LGFMS), 12 myxoid/round cell liposarcomas (M/RCLS) and 10 synovial sarcomas (SS). AMACR IHC was performed on select slides from all cases. Four pathologists independently scored the extent and intensity of staining using a 1+ to 3+ system. Final consensus scores for all sarcoma types were compared and used to correlate with tumor grade. Chi square test was used to determine statistical significance. Genomic DNA isolated from tissue blocks in selected cases of LMS that strongly expressed AMACR were evaluated for gene amplification (5p13.2) by aCGH.

Results: IHC staining for AMACR was present in 30/32 MFS (94%), 11/21 LMS (48%), 1/12 M/RCLS (8%), 0/8 LGFMS and 1/10 SS (10%). By histologic grade, AMACR was positive in 10/11 (90%) high grade (HG) MFS, 16/16 (100%) intermediate grade (IG) MFS, and 4/5 (60%) low grade (LG) MFS. There was no correlation between grade, clinical outcomes, and extent/intensity of staining. [Table]. Of the other sarcoma types, AMACR positivity correlated with grade (HG vs. IG-LG) in LMS, with positivity in 8/10 (72%) HG-LMS, 1/4 (33%) IG-LMS and 2/7 (22%) LG-LMS ($p < 0.01$). 4/4 cases of HG LMS with AMACR expression had low level gains in 5p13.2 by aCGH.

	n	NEG	1+	2+	3+
MFS-HG	11	1 (9%)	1 (9%)	4 (36%)	5 (45%)
MFS-IG	16	0	9 (56%)	4 (25%)	3 (19%)
MFS-LG	5	1 (20%)	1 (20%)	1 (20%)	2 (40%)
LMS-HG	10	3 (30%)	2 (20%)	3 (30%)	2 (20%)
LMS-IG	4	3 (75%)	1 (25%)	0	0
LMS-LG	7	5 (71%)	1 (14%)	0	1 (14%)
SS	10	9 (90%)	1 (10%)	0	0
LGFMS	6	6 (100%)	0	0	0
M/RCLS	12	13 (92%)	0	0	1 (8%)

Conclusions: In our study, AMACR immunoreactivity is seen in a majority of MFS and a portion of LMS, while few cases of other sarcomas showed significant expression. AMACR is a useful marker in the diagnosis of MFS, with 94% sensitivity, 76% specificity, and positive and negative predictive values of 71% and 95%, respectively. Since a high percentage of high-grade LMS also expresses AMACR, AMACR IHC should not be used in isolation; concurrent use of other stains, especially smooth muscle markers, is necessary to exclude LMS in cases with overlapping morphology.

87 Histiocyte-rich Rhabdomyosarcoma (RMS): A Potentially Deceptive Variant

Anthony Martinez[1], *Karen Fritchie*[2], *Andrew Folpe*[2]. [1]Mayo Clinic, Decatur, GA, [2]Mayo Clinic, Rochester, MN

Background: Current classification of RMS includes embryonal, alveolar, pleomorphic and spindle cell/ sclerosing subtypes. Some RMS may not show overt rhabdomyoblastic differentiation (e.g., solid alveolar RMS, sclerosing RMS), requiring ancillary immunohistochemical (IHC) studies for diagnosis, but the malignant nature of these lesions is usually readily apparent. Over the past several years, we have seen in consultation a small number of very unusual rhabdomyosarcomas, characterized by a very striking proliferation of non-neoplastic histiocytes, largely obscuring the underlying neoplasm.

Design: Archives were searched from 1990-present for cases of embryonal or spindle cell/sclerosing RMS in which the pathology report specifically mentioned the presence of large number of histiocytes. Previously treated tumors were excluded. All available routinely stained slides and IHC studies (desmin, myogenin, MyoD1, CD163) for cases meeting these criteria were re-reviewed. Clinical information and any follow up was obtained.

Results: 4 cases were identified in 3M and 1F, ranging from 26-69 years of age (median 54 yrs) and involving the left buttock, left knee, abdominal wall, and thoracic wall. Only 1 of 4 cases was considered by the initial pathologist to possibly represent RMS. Microscopically, the lesions consisted of infiltrative, sheet-like to nodular masses dominated by variably lipidized histiocytes and multinucleated giant cells, some of Touton-type. Close inspection revealed a variable number of cytologically atypical, mitotically active spindled cells, in one case showing overt rhabdomyoblastic differentiation in the form of strap cells with cross striations. By IHC, the spindled cells in all cases were strongly positive for desmin and more variably MyoD1-positive. Myogenin expression was limited in extent, typically confined to scattered tumor cells. CD163 was diffusely positive in histiocytes. Preliminary follow-up has shown 2 patients alive without disease following surgery and adjuvant radiotherapy.

Conclusions: We report an unusual variant of RMS, characterized by a dense, obscuring histiocytic infiltrate. Awareness of this potentially confusing histology in conjunction with appropriate use of ancillary studies should allow for recognition and correct therapy of these rare tumors. Histiocyte-rich RMS most likely represents a variant of spindle cell/sclerosing RMS, based on age and soft tissue location and age of occurrence, although genetic study will be necessary to confirm.

88 Osteochondromyxoma of Bone: A Clinicopathologic, Radiologic, and PRKAR1A Immunohistochemical Analysis of 12 cases

Anthony Martinez[1], *Doris Wenger*[2], *Kemal Kosemehmetoglu*[3], *Karen Fritchie*[2], *Carrie Inwards*[2]. [1]Mayo Clinic, Decatur, GA, [2]Mayo Clinic, Rochester, MN, [3]Hacettepe Universitesi, Ankara

Background: OCM is defined by the WHO as a rare chondroid and osteoid matrix producing tumor with extensive myxoid change originally described in 2001 by Carney *et al* in a series of 4 patients (pts) with/suspected of having Carney Complex (CNC). No cases have subsequently been added to the literature. *PRKAR1A* mutations are found in pts with CNC and loss of PRKAR1A by IHC has been shown to be a useful screen for CNC in cardiac myxoma pts. We expand the original series to include 8 additional pts in order to better define the clinical, radiologic and histologic features of OCM, and explore the utility of PRKAR1A IHC in the diagnosis of OCM.

Design: 12 cases of OCM were retrieved from our institutional archives. The clinical history, radiologic studies and histologic slides were evaluated, and IHC for PRKAR1A was performed.

Results: There were 6M and 6F. Age ranged from 8 days to 32 years (mean 9y; median 6y). 10/12 cases involved the nasal cavity and 2/12 involved the long bones (tibia, radius). CNC was diagnosed in 7/12 pts and 4 had CNC manifestations (11/12 total suspected/confirmed CNC cases).

Radiologically, all 12 tumors showed features suggestive of an indolent growth pattern. They were expansile, lytic, or mixed lytic and sclerotic masses with varying degrees of internal matrix and myxoid change.

Histologically, all OCM had a permeative growth pattern with entrapment of host bone and contained uniform, bland, stellate-shaped cells set in chondromyxoid background arranged in lobules and sheets. A variable amount of dense hyalinized eosinophilic matrix, often within the center of lobules, was present. 2 tumors were more cellular and contained enlarged round nuclei. All cases showed loss of PRKAR1A by IHC.

Of 11 pts treated surgically, 1 was lost to follow-up and 3 developed local recurrence. One (radius) spontaneously regressed after biopsy only. Follow-up information after surgical removal was available on

10 pts (mean 61m; median 33m). 9/10 pts are alive without disease. None had metastases. 1 died from an obstructed airway due to tumor.

Conclusions: OCM most commonly occurs in the nasal cavity of pediatric pts. Imaging shows indolent features. Despite a microscopic permeative growth and tendency for local recurrence, no pts developed metastases. Recognizing the distinct histologic and radiologic appearance will help avoid misdiagnosis as osteosarcoma or chondrosarcoma. OCMs show loss of PRKAR1A by IHC and should prompt further investigation for underlying CNC.

89 Angiosarcomas (AS) Showing Prominent Lymphoid Infiltration: A Potentially More Favorable Subgroup?

Anthony Martinez[1], *Sharon Weiss*[2], *Mark Edgar*[3], *Mauricio Zapata*[4], *Andrew Folpe*[5]. [1]Mayo Clinic, Decatur, GA, [2]Emory University Hospital, Atlanta, GA, [3]Atlanta, GA, [4]Northside Hospital, Atlanta, GA, [5]Mayo Clinic, Rochester, MN

Background: Most AS arise secondary to sun damage and show capillary endothelial differentiation. Although AS can arise in association with lymphatic abnormalities or express lymphatic markers, they are no longer subdivided into lymphangiosarcomas and hemangiosarcomas because the distinction often can't be reliably made and they share a similar poor prognosis. We have noted a distinctive subset of AS, showing some morphological features suggestive of lymphatic differentiation, such as "hobnail" endothelial cells, typically diffuse D240 expression, a striking lymphocytic reaction, and anecdotally behaving in an indolent fashion. We aim to better characterize this group of AS and determine if they should be distinguished from their more conventional counterparts.

Design: 21 cases coded as "AS," or "atypical hobnail hemangioendothelioma" with the above features were retrieved from our institutional/consultation from 1990-2017. Clinicopathologic features were analyzed and follow up was obtained.

Results: Tumors occurred in 12M and 9F (age range 32-95 yrs; median 65 yrs), involved the head/neck (N=11), trunk (N=5), lower extremity (N=4), upper extremity (N=1), and ranged from 0.8-8.5 cm (mean 3 cm). A history of lymphedema/lymphatic abnormality was noted in 4 cases; 2 arose in pre-existing post-radiation atypical vascular lesions and were not cMYC amplified. All were superficial lesions with a well-defined deep border. They showed areas of vasoformation, characterized by a branching network of irregularly anastomosing vascular lined by monomorphic, darkly staining "hobnail" endothelial cells with more solid and spindled areas, showing greater nuclear atypia and frequent mitoses. Necrosis was absent. All had a prominent lymphoid reaction, sometimes largely confined to the lumen of vascular channels. They were positive for CD31 (16/16) CD34 (9/15) and D240 (15/17). Follow-up (12 cases, 4-131 mo, median 43 mo) showed 9 patients alive without disease, 1 with disease, 1 dead of disease, and 1 dead of other causes. Local recurrences and lymph node metastases occurred in 7 and 2 patients, respectively. The patient who died from disease refused all adjuvant treatment and had presumed metastases.

Conclusions: We identified a group of AS, characterized by morphological and immunohistochemical features suggestive of lymphatic endothelial differentiation, a prominent host lymphocytic reaction, and relatively indolent clinical behavior which, we believe, warrant separation from conventional AS.

90 A Sub-population of Adamantinomas And Osteofibrous Dysplasia-Like Adamantinomas Show Loss of INI1

Reena Merard[1], *Lars-Gunnar Kindblom*[2], *VP SUMATHI*[3]. [1]The Royal Orthopaedic Hospital, Birmingham, United Kingdom, West Midlands, West Midlands, [2]The Royal Orthopaedic Hospital, Birmingham, United Kingdom, [3]Royal Orthopaedic Hospital, Birmingham

Background: INI1/SMARCB1 is a core subunit of the chromatin remodelling complex which are thought to act as tumour suppressors. SMARCB1/INI1 can be readily identified by immunohistochemistry. Loss of INI1 is observed in some soft tissue and CNS tumours. Immunohistochemistry for INI1 is therefore diagnostically helpful in these tumours. There is limited literature on INI1 expression in bone tumours. A recent study of INI1 expression in cytokeratin positive bone tumours shows that loss of INI1 expression occurs rarely in such bone tumours. We have observed a loss of INI1 in a few adamantinomas diagnosed in our department, prompting this study on the INI1 expression in adamantinomas and osteofibrous dysplasia-like (OFD-like) adamantinomas.

Design: All cases of adamantinomas and OFD-like adamantinomas diagnosed in our department during the last 7 years were included in the study. INI1 immunostain was done on selected tumor blocks. Depending on the staining pattern, the cases were categorized into three groups: INI1 retained, INI1 lost and focal faint positive staining.

Results: A total of 26 cases were studied, of which 9 were adamantinomas and 16 were OFD-like adamantinomas. 6 cases (23%) showed loss of INI1, while in 10 (38.5%) INI1 was retained and 10 cases (38.5%) showed focal faint staining for INI1. Of the 6 cases with loss of INI1, 4 were OFD-like adamantinomas and 2 were adamantinomas.

Out of the 26 cases, 6 were recently diagnosed cases and hence follow up information was not available. In the remaining 20 cases, only one, an OFD-like adamantinoma with loss of INI1, developed local recurrence after 2 years and none metastasized

Conclusions: A subpopulation of adamantinomas and OFD-like adamantinomas showed loss of INI1, possibly somewhat more common in OFD-like adamantinoma. Any prognostic significance of INI1 loss remains to be clarified.

91 Subcutaneous Atypical Fatty Tumors with P53 Overexpression, RB1 Gene Abnormalities and a Lack of MDM2 Gene Amplification. Expanding the Morphologic Spectrum of "Anisometric Cell Lipoma (ACL)"

Michael Michal[1], *Abbas Agaimy*[2], *Marian Svajdler*[3], *Dmitry Kazakov*[4], *Petr Steiner*[5], *Petr Grossmann*[6], *Ladislav Hadravsky*[7], *Kvetoslava Michalova*[8], *Peter Svajdler*[9], *Michal Michal*[10], *John F Fetsch*[11]. [1]Charles University, Prague, Czech Republic, [2]Friedrich-Alexander University Erlangen-Nuremberg, Erlangen, Bavaria, [3]Biopticka laborator s.r.o, Plzen, [4]Bioptical Laboratory SVO, Pilsen, Czech Republic, [5]Charles University in Prague, Bioptical Laboratory, Ltd, Pilsen, Czech Republic, [6]Bioptical Laboratory, Pilsen, Czech Republic, [7]Charles University in Prague, Czech Republic, Prague, [8]Biopticka laborator, Plzen, Czech Republic, [9]University hospital of PJ Safarik in Kosice, Kosice, SK, [10]Bioptical Laboratory s.r.o., Plzen, [11]The Joint Pathology Center, Silver Spring, MD

Background: ACL is a recently proposed tumor that shows variation in adipocytic size, patchy fat necrosis, scant stromal matrix, and only mild nuclear atypia. We have repeatedly encountered tumors of this type with more prominent atypia, invariably submitted to us as atypical lipomatous tumors for consultation. Moreover, we have noted significant p53 expression in all cases, which is a rare event in all other differential diagnostic entities.

Design: 20 cases were evaluated by two pathologists for the extent of atypia and graded on the scale from 1 to 3. Immunohistochemistry for p53, MDM2 and Retinoblastoma-1 (Rb1) protein was performed. Cases were tested for *MDM2* amplification, *RB1* deletion using FISH and for *TP53* mutation by Sanger sequencing.

Results: Patients were 18 men and 2 women, aged 34-74 yrs (mean:56 yrs). All tumors occurred in the subcutis of the upper back and neck. No recurrences were noted at follow-up of 14 patients (1-16yrs, mean:4.8 yrs). 15 cases exhibited mild atypia, 4 were moderately atypical and 1 case showed prominent atypia. All 20 cases exhibited strong expression of p53 in a subset of adipocytes with one or more atypical nuclei (~10%). 7/20 cases weakly expressed MDM2 in less than 1% of cells. Rb1 was consistently deficient in most cells. MDM2 FISH was negative in all analyzable cases (12) including the most atypical ones. Homozygous or heterozygous *RB1* deletion was present in all 4 analyzable cases. All 5 tested cases showed no *TP53* mutation.

Conclusions: Our study significantly expands the morphological spectrum of ACL, and suggests this tumor is best viewed as a special, biologically benign but atypical, fatty neoplasm that has a predilection for the subcutis of the neck and back region and features adipocytes with: 1) notable size variation and varying degrees of nuclear atypia, 2) no surrounding spindle cell stroma, 3) p53 overexpression, 4) absence of *MDM2* gene amplification by FISH and 5) *RB1* gene deletions. The mechanism behind p53 expression and the relationship to spindle cell/pleomorphic lipoma remains to be further explored.

92 Tenosynovitis with Psammomatous Calcifications (TPC): A Clinicopathologic Study of 23 Cases

Michael Michal[1], *Abbas Agaimy*[2], *Andrew Folpe*[3], *Iva Zambo*[4], *Radek Kebrle*[5], *Zdenek Kinkor*[6], *Marian Svajdler*[7], *Tomas Vanecek*[8], *Filip Heidenreich*[9], *Dmitry Kazakov*[10], *Kvetoslava Michalova*[11], *Ladislav Hadravsky*[12], *Michal Michal*[13]. [1]Charles University, Prague, Czech Republic, [2]Friedrich-Alexander University Erlangen-Nuremberg, Erlangen, Bavaria, [3]Mayo Clinic, Rochester, MN, [4]Masaryk University and St. Anne's University Hospital, Brno, Czech Republic, [5]Vysoke nad Jizerou, Czech Republic, [6]Biopticka Laborator, Plzen, CZE, [7]Biopticka laborator s.r.o, PPlzen, [8]Bioptical Laboratory, Pilsen, Czech Republic, [9]Charles University, Prague, Czech Republic, [10]Bioptical Laboratory

SVO, Pilsen, CZE, [11]Biopticka laborator, Plzen, Czech Republic, [12]Charles University in Prague, Czech Republic, [13]Bioptical Laboratory s.r.o., Plzen

Background: The term "idiopathic calcifying tenosynovitis" (ICT) refers to a clinically and radiologically defined syndrome of pain and tendinous calcification, most often involving the shoulder joint. A distinctive subset of ICT cases, termed "TPC", occurs in the distal extremities and shows characteristic morphology, in particular psammomatous calcifications. Some cases of TPC have been reported as examples of "tumoral calcinosis of distal extremity type", although abnormalities in calcium and/or phosphate metabolism have not been noted. To date, only 10 cases of TPC have been reported, and it remains poorly recognized by both pathologists and clinicians.

Design: 23 well-characterized cases of TPC from four institutions along with all available radiological and clinical information, including follow-up, were collected. Slides were reviewed and a subset of cases was immunostained for CD68. One case was subjected to clonality analysis using X-chromosomal inactivation pattern and HUMARA locus.

Results: Cases occurred in 21F, 1M and 1 patient of unknown gender (mean 41 years of age, range 16-75 years), and almost exclusively involved the fingers and toes, except for one case in the elbow and one in the knee joint. The masses ranged from 2 to 30 mm (mean 10mm). Pain was the most common presenting symptom (11/16 patients). A history of trauma or repetitive activity was present in 6 of 12 patients; none were known to have disorders in calcium or phosphate metabolism. Radiographic studies showed a non-specific, calcified mass. Typical morphological features of TPC were invariably present, with degenerating tendinous tissue containing a variable number of psammomatous calcifications, surrounded by a moderately cellular, CD68-positive histiocyte-rich host reaction (Fig). HUMARA assay in one case showed polyclonality. Clinical follow-up (19 patients; mean 5.2 years; range 1-14 years) showed no local recurrences.

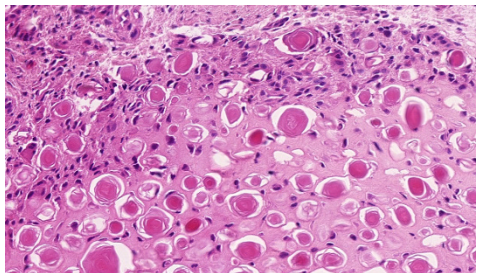

Conclusions: Our study confirms the striking predilection of TPC for the fingers and toes of young to middle-aged women. TPC should be rigorously distinguished from other forms of ICT, which typically involve large, proximal joints and show simply dystrophic calcification involving tendinous tissues, and from tumoral calcinosis, which also involves large joints and often is associated with calcium and/or phosphate abnormalities. TPC appears to be related to trauma and/or repetitive activity and is cured with simple excision.

93 Clinicopathologic and Prognostic Features of Radiation-Associated Sarcomas: A Single Institution Study of 188 Cases

Jeffrey Mito[1], *Devarati Mitra*[2], *Constance M Barysauskas*[3], *Christopher D Fletcher*[1], *Chandrajit P Raut*[2], *Elizabeth H Baldini*[2], *Leona A Doyle*[4]. [1]Brigham and Women's Hospital, Boston, MA, [2]Brigham and Women's Hospital, [3]Dana Farber Cancer Institute, [4]Brigham and Women's Hospital, Brookline, MA

Background: Although rare, radiation-associated sarcomas (RAS) are a significant consequence of radiation therapy, and may arise months to decades following radiation. Previous studies have shown that these tumors have a poor prognosis, but little is known about the clinicopathologic features of RAS that are associated with outcomes.

Design: Patients with RAS diagnosed from 1994-2016 attending our institutional multidisciplinary sarcoma clinic were identified. Patients with <3 months of available follow up were excluded, resulting in a cohort of 188 patients. All available histologic material was reviewed and confirmatory immunostains were performed when appropriate; pathology reports and clinical notes were reviewed for clinical demographics, history and follow-up data.

Results: The median patient age was 62 yrs (27-85 yrs), and most were female (78.2%). RAS arose with a median latency of 10 yrs (1-61 yrs). Common sites of RAS were breast/chest wall (57%), pelvis (13%), head and neck (11%) and extremities (10%). The most common histologic subtypes of RAS were unclassified sarcoma (75/188; 40%) and angiosarcoma (73/188; 39%), followed by leiomyosarcoma (18/188; 9.6%), malignant peripheral nerve sheath tumor (11/188; 5.9%), and osteosarcoma (5/188; 2.7%). Among patients presenting with localized disease, the 5-yr OS was 68% and in contrast to prior studies, excluding radiation-associated breast angiosarcoma (RABA), histologic subtype of RAS was not found to have a significant impact on patient outcome. Patients with RABA tended to be younger (57 vs 71 years, p<0.001), had a shorter latency to develop their RAS (7 vs 14.3 years, p<0.001), and were less likely to develop distant metastases compared to other RAS types (p=0.001). Irrespective of sarcoma subtype, most patients presented with localized disease (176/188) and underwent attempted definitive resection (155/188). Of those with localized disease, tumors were predominantly high grade (77.2%), which was associated with worse event free (p=0.01) and overall survival (p<0.001). Among the patients who underwent surgery, intra-abdominal or -thoracic locations (p=0.01) and positive margin status (p<0.001) were associated with worse overall survival.

Conclusions: With the exception of radiation-associated breast angiosarcoma, histologic subtyping had no association with outcomes in our cohort. Tumor locations allowing definitive resection with negative margins and lower tumor grade were strong predictors of better patient outcomes.

94 MYC Expression and Loss of Histone H3K27 Trimethylation are Infrequent Among Unclassified Radiation-Associated Sarcomas

Jeffrey Mito[1], *Vickie Y Jo*[2], *Leona A Doyle*[3]. [1]Brigham and Women's Hospital, Boston, MA, [2]Brigham & Women's Hospital, Boston, MA, [3]Brigham and Women's Hospital, Brookline, MA

Background: Recent advances in understanding the pathogenesis of radiation-associated sarcomas (RAS) have identified several recurrent molecular alterations including *MYC* amplification, most notably in radiation-associated breast angiosarcoma, and recurrent mutations in *EED* or *SUZ12*, which encode subunits of the polycomb repressive complex 2 (PRC2), in radiation-associated malignant peripheral nerve sheath tumors (MPNST). Mutations in PRC2 lead to loss of histone H3 K27 trimethylation (H3K27me3), a repressive epigenetic mark associated with gene silencing. Previous studies have shown immunohistochemistry (IHC) for MYC and H3K27me3 to be reliable surrogate markers for their respective genetic alterations. We investigate the potential diagnostic utility and prevalence of expression of these markers in a cohort of non-angiosarcoma RAS (NARAS).

Design: Seventy-one cases of NARAS diagnosed between 2001 and 2016 with material available for additional immunohistochemical studies were identified including: 63 undifferentiated pleomorphic sarcoma/unclassified spindle cell sarcomas, 4 leiomyosarcomas, and 4 MPNST. IHC for MYC and H3K27me3 was performed on whole tissue sections. The presence and extent of nuclear expression (MYC) and loss (H3K27me3, in the presence of positive internal control) were scored semi-quantitatively.

Results: Among NARAS, expression of MYC (5/62, 8%) and complete loss of H3K27me3 (7/71, 10%) were infrequent events. The 5 MYC positive cases included 3 unclassfied spindle cell sarcomas with multifocal expression (6-40% of cells) and 2 unclassified spindle cell sarcomas with focal staining (1-5% of cells), all of moderate intensity. The 7 cases with complete loss of H3K27me3 included 3 MPNST and 4 unclassified spindle cell sarcomas that lacked morphologic or immunohistochemical features of MPNST. No case showed concomitant H3K27me3 loss with MYC expression.

Conclusions: 1. Despite the presence of *MYC* amplification in a significant subset of NARAS, corresponding MYC protein expression is infrequent, and when present is usually limited in extent and intensity. MYC expression outside the setting of radiation-associated breast angiosarcoma is therefore of limited utility in the evaluation of NARAS. 2. Although helpful in confirming a diagnosis of radiation-associated MPNST in the context of suggestive morphologic or immunophenotypic features, complete loss of H3K27me3 occasionally occurs in unclassified RAS; loss of expression is therefore not specific to radiation-associated MPNST.

95 Inflammatory Pseudotumors Arising in Metal-on-Metal Versus Metal-on-Polyethylene Hip Replacements Demonstrate a Similar Lymphocytic Response Based on Immune Profiling

Nissreen Mohammad[1], *Felipe Eltit*[2], *Donald Garbuz*, *Clive Duncan*[3], *Bassam Masri*, *Nelson Greidanus*[3], *Manju Sharma*[4], *Rizhi Wang*[5], *Michael Cox*[6], *Tony Ng*[7]. [1]University of British Columbia, Vancouver, BC, Canada, [2]Centre for Hip Health and Mobility and University of British

Columbia, Vancouver, BC, Canada, [3]University of British Columbia, Vancouver, BC, Canada, [4]Vancouver Prostate Centre, Vancouver, BC, Canada, [5]Centre for Hip Health and Mobility and University of British Columbia, Vancouver, BC, Canada, [6]Vancouver Prostate Centre and University of British Columbia, Vancouver, BC, Canada, [7]Vancouver General Hospital and University of British Columbia, Vancouver, BC, Canada

Background: Inflammatory pseudotumors secondary to adverse local tissue reactions (ALTR) are the main cause of implant failure of hip replacements due the uncontrolled inflammatory reaction to metal-on-metal (MoM) and metal-on-polyethylene (MoP) articulations. Due to the higher prevalence of ALTRs in MoM systems and differences in the histological description of ALTRs in MoM and MoP, it has been proposed that differences could exist in the immune profiles associated with implant type in ALTRs.

Design: We reviewed the histopathologic findings of eighteen cases of failed hip replacement secondary to ALTR (nine MoM and nine MoP). We then characterized immune reactions in ALTR through the quantification of cytokines in the synovial fluid of patients, and RNA expression analysis of aseptic lymphocytic vasculitis-associated lesion (ALVAL) aggregates using a NanoString-based immune profiling assay.

Results: Histologically, all cases showed inflammatory pseudotumor scored using the criteria of aseptic lymphocytic vasculitis-associated lesion (ALVAL Score). MoM cases differed from MoP by having more prominent and extensive perivascular lymphoid aggregates, while MoP cases were characterized by extensive necrosis with associated garland-like histiocytic reaction. We found a distinctive pattern of cytokines in the synovial fluid of the patients with ALTRs, characterized by the elevated concentration of pro-inflammatory chemokines as well as dual-function cytokines. Some of these chemokines and cytokines, especially the monocyte chemoattractants, were highly concentrated in the synovial fluid of the patients. The gene expression of the T cells in the perivascular aggregates of the lesions showed a high expression of inflammatory cytokines and chemokines, but no differences were found between the MoM and MoP ALTRs. Ingenuity pathway analysis found highly significant association with leucocyte adhesion and diapedesis, and Th1 and Th2 activation pathways, but not Th17.

Conclusions: The similar gene expression found in the lymphocyte aggregates, suggests a similar etiology and pathogenesis for MoM and MoP hip replacements, regardless of the differences in histologic findings, metal ion concentrations and wear particles found in these two types of implants.

96 Characterization of IDH1/IDH2 Mutation and D-2-Hydroxyglutarate Oncometabolite Level in Dedifferentiated Chondrosarcoma

Nissreen Mohammad[1], *Amy Lum*[2], *Jonah Lin*[3], *Derek Wong*[3], *Julie Ho*[4], *Cheng-Han Lee*[5], *Tony Ng*[6], *Stephen Yip*[7]. [1]University of British Columbia, Vancouver, BC, Canada, [2]British Columbia Cancer Research Centre, Vancouver, BC, Canada, [3]British Columbia Cancer Research Centre, Vancouver, BC, Canada, [4]Vancouver General Hospital, [5]British Columbia Cancer Agency, Vancouver, British Columbia, [6]Vancouver General Hospital and University of British Columbia, Vancouver, BC, Canada, [7]University of British Columbia and Vancouver General Hospital, Vancouver, BC, Canada

Background: Dedifferentiated chondrosarcoma (DDCHS) is an aggressive type of chondrosarcomas, and results from high-grade transformation of a low-grade chondrosarcoma. Isocitrate dehydrogenase 1 (*IDH1*) and *IDH2* mutations have been recently described in low-grade cartilaginous neoplasms. These mutations lead to increased D-2-hydroxyglutarate (2HG) oncometabolite production, promoting tumorigenesis through CpG island and histone hypermethylation. Our aim is to determine the frequency of *IDH1/2* mutations in DDCHS and correlate it with 2HG levels.

Design: We examined a series of 21 resection specimens of primary DDCHS using Sanger sequencing and qPCR genotyping to interrogate for *IDH1/2* mutations, and using a fluorimetric assay to evaluate the level of 2HG in formalin-fixed paraffin-embedded (FFPE) tumor and matched normal tissue samples.

Results: Seventy-six percent of DDCHS (16/21) harbored either *IDH1* or *IDH2* mutations, with R132L (3/16), R132H (2/16), R132S (3/16), R132C (1/16) and R132G (1/16) in *IDH1*, and R172S (4/16) and R172M (2/16) in *IDH2*. *IDH1/2*-mutated DDCHS showed elevated 2HG in the tumor relative to matched normal tissue, with 2HG level being highest in tumors with *IDH2* R172S mutation, whereas DDCHS with wild-type *IDH1/2* showed no elevation in 2HG level. There were no consistent histologic differences between *IDH1/2*-mutated tumors and wild-type tumors. The mean age of patients with *IDH1/2*-mutated DDCHS was 65.7 years. Amongst these 16 mutation-positive patients, follow-up data was available for 14 patients, with an average follow-up period of 11 months. 11 of 14 patients (78%) died from their disease, most within a year of diagnosis, while 2 patients were alive with recurrent disease.

Conclusions: Our study confirms the frequent presence of *IDH1/2* mutations in DDCHS, which is seen in about three-quarter of the cases. A broad range of *IDH1/2* mutation variants is seen, indicating that a sequencing-based approach to mutation analysis is required for DDCHS if it is to be used as a diagnostic marker. As seen in other *IDH1/2*-mutated tumor types (i.e. glioma and acute myeloid leukemia), *IDH1/2*-mutated DDCHS also shows elevated 2HG level, indicating that it may depend at least in part on the oncometabolite activity for its oncogenesis.

97 PREVIOUSLY PUBLISHED

98 Co-Gain of the MDM2 Gene and Chromosome 12 Centromere and MDM2 Protein Expression in Spindle Cell Lipoma: a Potential Diagnostic Pitfall

Toru Motoi[1], *Masumi Ogawa*[2], *Ikuma Kato*[3], *Fumie Kakizaki*[1], *Rin Yamada*[2], *Akiko Tonooka*[2], *Shinichiro Horiguchi*[2], *Tomotake Okuma*[4], *Akihiko Yoshida*[5], *Takahiro Goto*[2], *Tsunekazu Hishima*[2]. [1]Tokyo Metropolitan Cancer and Infectious Diseases Center Komagome Hospital, Bunkyo-ku, Tokyo, [2]Tokyo Metropolitan Cancer and Infectious Diseases Center Komagome Hospital, [3]Tokyo Metropolitan Cancer and Infectious Diseases Center Komagome Hospital, Tokyo, Japan, [4]Tokyo Metropolitan Cancer and Infectious Diseases Center Komagome Hospital, Tokyo, [5]Chuo-ku, Tokyo, Japan

Background: Spindle cell/pleomorphic lipoma (SL) is a benign lipogenic tumor whose differentiation from atypical lipomatous tumor (ALT) can be challenging. The *MDM2* gene amplification and the resultant MDM2 protein overexpression are key diagnostic features of ALT, which are routinely used to separate ALT from SL. However, because cytogenetic and protein status of MDM2 in SL has been poorly studied, the accuracy of MDM2 testing for this distinction remains to be determined. We therefore explored them in SL.

Design: Formalin-fixed paraffin embedded samples of 34 SLs were subjected to immunohistochemistry using MDM2 antibody. Six fibrolipomas (FLs) were used as references. The immunostaining was judged as positive when definite nuclear staining of MDM2 was present in more than 10 spindle and/or pleomorphic cells per 50HPF. The *MDM2* gene status was examined by chromogenic in situ hybridization (CISH) using dual-color *MDM2* and chromosome 12 centromere (CEN12) probes. Co-gain was defined as positive when ≥10% of nuclei of spindle and/or pleomorphic cells contained ≥3 copies of both MDM2 and CEN12 signals with a ratio of <2.0 by counting 100 nuclei. Then the mean copy number of *MDM2* gene was calculated.

Results: Co-gain of the *MDM2* gene and CEN12 was observed in 8/32 (25%) of SLs successfully tested, while all FLs were negative. The mean copy number of *MDM2* gene was low (3.1-4.8) and all SLs lacked selective *MDM2* gene amplification or aggregated *MDM2* signals. An average of 32% of SL tumor cells (range, 10-55%) demonstrated the co-gain, and it was more frequently found in pleomorphic cells. On the other hand, MDM2 immunoexpression was positive in 5/34 (15%) of SLs, whereas it was negative in all FLs. In MDM2-positive cases, the number of immunoreactive cells was 10-89 (mean, 43) per 50HPF. Staining intensity was weaker than what is typically seen in ALT. MDM2 expression was significantly more common in co-gain-positive SLs (3/8; 38%) than co-gain-negative SLs (2/24; 9%) ($p<0.05$).

Conclusions: Although the nuclear staining intensity was generally weaker than that in ALT and incidence of the co-gain was lower than a previous report (Weaver et al., 2008), abnormal MDM2 status that is uncommonly found in SL may potentially cause diagnostic problems. Although whether the co-gain indicates true polysomy 12 remains unclear, this abnormality may characterize SL in part, in addition to 13q14 deletion. Low-level of copy number gain may be a cause of limited MDM2 expression in SL.

99 Immunohistochemical analysis of mismatch repair deficiency in 188 sarcomas

Nya D Nelson[1], *Hongxing Gui*[2], *John Brooks*[3], *Paul J Zhang*[4]. [1]Hospital of the University of Pennsylvania, Philadelphia, PA, [2]Pennsylvania Hospital, Philadelphia, PA, [3]Pennsylvania Hospital of UPHS, Philadelphia, PA, [4]Hospital of the University of Pennsylvania, Media, PA

Background: The identification of mismatch repair deficient (dMMR) tumors has become even more critical with the recent FDA approval of pembrolizumab for the treatment of unresectable or metastatic

dMMR solid tumors. For many cancers, most notably colorectal and endometrial adenocarcinoma, the incidence of sporadic dMMR has been well established. dMMR and MSI (microsatellite instability) have been reported in a small number of sarcomas but large scale analyses of dMMR have been lacking. We present a large scale analysis of mismatch repair protein expression in sarcomas on TMA material.

Design: TMA sections containing 188 various sarcomas each represented by 1 mm triplet cores were stained with antibodies to MLH1 (Biocare G168-15), PMS2 (BD Biosciences A16-4), MSH2 (Biocare FE11), and MSH6 (Biocare BC/44). Immunohistochemical staining was scored as present, or absent for each core. Complete loss of nuclear staining in all three cores for any given tumor was required for staining to be considered truly absent.

Results: Staining was present in all positive controls. The data is summarized below in table 1.

		dMMR			
Diagnosis	Re-tained	Isolat-ed PMS2 loss	PMS2 and MLH1 loss	MSH6 and/or MSH2 loss	PMS2, MLH1, MSH2, and MSH6 loss
Angiosarcoma (n=13)	69%	31%	0%	0%	0%
Epithelioid sarcoma (n=5)	80%	20%	0%	0%	0%
Rhabdomyosarcoma (n=5)	80%	0%	20%	0%	0%
Leiomyosarcoma (n=27)	82%	11%	7%	0%	0%
Myxoid liposarcoma (n=8)	87%	0%	13%	0%	0%
Malignant SFT (n=10)	90%	0%	10%	0%	0%
Well differentiated liposarcoma (n=12)	92%	8%	0%	0%	0%
Epithelioid hemangioendo-thelioma (n=4)	50%	0%	0%	0%	50%
Dedifferentiated liposarcoma (n=28), MPNST (n=19), giant cell tumor of tendon sheath (n=15), IMT (n=11), synovial sarcoma (n=7), fibrosarcoma (n=6), low grade fibromyxoid sarcoma (n=5), desmoplastic small round cell (n=4), EWS (n=3), kaposi sarcoma (n=2), pleomorphic liposarcoma (n=2), clear cell sarcoma (n=1), alveolar soft parts sarcoma (n=1)	100%	0%	0%	0%	0%

Conclusions: Overall, 16 of 188 sarcomas (8.5%) displayed dMMR with most of the dMMR tumors showing absence of PMS2 and/or MLH1. Angiosarcoma had the highest incidence of dMMR (31%), followed by epithelioid sarcoma (20%), rhabdomyosarcoma (20%), and leiomyosarcoma (18%). Interestingly, loss of all 4 MMR proteins was seen in 2 of 4 epithelioid hemangioendotheliomas (50%), another malignant endothelial tumor, which could be due to concurrent loss of MLH1 and MSH2, or possibly an artifact. No isolated or concurrent loss of MSH2 and MSH6 was seen. dMMR was not restricted to high grade tumors and was also detected in low grade tumors such as well differentiated liposarcoma and myxoid liposarcoma. The biologic significance of the preference of dMMR in sarcomas is unknown. While further genetic and MSI studies are needed, these results provide an argument for routine testing for dMMR in patients with unresectable or metastatic sarcoma to identify patients who are candidates for pembrolizumab treatment. In particular, MMR testing should be considered in those tumors with a high prevalence of dMMR, such as angiosarcoma and leiomyosarcoma.

100 INI1 Expression in Neurofibromas and Malignant Peripheral Nerve Sheath Tumors Reveals "Mosaic" Pattern in a Subset of Cases

Gauri Panse[1], *Davis Ingram*[2], *Ghadah Al Sannaa*[3], *Khalida Wani*[2], *Alexander Lazar*[4], *Wei-Lien Billy Wang*[5]. [1]Yale School of Medicine, New Haven, CT, [2]M D Anderson Cancer Center, [3]Houston Methodist, [4]M. D. Anderson Cancer Center, Houston, TX, [5]UT MD Anderson Cancer Ctr, Houston, TX

Background: Integrase interactor 1 (INI1, also known as SMARCB1/BAF47/hSNF5) is a tumor suppressor gene that encodes a subunit of the SWI/SNF chromatin remodeling complex encoded at chromosomal position 22q11.2. Complete loss of INI1 expression is observed in multiple tumor types including a subset of nerve sheath tumors such as epithelioid schwannoma and epithelioid malignant peripheral nerve sheath tumor (MPNST). Additionally, "mosaic" or partial loss of INI1 has been reported in schwannomatosis, ossifying fibromyxoid tumors and gastrointestinal stromal tumors secondary to chromosome 22q abnormalities in these neoplasms. Given that losses at chromosome 22q are also observed in both neurofibromas and MPNSTs, we evaluated INI1 labeling in a large cohort of these tumors, hypothesizing that INI1 expression might also be altered in a subset of tumors.

Design: Forty-nine cases of neurofibroma (45 from patients with neurofibromatosis 1 [NF1] and 4 sporadic) and 89 cases of conventional/non-epithelioid MPNST (59 NF1-associated and 30 sporadic) from a clinically annotated tissue microarray were evaluated for percentage of nuclear INI1 expression within the tumor cells in the presence of positive internal control.

Results: Twenty-three (47%) neurofibromas had a mosaic / partial loss of INI1 (INI1 lost in 20-80% of tumor cells) while INI1 labeling was retained (≥90% tumoral labeling) in the remaining cases. Of the 89 MPNST cases, 14 (15.8%) showed mosaic / partial loss of INI1 and 75 (84.2%) had retained INI1 expression. Mosaic /partial loss of INI1 was more frequent in neurofibromas than in MPNSTs (p=0.0002). Mosaic expression of INI1 did not correlate with factors such as site, prognosis and sporadic or NF1 associated disease. Complete loss of INI1 expression was not observed in any of the cases.

Conclusions: A subset of neurofibromas and MPNSTs show mosaic pattern of INI1 expression, suggesting heterogeneous and subclonal chromosomal 22q abnormalities in these tumors. Mosaic INI1 was more frequent in neurofibromas than in MPNSTs in our series.

101 Evaluation of H3.3 G34W expression in denosumab-treated giant cell tumor of bone and histologic mimics

Vatsal Patel[1], *John D Reith*[2], *Bonnie Balzer*[3], *Earl W Brien*[4], *Wonwoo Shon*[5]. [1]Mayo Clinic, Rochester, MN, [2]Cleveland Clinic, Cleveland, OH, [3]Cedars-Sinai Medical Center, Los Angeles, CA, [4]Cedars-Sinai Medical Center, [5]Cedars-Sinai Medical Center, Studio City, CA

Background: The receptor activator of NF-KB ligand (RANKL) pathway has been shown to play a key role in the pathogenesis of giant cell tumor of bone (GCTB). Denosumab, a human monoclonal antibody acting as a RANKL inhibitor, offers a new treatment option for a subset of patients with previously unresectable tumors. Denosumab-treated GCTBs exhibit significant post-treatment histologic alterations, mimicking other primary benign and malignant bone lesions. Recently, *H3.3 G34W* mutations and protein overexpression were documented in GCTBs. The purpose of this study was to evaluate H3.3 G34W immunoreactivity in a series of denosumab-treated GCTBs and other bone tumors commonly considered in the differential diagnosis.

Design: Formalin-fixed, paraffin-embedded whole tissue sections of bone tumors were evaluated: 9 denosumab-treated GCTBs (from 6 patients), 10 non-treated GCTBs, 13 osteosarcomas (5 conventional, 5 low-grade central, and 3 giant cell-rich), 8 chondroblastomas, 8 nonossifying fibroma, 6 aneurysmal bone cysts, 5 giant cell reparative granulomas, 3 fibrous dysplasia, 3 brown tumors, and 2 osteoblastomas. Immunohistochemical analysis for H3.3 G34W (clone RM263; RevMAb Biosciences, San Francisco, CA) was performed with an automated system (Ventana BenchMark XT, Ventana Medical Systems Inc., Tucson, AZ), according to the manufacturer's instructions.

Results: Denosumab-treated GCTBs were predominantly composed of ovoid to spindled mononuclear cells with various degrees of collagen/osteoid matrix deposition and stromal fibrosis. There was a marked decrease in the number of giant cells. Two cases also showed areas of peculiar purple lace-like mineralization. By immunohistochemistry, diffuse strong nuclear staining for H3.3 G34W was present in 18/19 GCTBs, including all 9 denosumab-treated tumors. Of note, one negative GCTB case was decalcified. All the other evaluated tumor types were completely negative for H3.3 G34W.

Conclusions: H3.3 G34W immunohistochemistry is a highly sensitive and specific diagnostic marker for denosumab-treated GCTB. The presence of persistent H3.3 G34W-positive cells in post-treatment tumors further reinforces the notion that denosumab therapy simply inhibits the resorptive activity of the tumor cells instead of eliminating them.

102 New Potential Immunohistochemical Markers to Help Discriminating Between Different Steps of Malignant Transformation from Plexiform Neurofibromas (PNFs) to Malignant Peripheral Nerve Sheath Tumors (MPNSTs)

Irma Ramos-Oliver[1], *Carolina P Montecino*[2], *Gabriela Bernal*[3], *Eduard Serra*[4], *Meritxell Carrió*[5], *Ernest Terribas*[6], *Teresaq Moliné*[3], *Santiago Ramon y Cajal*[7], *Cleofe Romagosa*[8]. [1]H.U.Vall d'Hebron, Barcelona, [2]Vall d' Hebron University Hospital, Barcelona, [3]Vall d'Hebron

University Hospital, [4]Institute for Health Science Research Germans Trias i Pujol (IGTP)-CIBERONC, Badalona, Barcelona, [5]Institute for Health Science Research Germans Trias i Pujol (IGTP), [6]Institute for Health Science Research Germans Trias i Pujol (IGTP), Badalona, Barcelona, [7]Hospital Universitari Vall d'Hebron, Barcelona, [8]Hospital Vall d'Hebron, Barcelona, Spain

Background: Neurofibromatosis Type 1 (NF1) is a genetic disease characterized by the development of multiple neurofibromas (NFs). A subgroup of them, plexiform neurofibromas (PNFs), can progress into malignant peripheral nerve sheath tumors (MPNSTs). A new nomenclature for NF1-associated nerve sheath tumors has been recently proposed and the term "atypical neurofibromatous neoplasms of uncertain biologic potential" (ANNUBPs) has been proposed for lesions that are considered at higher (but uncertain) risk of malignization compared to cellular neurofibromas (CNFs) and neurofibromas with atypia (NFAs). ANNUBPs exhibit 2 or more of the following morphological criteria: cytological atypia, loss of NF architecture, hypercellularity and mitotic index >1/50 HPF but <3/10HPF. In this study we compared current and previous classifications and we also tried to find immunohistochemical markers to help discriminating between the different steps of tumor progression, using current (p16, S100, H3K27me and ki67) and potential (KIF15) markers.

Design: Clinical-pathological characteristics of 62 nerve sheath tumors were evaluated. Tissue microarrays were developed including three samples of each lesion type. Immunohistochemistry (IHC) for p16, S100, H3K27ME3(H3), KI67 and KIF15 was performed.

Results: Sixty-two lesions were reclassified according to the new nomenclature as: 9 PNFs, 3 CNFs (before 2 PNFS/ 1 ANF), 10 NFA (before 7 NF/ 3 ANF), 19 ANNUBP (before 1 NF/ 16 ANFs / 2 MPNSTs-LG) and 21 MPNSTs (before 20 MPNSTs / 1 ANF), (17/21 NF1 associated). NFs, CNFs and NFAs were grouped together as benign NFs.

Significant differences in the cytoplasmic KIF15 staining between benign NFs and ANNUBPs; and in p16, S100, H3, Ki67 and nuclear KIF 15 between ANNUBP and MPNST were observed. Cytoplasmic KIF15 staining was associated to a premalignant or malignant lesion (p= 0,001), whereas a purely nuclear staining indicated a benign lesion (p=0,029). The lack of expression of p16 (p=0,019), H3 (p=0,029) and S100 (p=0,004) supported the diagnosis of malignancy.

Conclusions: Although the current histological classification of NF1-associated tumors provides more objective criteria than the previous one and has helped to classify these tumors, some of the criteria, such as cell density and atypia, continue to imply a degree of subjectivity. In case of doubt, IHC may be helpful in discriminating between benign, premalignant, or malignant lesions.

103 Primary Epithelioid Vascular Tumors Of Bone: A Monocentric Retrospective Analysis Of 129 Patients

Alberto Righi[1], *Marco Gambarotti*[2], *Marta Sbaraglia*[3], *Daniel Vanel*[1], *Piero Picci*[1], *Angelo Dei Tos*[4]. [1]Rizzoli Institute, Bologna, Italy, [2]Bologna, [3]Ospedale Regionale di Treviso, Treviso, [4]Hospital of Treviso, Treviso, Italy

Background: Recently, several important refinements in the classification of epithelioid vascular tumors of bone have occurred.

Design: To further investigate the clinical relevance of a refined classification of epithelioid vascular tumor of bone, we reviewed all primary bone vascular tumors treated at our institutions. Based on morphology cases were assessed immunohistochemically (FOS-B, CAMTA1 and TFE3) and molecularly (*WWTR1-CAMTA1* gene fusion *FOSB-SERPINEB* by RT-PCR, and *CAMTA1, FOS* and *TFE3* gene rearrangements by FISH).

Results: One hundred and twenty-nine cases of primary epithelioid vascular tumor of bone (32 epithelioid hemangioma [EH], 24 pseudomyogenic hemangioendothelioma [PMEHE], 26 epithelioid hemangioendothelioma [EHE] and 45 epithelioid angiosarcoma [EAS]) with long-term follow-up were retrieved. Five EH, treated with curettage, recurred with a mean of 76 months after the first diagnosis. At the last follow-up (mean 111 months), 3 patients were alive with local disease and 29 patients were alive without disease. Among 24 PMEHE 3 recurred locally following curettage. At the last follow-up (mean 121 months), 3 patients died of other cause, 5 are alive with disease and the remaining 16 patients were alive without disease. Among 26 patients with EHE a patient developed local recurrences one month after the surgical curettage and, at the last follow-up (mean 98 months), 5 patients died of disease with a mean of 78 months after the first diagnosis, 6 patients were alive with local disease without distant metastases, 2 patients died of other reasons and the remaining 13 patients were alive without disease. Thirty-two out of 45 patients with EAS died of disease with a mean of 12 months from diagnosis; 3 patients died of other diseases; 5 patients were alive with multicentric disease and 6 patients were disease-free at last follow-up (mean 112 months). Log-rank test analysis showed significant statistical differences in terms of DFS and OS between EH and EHE (p=0.004 for DFS and p=0.001 for OS) and between EHE and EAS (p<0.001 both for DFS and for OS). PMEHE appears to overlap clinically more with EH than with EHE.

Conclusions: The integration of morphology, immunohistochemical and molecular features allows better stratification of primary epithelioid vascular tumors of bone. EH, EHE and EAS all exhibit statistically significant differences in clinical behavior. PMEHE further emerges as an indolent multifocal disease.

104 Novel t(5;15)(p15;q21) Resulting in CLPTM1L-FBN1 Fusion in Two Cases of High Grade Sarcoma with Similar Histology, IHC Findings and Demographics

Aaron P Rupp[1], *Jin Wu*[2], *Erika L Garbrecht*[3], *Scott Ness*[4], *Kathryn J Brayer*[4], *Cory Broehm*[5], *Therese J Bocklage*[6]. [1]University of New Mexico, Albuquerque, NM, [2]UNM SOM, [3]UNMH, Albuquerque, NM, [4]UNM SOM, [5]Albuquerque, NM, [6]University of Kentucky College of Medicine, Lexington, KY

Background: Half of mesenchymal tumors show fusion translocations. With molecular genetic techniques, new fusions are detected regularly. We report a new fusion translocation in two patients with a distinctive high grade sarcoma and identify the gene partners.

Design: A histologically unusual sarcoma was assessed by IHC and karyotyping. Distinctive features prompted a search of the institution's tumor database, and a second case with similar histology was found with the same chromosomal fusion, t(5;15)(p15;q21). RNA-Seq analysis was subsequently performed using FFPE tumor tissue. cDNA was synthesized using the Clontech SMARTer Universal Low Input RNA kit for Sequencing from ribosomally depleted, purified total RNA. Libraries were barcoded and amplified using the Ion Total RNA-Seq Kit v2 and sequenced using the Ion Proton s5xl platform. Sequence reads were mapped to the human genome (hg19) by STAR alignment, and translocations were detected by visual inspection using IGV (Broad Institute).

Results: Two females aged 79 (Case 1) and 62 years (Case 2), presented with growing soft tissue masses in the knee and gluteal region, respectively. Both tumors involved superficial soft tissue; Case 1 also involved deep soft tissue. Both tumors comprised cellular, storiforming aggregates of plump spindled cells with nuclear pleomorphism, prominent inflammation and an HPC to lattice-like pattern of small vessels. On IHC staining, tumor cells showed partial loss of Rb1 and no expression of: SMA, desmin, S-100 protein, calponin, keratins, CD34, CD31, STAT6, or HMB45. By karyotyping, both tumors shared a t(5;15)(p15;q21) translocation and also showed additional, non-shared complex changes. RNA-Seq data analysis showed both translocations resulted in similar fusion products of *FBN1* (15q21) and *CLPTM1L* (5p15). Patient 1 died of widespread metastatic disease <1 year after diagnosis. Patient 2 presented with lung metastases and is alive (F/U of 7 months).

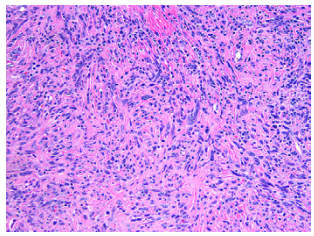

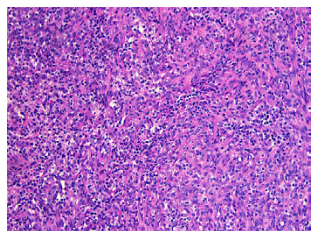

Conclusions: We report the first two cases of a novel fusion, t(5;15)(p15;q21); *CLPTM1L- FBN1* in two cases of a histologically distinctive and behaviorally aggressive sarcoma. Mutations, translocations or altered expression levels of the genes involved in this novel fusion (FBN1 and *CLPTM1L*) have recently been implicated in carcinogenesis and progression in malignancies including B-cell lymphomas, prostate and colorectal carcinoma and GIST. Work is ongoing to evaluate specifics of this fusion, its potential oncogenic effects and relationship to known sarcoma types.

105 Inflammatory myofibroblastic tumors and leiomyosarcomas: a clash between morphological and molecular diagnosis

Wesley Samore[1], *Jochen Lennerz*[2], *Vikram Deshpande*[3]. [1]Boston, MA, [2]Massachusetts General Hospital and Harvard Medical, Boston, MA, [3]Massachusetts General Hospital, Boston, MA

Background: Leiomyosarcomas (LMS) and inflammatory myofibroblastic tumors (IMT) have broad morphological spectrums that sometimes overlap. However, histologically classic LMSs are traditionally thought to be negative for the ALK-1 or ROS1 rearrangements that have come to define IMTs. In this study, we demonstrate that a histologically classic low-grade LMS harbored an ALK-1 rearrangement to a previously undescribed fusion partner ACTG2 (actin gamma 2, smooth muscle). Following the discovery of this case, we examined 42 additional LMSs for ALK-1 and ROS1 by immunohistochemistry (IHC). In addition, we searched for ALK-1 translocations in the LMS series within The Cancer Genome Atlas (TCGA).

Design: A tissue microarray of 42 LMSs was generated. The tissue microarrays slides were stained by IHC for antibodies against ALK-1 and ROS1. On our index case, fluorescence-in-situ-hybridization (FISH) of paraffin tumor tissue was performed using a break-apart probe to the ALK gene. Anchored Multiplex PCR was used for targeted fusion transcript detection via next generation sequencing (ArcherDx FusionPlex Solid Tumor Kit primers). Using TCGA data, a search for ALK-1 and ROS1 related translocations was conducted in 105 leiomyosarcomas.

Results: All 42 LMSs tested on the microarray were negative for both ALK-1 and ROS1 by IHC. Our index case of a LMS demonstrated positive staining for ALK-1 by IHC and was positive for rearrangement by FISH (ALK x 2)(5'ALK sep 3'ALK x 1) [9/50]). With our translocation assay, a novel fusion transcript was identified involving ACTG2 (Exon2) and ALK (Exon18). Upon further investigation of the clinical data, the patient with the ALK-1-ACTG2 fusion had been previously diagnosed with a leiomyoma in a morcellated uterus specimen. Workup of the uterine tumor demonstrated positive ALK-1 IHC staining and the identical ALK-ACTG2 fusion transcript. A review of the TCGA series revealed a single LMS (1 of 105) with an ALK-ACTG2 fusion. Both our index case and the case in the TCGA series showed characteristic morphologic and immunohistochemical features of a LMS.

Conclusions: While further studies are needed, our series demonstrates that ALK-1 translocations rarely occur in LMSs. Intriguingly, this subset of LMS had the same fusion partner to the ACTG2, a protein highly expressed in smooth muscle tissues. Although uncommon, ALK-1 translocations warrant attention, particularly given the availability of targeted therapy with tyrosine kinase inhibitors.

106 Nicotinamide Phosphoribosyl Transferase is Increased in Osteosarcomas and Chondrosarcomas Compared to Benign Bone and Cartilage

Rodney Shackelford[1], *YASIR ALZUBAIDI*[2], *Jehan Abdulsattar*[3], *Junaid Ansari*[4]. [1]LSU Health Shreveport, Shreveport, LA, [2]LSU Health, Shreveport, LA, [3]LSUHSC, Shreveport, LA, [4]LSU Health Shreveport

Background: Osteosarcomas (OS) are rare malignancies of bone that occur predominately in young adults. Chondrosarcomas (CS) are rare heterogenous cartilaginous soft tissue neoplasms that can occur at many anatomic sites. Both OS and CS have different histologic subtypes and CSs are often graded into well-differentiated, intermediate, and high-grade CS. Nicotinamide phosphoribosyl transferase (Nampt) catalyses the rate limiting step of NAD^+ synthesis. Nampt expression is increased in several different tumor types and serves as a measure of overall cellular NAD^+ consumption and metabolic activity. In several malignancies increased Nampt expression correlates with tumor clinical aggressiveness. The expression of Nampt has not been examined in OS or CS. Here we looked at Nampt expression in osteoblastic OS (OOS), telangiectatic OS (TOS), and different grades of CS and compared these to benign bone and catilage Nampt levels.

Design: We used tissue microarray technology to examine Nampt immunohistochemical intensity expression in 25 cases of benign bone, 7 cases of benign cartilage, 52 cases of OOS, 8 cases of TOS, and 43, 10, and 6 cases of well-differentiated, intermediate, and high-grade OS. Nampt immunohistochemical expression was determined as immunostain intensity scored on a 0-3 scale, with 3 being maximal. Immunostain intensity was scored with no staining being 0, light staining as 1, moderate staining as 2, and heavy staining as 3. The percentage of cells stained was measured with no detectable staining as 0, 1-33% as 1, 34-66% as 2, and 67-100% as 3. The final IHC score was the product of the percent of cells stained multiplied by the intensity score, allowing for a maximal score of 9 and a minimal score of 0.

Results: Nampt expression was increased in both OS and CS compared to the counterpart benign tissues (benign bone 1.24+/-0.25, OOS 6.73+/-1.23, TOS 5.63+/-0.61, intensity x percentage score+/-standard error of the mean). Interestingly, Nampt expression dramatically increased with increasing CS grades, correlating with increasing clinical aggressivity and dedifferentiation (benign cartilage 1.00+/-0.00, well-differentiated 1.79+/-0.84, intermediate 3.90+/-0.84, high-grade 9.00+/-0.00).

Conclusions: Here we show for the first time that OS and CS show significantly increased Nampt expression compared to their benign tissue counterparts. Our data also suggests that for the case of CS, Nampt immunohistochemistry might have value in degerming the CS grade and predict clinical aggressivity.

107 Clinicopathologic Characteristics of Poorly Differentiated Chordoma

Angela R Shih[1], *Gregory M Cote*[2], *Ivan Chebib*[3], *Vikram Deshpande*[1], *Ruoyu Miao*[2], *Yen-Lin Chen*[2], *G. Petur Nielsen*[1]. [1]Massachusetts General Hospital, Boston, MA, [2]Massachusetts General Hospital, [3]Massachusetts General Hospital and Harvard Medical School, Boston, MA

Background: Chordoma is a rare malignant tumor of bone with a very high morbidity and mortality. Recently, pediatric poorly differentiated chordoma with an aggressive clinical course and absent INI1 expression has been described. This study aims to summarize the clinicopathologic features of poorly differentiated chordoma in the largest series to date.

Design: A search of the clinical and surgical pathology files between 1990 and 2017 at our tertiary referral institution identified 19 patients with a diagnosis of poorly differentiated chordoma. Immunohistochemistry for keratin, S100, brachyury, and INI1 was evaluated. Kaplan-Meyer survival statistics and a log-rank (Mantel Cox) test were used to compare survival with other subtypes of chordoma.

Results: The patients (n = 19) were diagnosed at a median age of 11 (range: 1 to 29) years with a M:F ratio of 0.46. Tumors arose in the skull base and clivus (n = 9/19; 47%); cervical spine (n = 7/19; 37%); and sacrum or coccyx (n=3/19; 16%). The clinical stage of these patients (AJCC 7e) was Stage 2A (n=7/16; 44%); Stage 2B (n=6/16; 38%); Stage 4A (n=1/16; 6%); and Stage 4B (n=2/16; 13%). Morphologically, the tumors were composed of sheets of epithelioid cells remarkable for nuclear pleomorphism, abundant eosinophilic cytoplasm, and increased mitoses. Tumors were positive for cytokeratin (n = 18/18; 100%) and brachyury (n = 18/18; 100%), and negative for INI1 (n = 17/17; 100%). Patients were treated with variable combinations of excision, radiation therapy, and chemotherapy. Clinical follow-up reveals that six patients were found to have local recurrence at a median of 11 (range: 3 to 26) months from the initial diagnosis. The mean overall survival (OS) is 52.7 months (SD = 9.0 months); mean progression free survival (PFS) is 28.1 months (SD = 7.6 months); mean local control (LC) time is 39.4 months (SD = 9.1 months); and mean metastasis-free survival (MFS) is 37.1 months (SD = 7.7 months). Compared to other subtypes, poorly differentiated chordoma has a statistically significant decreased OS ($p = 0.012$), PFS ($p < 0.0005$), LC ($p = 0.002$), and MFS ($p < 0.0005$).

Conclusions: Pediatric poorly differentiated chordoma has a distinct clinical and immunohistochemical profile, with characteristic INI1 loss and a more aggressive clinical course with decreased OS, PFS, LC, and MFS compared to conventional and chondroid chordoma. Recognition of this subtype of chordoma is important because these malignancies should be treated aggressively with multimodality therapy.

108 Localized tenosynovial giant cell tumors: A clinicopathologic analysis of 222 cases with emphasis on morphologic patterns and outcome.

Natalya Shlyakhova[1], *Sarah M Jenkins*[2], *Karen Fritchie*[3]. [1]Mayo Clinic, Rochester, Minnesota, [2]Mayo Clinic Rochester, [3]Mayo Clinic, Rochester, MN

Background: Background: The localized variant of tenosynovial giant cell tumor (LTSGCT, giant cell tumor of tendon sheath) typically presents as a discrete mass on the distal extremities. Classically, these tumors are composed of a polymorphous proliferation of multinucleated giant cells, mononuclear cells, foamy histiocytes and hemosiderin-laden macrophages. However, the proportion and distribution of these cell types varies. Furthermore, giant cell-poor cases or tumors with abundant foamy histiocytes make cause diagnostic difficulty.

Design: Design: Primary LTSGCT were retrieved from our archives. H&E slides were reviewed to confirm the diagnosis and to evaluate specific histologic features including: low power architecture, diffuse hyalinization, giant cell-poor and histiocyte-rich zones, mitotic rate (per 10/hpfs), and necrosis. Clinical variables were recorded.

Results: Results: 222 LTSGCT were identified from 148 females and 74 males ranging in age from 3 to 87 years (median 51 years). Sites

included fingers (178), wrist (15), hand (13), knee (8), toe (3), ankle (2), foot (2), shoulder (1). Size ranged from 0.3 to 7 cm (median 1.4 cm). Low power examination revealed a single nodule in the majority of cases (n=136; 61.3%) while the remaining cases (n=86, 38.7%) exhibited a multinodular growth pattern. Morphologic patterns included: diffuse hyalinization (n=129, 58.1%), histiocyte-rich zones (n=66, 29.7%), giant-cell poor zones (n=52, 23.4%), and necrosis (n=3, 1.4%). The mitotic rate ranged from 1 to 23/10 hpfs (median 6/10 hpfs). 20 (9%) patients experienced recurrence (follow up 0-24.7 years, median 13.5 years, overall 5-year recurrence-free survival 92.1%). Neither size, mitotic rate nor necrosis correlated with recurrence, although there was a trend toward lower 5-year recurrence-free survival in multinodular tumors (89.2%) compared to those presenting as a single nodule (94.1%), p=0.053. Hyalinization/histiocytes also failed to correlate with clinical variables including age, location and size.

Conclusions: Conclusions: LTSGCT may exhibit a broad range of morphologic patterns, and cases commonly harbor giant-cell poor and histiocyte-rich regions, as well as large zones of hyalinization. We confirm that mitotic rate and necrosis do not correlate with recurrence. However, the 5-year recurrence-free estimates appear lower for multinodular lesions.

109 Detection of MDM2 Overexpression by RNA In Situ Hybridization (RNA-ISH) in Liposarcomas

Reena Singh[1], *Lisha Wang*[2], *Dafydd Thomas*[3], *Jonathan McHugh*[4], *David Lucas*[4], *Aaron M Udager*[5], *Rohit Mehra*[2], *Rajiv Patel*[6]. [1]Michigan Medicine, Ann Arbor, MI, [2]University of Michigan, Ann Arbor, MI, [3]Univ. of Michigan Hosps, Ann Arbor, MI, [4]University of Michigan Health System, Ann Arbor, MI, [5]University of Michigan Medical School, Ann Arbor, MI, [6]Univ. of Michigan, Ann Arbor, MI

Background: Detection of *MDM2* amplification by fluorescence *in situ* hybridization (FISH) or MDM2 overexpression by immunohistochemistry (IHC) aids in distinguishing atypical lipomatous tumor/well-differentiated liposarcoma (ALT/WDLPS) and dedifferentiated liposarcoma (DDLPS) from their differential diagnostic considerations. FISH is highly sensitive but expensive and time-consuming, while lower sensitivity and specificity and discordance with molecular analysis limit the utility of IHC. The purpose of this study was to assess the diagnostic utility of RNA-ISH for detecting *MDM2* overexpression in liposarcomas.

Design: *MDM2*, positive RNA control (*PPIB*) and negative RNA control (*DapB*) RNA-ISH (Advanced Cell Diagnostics) was performed on representative formalin-fixed paraffin-embedded whole tissue sections from retrospectively identified lipomas and DDLPS (cases from 2017) and previously constructed tissue microarrays (TMAs) containing DDLPS, WDLPS, and spindle cell lipomas (cases from 1999-2007). Cases with positive corresponding PPIB staining were manually and independently scored for MDM2 staining by two study pathologists. For whole-section cases, a single 40X field with maximal staining was scored. For TMAs scores were averaged across all evaluable tissue cores from a given case. RNA-ISH signal intensity for individual tumor cells was scored as indicated by the manufacturer (0-4). A cumulative H-score was determined from the products of signal intensity and percentage of cells (i.e. H-score = [A% × 0] + [B% × 1] + [C% × 2] + [D% × 3] + [E% × 4]; total range = 0 to 400).

Results: *MDM2* RNA-ISH scores were highly concordant between the two study pathologists for all TMA cases scored (r = 0.983; P < 0.05). Whole-section cases demonstrated high *MDM2* expression by RNA-ISH in DDLPS (median = 295, range = 220-325; n = 5), with low expression in lipomas (median = 0, range = 0-20; n = 5). Only fourteen (13.6%) of 103 lipomatous tumors were able to be scored for *MDM2* expression from the TMAs; the vast majority of cases failed to show corresponding PPIB staining. Regardless, high *MDM2* expression was observed in DDLPS (median = 238, range = 115-326; n = 11) and WDLPS (H-score = 400, n = 1) with low expression in spindle cell lipomas (H-score < 10; n = 2).

Conclusions: RNA-ISH is useful for detecting *MDM2* overexpression in DDLPS. Analysis of additional lipomatous tumors (WDLPS, pleomorphic liposarcoma, myxoid liposarcoma, etc.) and comparison to MDM2 FISH and MDM2 IHC is ongoing.

110 RANKL In-situ Hybridization Indicates Chondroblastoma May Respond to Denosumab Therapy

David Suster[1], *Ivan Chebib*[2], *G. Petur Nielsen*[3], *Vikram Deshpande*[3]. [1]Boston, MA, [2]Massachusetts General Hospital and Harvard Medical School, Boston, MA, [3]Massachusetts General Hospital, Boston, MA

Background: Primary lesions of bone featuring osteoclast-like giant cells comprise a diverse group of entities, including giant cell tumor (GCT) of bone, chondroblastoma, chondromyxoid fibroma, conventional osteosarcoma with giant cells, and others. The receptor activator of nuclear factor kappa-B ligand (RANKL) has been implicated in the pathogenesis of GCT of bone. These tumors have been successfully treated with denosumab, a monoclonal antibody with high affinity for RANKL. Herein, we examine RANKL expression by in-situ hybridization in various giant cell rich osseous lesions.

Design: Thirty patients with primary osseous lesions were identified including 5 chondroblastomas, 7 GCT of bone, 6 fibrous dysplasia, 3 chondromyxoid fibromas, and 9 conventional osteosarcomas (7 osteoblastic, 1 fibroblastic, 1 chondroblastic). Tissue microarrays comprised of 56 osteosarcomas and 23 chondrosarcomas were also evaluated. RANKL in-situ hybridization was performed using a branch chain in-situ hybridization assay. A housekeeping gene (HKG) control was performed on each case and cases negative for the HKG were excluded. The percentage of positive tumor cells was then estimated for each case.

Results: 6/7 (86%) cases of giant cell tumors of bone were positive; of the positive tumors, three tumors showed staining in 50-80% of tumor cells and three showed staining in 5-20% of tumor cells. 4/5 (80%) chondroblastomas showed positive staining in 5-80% of tumor cells (mean=29% of neoplastic cells). 2/6 (33%) cases of fibrous dysplasia showed focal positive staining in 1-5% of lesional cells. The chondromyxoid fibromas (n=3), osteosarcomas (n=65) and chondrosarcomas (n=23) were negative for RANKL.

Conclusions: The majority of chondroblastomas and GCTs of bone express RANKL by in situ hybridization as compared to other osseous lesions. Based on the success of denosumab therapy for GCTs, the increased expression of RANKL in chondroblastoma indicates that it may play a role in the pathogenesis of this neoplasm and may be a therapeutic target in selected patients with aggressive/recurrent lesions.

111 SETD2 Mutation Is a Recurrent Secondary Alteration in Synovial Sarcoma Associated With Loss of the H3k36me3 Histone Mark

Huichun Tai[1], *Tatsuo Ito*[2], *Achim Jungbluth*[3], *Marc Ladanyi*[4]. [1]Changhua Christian Hosp., Changhua, Taiwan, [2]Okayama University, [3]MSKCC, New York, NY, [4]Memorial Sloan-Kettering CC, New York, NY

Background: Synovial sarcoma (SS) is an aggressive soft tissue sarcoma occurs predominantly in adolescents and young adults. Aside from the pathognomic translocation t(X;18), SS18-SSX fusion, SS samples show very quiet genomes with few other recurrent alterations. One of the few genomic regions recurrently lost in SS is chromosome arm 3p (PMID: 20601955) which includes SETD2, a histone methyltransferase necessary for trimethylation of lysine 36 of histone H3 (H3K36me3). Recently, truncating mutations in SETD2 have been reported in SS (PMID: 24190505). Our aim was to determine the frequency of SETD2 mutation in SS, to validate the use of H3K36me3 IHC to identify this novel molecular subset of SS, and to examine the effects of SETD2 loss in SS cells.

Design: Prospective clinical genomic data on 51 SS cases tested using the MSK-IMPACT large panel NGS assay (PMID: 28481359) were reviewed for SETD2 alterations. Immunohistochemistry (IHC) for H3K36me3 was performed on FFPE whole sections or TMA slides and correlated with the genomic status of SETD2. Experimental inactivation of SETD2 was achieved by CRISPR-Cas9 genome editing.

Results: Inactivating alterations of SETD2 were found in 6% of SS (3/51), including two truncating mutations and one case of homozygous deletion. IHC for H3K36me3 showed a striking difference between SETD2 intact SS, which uniformly showed moderate to strong nuclear staining, and SETD2 inactivated SS, which showed lack of IHC staining for H3K36me3. SETD2 inactivation by CRISPR-Cas9 in the SYO-1 SS cell line resulted in loss of H3K36me3 by western blotting.

Conclusions: Inactivation of SETD2 emerges as one of the few recurrent secondary mutations in SS and is of particular interest given the known role of SS18-SSX in chromatin dysregulation. The use of H3K36me3 IHC stain to identify this molecular subset of SS should facilitate studies of its clinical and prognostic correlates. SYO-1 cells with SETD2 knockdown provide a cellular model in which to examine the effects of SETD2 mutations on cell phenotype, epigenetic regulation, and sensitivity to epigenetic targeted therapies.

112 Histological Diversity of Spindle Cell/Sclerosing Rhabdomyosarcomas: Clinicopathological, Immunohistochemical, And Molecular Analysis of 7 Cases

Jen-Wei Tsai[1], *Cher-wei Liang*[2], *Jen-Chieh Lee*[3], *Wan-Shan Li*[4], *Hsuan-Ying Huang*[5]. [1]E-DA Hospital/I-Shou University, Kaohsiung, [2]Fu Jen Catholic University Hospital, New Taipei City, Taiwan, [3]National Taiwan University Hospital, Taipei City, [4]Kaohsiung Medical University Hospital, Chiayi City, Taiwan, [5]Chang Gung Memorial Hospital, Kaohsiung City, Taiwan

Background: Spindle cell/sclerosing rhabdomyosarcomas (SCSRs) are typified by bundles of atypical spindle cells admixed with organoid arrangements of primitive rounded cells in a variably hyalinized stroma and harbor a driving neomorphic *MYOD1* (L122R) mutation, with or without coexisting PI3K-AKT pathway mutations. However, the histological spectrum of molecularly confirmed SCSRs is insufficiently defined.

Design: Seven SCSRs with diffuse MYOD1 expression were retrieved to analyze histological features, including predominance of spindle vs. primitive-appearing cells, the proportion and deposition pattern of collagenous stroma, the extent of rhabdomyoblasts, mitosis, necrosis, and other variant histology. In 6 SCSRs with available tissues, Sanger sequencing for *MyoD1* and *PIK3CKA* was performed, including one case additionally laser-microdissected for the focal area featuring lipoblastic differentiation.

Results: Four females and 3 males aged between 15 and 64 years (median, 34) had primary SCSRs in the head and neck in 3 cases (parapharynx, 2; buccal, 1), extremities in 3, and mediastinum in 1, with the median size being 6.4 cm (range, 2.3-22). Four SCSRs exhibited predominantly hypercellular spindle histology, including one with lipoblasts in focally myxoid stroma. Another 3 showed prominent sclerotic stroma embracing nests, cords, or pseudoalveoli formed by rounded cells, including one with multinucleated tumor cells reminiscent of alveolar rhabdomyosarcoma. The median mitotic count was 6 (range, 2-38) per 10 HPFs, and tumor necrosis was present in 4 cases, with 1 being extensively necrotic in >50% of cells. In all 7 cases, MYOD1 expression was diffusely strong, and myogenin reactivity was focally patchy, with remarkable co-expression of SMA and desmin in 3. *MYOD1* L122R mutation, 5 heterozygous and 1 homozygous, was detected in in all 6 cases sequenced. Concurrent *PIK3CA* (H1047R) mutation was only detected the SCSR harboring identical *MYOD1* L122R mutation in both classical spindle and lipoblasts-containing areas. After a median follow-up of 12.4 months, 3 patients were alive without disease, 3 alive with disease, and 1 dead of disease.

Conclusions: SCSRs are genetically distinctive, aggressive rhabdomyosarcomas constantly harboring the driver *MYOD1* L122R mutation, while the coexistent *PI3KCA* mutation is uncommon. Besides spindle cell/sclerosing features, our series expands the histological spectrum of SCSRs by highlighting the variant lipoblastic differentiation and multinucleated cells.

113 Extensive Survey of panTRK Expression in a Large Series of Sarcomas

David P Wang[1], *Samia Khan*[2], *Davis Ingram*[3], *Russell Broaddus*[4], *Alexander Lazar*[5], *Wei-Lien Billy Wang*[6]. [1]MD Anderson Cancer Center, Houston, TX, [2]MD Anderson Cancer Center, [3]M D Anderson Cancer Center, [4]M.D. Anderson Cancer Center, Houston, TX, [5]M. D. Anderson Cancer Center, Houston, TX, [6]UT MD Anderson Cancer Ctr, Houston, TX

Background: The neurotrophic tyrosine kinase receptor family includes TrkA, TrkB and TrkC proteins encoded by 3 genes - *NTRK1*, *NTRK2* and *NTRK3*, respectively. These proteins are involved in neuronal development, with limited expression in benign smooth muscle, testes and neural tissues. Recently, malignancies, including a subset of sarcomas, have been found to harbor fusions involving *NTRK* genes suggesting efficacy of available targeted therapy. Immunohistochemistry with anti-pan-Trk (EPR17341), can be an effective screening tool for this fusion. However, the prevalence of panTRK labeling in various sarcomas are not known. We evaluated a large series of sarcomas for panTRK expression.

Design: Unstained slides were prepared from tissue microarrays of formalin-fixed paraffin-embedded tissue consisting of 251 leiomyosarcomas, 61 angiosarcomas, 22 alveolar soft part sarcoma (ASPS), 115 chordomas, 110 solitary fibrous tumor (SFT), 63 desmoplastic small round cell tumor (DRSCT), 79 Ewing sarcomas, 334 atypical lipomatous tumor/dedifferentiated liposarcoma (ALT/DDLS), 70 malignant peripheral nerve sheath tumor (MPNST), 57 synovial sarcomas, 3 low-grade fibromyxoid sarcoma (LGFMS), 3 dermatofibrosarcoma protuberans (DFSP) and 107 undifferentiated pleomorphic sarcomas (UPS). Immunohistochemical study used a monoclonal anti-pan-Trk antibody (Abcam, EPR17341, 1:125) on Leica Bond III autostainer. Both extent (% tumor reactivity) and intensity (1+, 2+, 3+) of labeling were evaluated, with positivity defined as 1+ labeling of > 10% tumor cells.

Results: Overall, 133/1275 (10%) sarcomas expressed panTRK. By subtype, 61 DSRCTs (97%), 16 SFTs (15%), 7 synovial sarcomas (12%), 8 MPNSTs (11%), 17 leiomyosarcomas (7 %), 15 ALT/DDLSs (5%), 4 chordomas (4%), 2 Ewing sarcomas (3%), 2 UPSs (2%), and 1 angiosarcoma (2%) were positive. None of the ASPS, LGFMS, or DFSP were positive.

Conclusions: PanTrk expression is overall low in sarcomas; however, there is considerable variability by subtype. Notably desmoplastic small round cell tumors demonstrate high prevalence of panTRK expression. This expression is unlikely to be related to TRK fusion status as these tumors already harbor a known oncogenic fusion. Accuracy of panTRK immunohistochemistry as an indicator of *NTRK* fusion may vary by subtype/tumor type and warrants prudence utilizing immunohistochemistry alone to qualify patients for targeted therapy. Additional confirmatory molecular testing is ongoing.

114 Loss of H3K27Me3 Expression in Osteosarcoma

Wei-Lien Billy Wang[1], *John A Livingston*[2], *Yu Liang*[3], *Cheuk Hong Leung*[4], *Heather Lin*[2], *Alexander Lazar*[5]. [1]UT MD Anderson Cancer Ctr, Houston, TX, [2]The University of Texas MD Anderson Cancer Center, [3]City of Hope National Medical Center, Duarte, CA, [4]The University of Texas MD Anderson Cancer Center, Houston, Texas, [5]M. D. Anderson Cancer Center, Houston, TX

Background: Loss of H3K27 trimethylation demonstrated by immunohistochemistry has been proposed to be a useful diagnostic and poor prognostic marker for malignant peripheral nerve sheath tumors (MPNSTs). These tumors have mutations in genes involved in the polycomb receptor complex 2 which regulates histone methylation. Recently, other studies have reported occasional loss in other spindle cell soft tissue tumors and melanoma. H3K27me3 expression has not been extensively studied in osteosarcomas.

Design: Tissue microarray from formalin-fixed paraffin embedded decalcified osteosarcoma specimens were prepared from 260 patients: 184 resections and 94 metastases. Anti-H3K27me3 (Cell Signaling, clone C36B11, 1:200) immunohistochemistry was performed by autostainer. Both extent and intensity of labeling were recorded. Loss of expression was defined as <10% of tumoral cells labeling. Clinical outcomes were tabulated.

Results: 159 cores were analyzable (98 primaries; 61 metastases). Loss of H3K27me3 was seen in 29 cases (18/98 primaries and 11/61 metastases). In primary resection specimens, loss of expression of H3K27me3 was associated with poor overall survival (HR 2.40, p=0.008) as well as relapse free survival (HR:2.9, p=0.002).

Conclusions: Loss of H3K27Me3 can occasionally be seen in osteosarcomas, suggesting that a subset of these tumors may also have dysregulation of polycomb repressor complex 2. Loss of expression was associated with a poor prognosis and thus may be a marker of aggressive disease. The biological underpinnings of this loss of expression are the topic of further investigation.

115 Atypical lipomatous tumor/well-differentiated liposarcoma and dedifferentiated liposarcoma in patients <40 years: A study of 91 patients.

Rebecca E Waters[1], *Andrew Horvai*[2], *Armita Bahrami*[3], *Patricia Greipp*[1], *Ivy John*[4], *Elizabeth Demicco*[5], *Brendan C Dickson*[6], *Munir Tanas*[7], *Brandon Larsen*[8], *Nasir Ud Din*[9], *David Creytens*[10], *Leona Doyle*[11], *Alyaa Al-Ibraheemi*[12], *Vickie Y Jo*[13], *Andrew Folpe*[1], *Karen Fritchie*[1]. [1]Mayo Clinic, Rochester, MN, [2]Univ of California San Francisco, San Francisco, CA, [3]St. Jude Children's Res Hosp, Memphis, TN, [4]University of Pittsburgh Medical Center, Pittsburgh, PA, [5]Mount Sinai Hospital, [6]Mount Sinai Hospital, Toronto, ON, [7]University of Iowa, Iowa City, IA, [8]Mayo Clinic Arizona, Scottsdale, AZ, [9]Karachi, Sindh, [10]Ghent University Hospital- Belgium, [11]Brigham and Women's Hospital, Boston, MA, [12]Boston Children's Hospital, Boston, MA, [13]Brigham & Women's Hospital, Boston, MA

Background: Atypical lipomatous tumor (ALT)/well-differentiated liposarcoma (WDL) and dedifferentiated liposarcoma (DDLPS) typically present in the 6th and 7th decades of adulthood. Limited data exists on these tumors in children and young adults.

Design: Cases of ALT/WDL/DDLPS arising in patients ≤40 years with either 1) morphologic criteria, 2) MDM2 amplification by FISH, 3) MDM2/CDK4 immunoreactivity, or 4) ring/marker chromosomes were collected from multiple institutional and consultation archives. Clinical variables were recorded.

Results: 57 ALT/WDL and 34 DDLPS were identified. The patients (48M,43F) ranged from 20 to 40 years (median 36 years) in age. Sites included abdomen/retroperitoneum (RP) (n=49), extremities (n=33; intramuscular=24, subcutis=2, unknown=7), head/neck (n=6), mediastinum (n=1), flank (n=1) and back (n=1). Of those in the abdomen/RP, 27 of the 49 (55%) were DDLPS, compared to 4 of the 33 (12%) in the extremity. 23 patients received adjuvant chemo/radiation therapy. Follow-up was available for 72 patients (range 1-211 months, median 32 months). Of these, 31 (43%) recurred (5-100 months, median 24.5 months) and 9 (13%) metastasized (5-117 months, median 22 months). By site, 3 of 33 (9%) extremity lesions recurred (1 ALT, 2 DDLPS) and 1 (3%) metastasized (DDLPS), while 23 of 49 (47%) abdomen/RP tumors recurred (9 WDL, 14 DDLPS) and 6 (12%) metastasized (6 DDLPS). 4 of 5 (80%) head/neck tumors recurred (2 WDL, 2 DDLPS) with one patient experiencing metastasis (DDLPS). The single mediastinal tumor (DDLPS) recurred and metastasized. At last follow-up, 61 (85%) patients are alive, 7 (10%) patients died of disease, and 1 died of other causes.

Conclusions: ALT/WDL/DDLPS may arise in young adults (20-40 years) but appear to be exceedingly rare in the pediatric population. ALT/WDL typically presents as an intramuscular mass in the extremity or within the abdomen/RP, while DDLPS in this age group predominantly affects deep-seated central sites. As in older adults, ALT/WDL/DDLPS arising in the abdomen/RP or mediastinum exhibit high rates of local recurrence, and those which are dedifferentiated are capable of distant metastasis. Tumors arising in the head/neck also appear to behave in a more aggressive fashion.

116 Loss of H3K27me3 Expression Distinguishes MPNST from ANNUBP but Lacks Prognostic Significance

Erik Williams[1], *Ana B Larque Daza*[1], *Tareq Juratli*[2], *Vikram Deshpande*[1], *Ivan Chebib*[3], *G. Petur Nielsen*[1], *Anat Stemmer-Rachamimov*[1]. [1]Massachusetts General Hospital, Boston, MA, [2]Massachusetts General Hospital, [3]Massachusetts General Hospital and Harvard Medical School, Boston, MA

Background: Loss of H3K27 trimethylation (H3K27me3) expression has been recognized in many sporadic, radiation-induced, and NF1-associated malignant peripheral nerve sheath tumors (MPNSTs), and has been associated with inferior survival. H3K27me3 has also been demonstrated to be retained in several small series of various neurofibromas, and epithelioid MPNSTs. This study aims to further evaluate the diagnostic and prognostic utility of H3K27me3 in MPNSTs, by specifically examining H3K27me3 status in a large cohort of MPNSTs and atypical neurofibromatous tumors with unpredictable biological behavior (ANNUBP), with focus on neurofibromas directly associated with MPNSTs, and epithelioid MPNSTs.

Design: We identified 58 MPNSTs in 49 patients and 12 ANNUBPs in 8 patients, 5 of which were directly associated with MPNSTs. Demographic data (including neurofibromatosis, radiation-induced, and sporadic status), primary site, development of recurrences and metastasis, and survival were recorded. Additional histologic features, such as epithelioid or heterologous features and vascular invasion, were noted. We performed immunohistochemistry (IHC) using anti-H3K27me3 monoclonal antibody clone C36B11 on whole slide sections and tissue microarray.

Results: The mean age of the MPNST cohort at first resection was 44.3 years with 47% of patients male. Clinical presentations included NF1-related (23%), radiotherapy-related (8%), and sporadic MPNSTs (69%). The mean age of the ANNUBP cohort was 32.4 years at first resection with 63% male, all in NF1 patients. In the MPNST cohort, complete loss of H3K27me3 was identified in 80% of tumors of NF1 cases (12/15), all radiation-related cases (6/6), and 46% of sporadic cases (17/37) (Fig 1). H3K27me3 was also lost in 2/7 epithelioid MPNSTs, all sporadic cases. H3K27me3 was lost in 4/5 MPNSTs with heterologous features. No significant correlation was identified between loss of H3K27me3 and grade, vascular invasion, development of recurrences or metastasis, or overall survival, in any subgroup. H3K27me3 was retained in all stained cases of ANNUBPs, including those with direct association with MPNSTs.

Conclusions: H3K27me3 IHC may play a critical role in differentiating ANNUBPs from MPNSTs. This MPNST cohort showed no prognostic significance to loss of H3K27me3 in MPNSTs.

117 Epigenetic Dysregulation Unites Ossifying Fibromyxoid Tumor and Endometrial Stromal Sarcoma Pathogenesis

John Wojcik[1], *Dipti Sajed*[2], *Esther Oliva*[3], *Sarah Chiang*[4], *Benjamin A Garcia*[5]. [1]Hospital of the University of Pennsylvania, Philadelphia, PA, [2]University of California at Los Angeles, [3]Massachusetts General Hospital, Boston, MA, [4]Memorial Sloan Kettering Cancer Center, New York, NY, [5]University of Pennsylvania

Background: Low-grade endometrial stromal sarcoma (ESS) and ossifying fibromyxoid tumor (OFMT) are translocation-associated tumors with distinct clinical, histologic and immunohistochemical features. Molecular studies have identified fusions involving genes with similar functions and/or identical fusion partners in both tumor types. In both, the involved genes encode proteins involved in histone post-translational modifications (PTMs), most notably those responsible for histone H3 lysine 27 trimethylation (H3K27me3), a PTM associated with gene silencing. While this suggests that altered epigenetic regulation drives these tumors, the mechanism remains unclear.

Design: H&E and IHC stains for H3K27me3 were reviewed for representative sections of 17 tumors (11 ESS, 6 OFMT) and a tissue microarray containing 70 ESS. Histones were isolated from FFPE tissue for 5 ESS, 4 OFMT and controls. PTMs were quantified using nano-liquid chromatography and tandem mass spectrometry (LC-MS/MS). Statistical analysis was performed using Student's t-test for pairwise comparison of histone modifications between tumor and control.

Results: In contrast to recently published data suggesting loss of function by fusion proteins, ESS and OFMT exhibit retained H3K27me3 levels as assessed by immunohistochemistry. This was true regardless of fusion type. 51/67 ESS represented on tissue microarray and all 17 combined ESS and OFMT whole-tissue sections exhibited strong nuclear reactivity in the majority of cells. The remaining microarray cases exhibited weak internal control staining, suggesting that decreased staining in tumors was a technical artifact. By quantitative mass-spectrometry, both tumor types showed highly similar global PTM profiles. Both exhibited retained H3K27 trimethylation and demonstrated loss of PTMs typically associated with active transcription, including histone H3 and H4 acetylation among others. Loss of 'active' histone marks was accompanied by an increase in adjacent 'repressive' marks, suggesting a gain-of-silencing function for the fusion proteins.

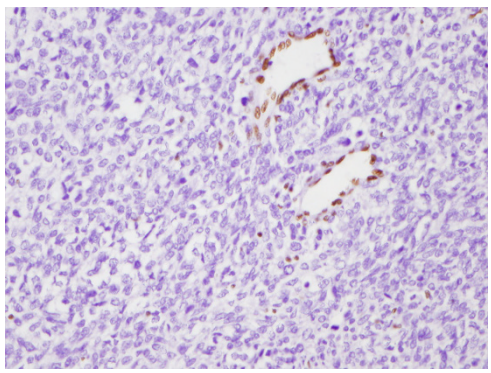

Conclusions: Through a combination of immunohistochemistry and quantitative mass spectrometry on human tissue samples, we demonstrate that ESS and OFMT exhibit similar global epigenetic changes, and that these changes are shared across various fusion types. This points to a unified mechanism for translocation-mediated pathogenesis in which genetic rearrangements promote spread of silencing histone marks to previously active genomic regions.

118 Whole Block Imaging in Bone Tumor

Yukako Yagi[1], *Kazuhiro Tabata*[1], *Alexei Teplov*[1], *Sinchun Hwang*[2], *Meera Hameed*[3]. [1]Memorial Sloan Kettering Cancer Center, New York, NY, [2]Memorial Sloan Kettering Cancer Center, [3]Memorial Sloan-Kettering CC, New York, NY

Background: In Orthopedic Pathology, correlation of imaging characterstics to histopathology is important for a meaningful and accurate diagnostic interpretation. This traditional practice has given many insights on tumor characteristics such as growth pattern, relationship to adjacent normal bone, matrix production, tumor aggressiveness etc., While in Radiology practice 3D reconstruction of digital images is an easily available technique, traditional Pathology provides only a 2D image of 3D anatomical structures albeit with much higher resolution than radiological images. While 3D histological reconstruction is possible, it requires automated sectioning of 100s of slides with 3D reconstruction with appropriate software. 3D Whole block imaging (WBI) by MicroCT provides a new imaging modality to create 3D reconstruction of tissue sections with microscopic level resolution potentially up to 10x without the need for tissue sectioning.

Design: To create 3D reconstruction images from tissue blocks, two osteosarcomas (great toe and spine) and 2 chondrosarcomas (distal femur and metacarpal) were chosen and whole mounted tissue blocks were scanned using the custom-built Nikon Metrology microCT scanner. The data was reconstructed into 3D volumetric images then digitally stained H&E for visualization. Scanning per block took 7 hours. Images were compared to corresponding adjacent histology whole slide images and with MRI studies performed in vivo.

Results: In all cases, tumor characterisctics were readily identifiable on microCT images and matched to that seen on whole mounted section. In addition 3D reconstruction allowed examination of tissue section through the entire block allowing for potential detection of additional morphological features in the same block. The resolution was equivalent with 2x objective lenses with microscope due to the size of the whole mounted tissue block.

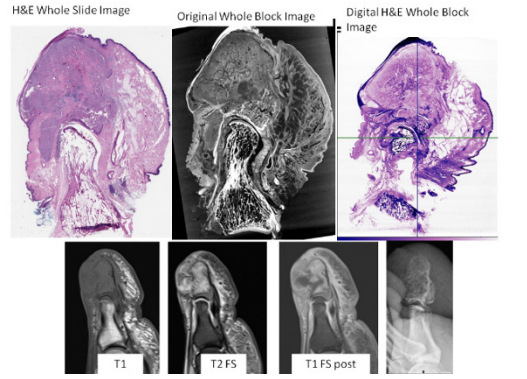

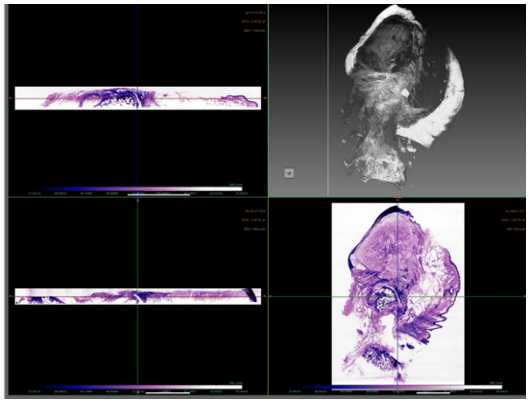

Conclusions: MicroCT scanning technology can add another dimension to correlate radiologic images, 2D and 3D histology

These preliminary results show that microCT has the potential to analyze tumor relationship with normal structures, tumor spread along marrow cavity, cortical bone and surrounding soft tissue.

Additional studies on various specimens has the potential to yield interesting and useful information which could not be obtained on 2D histological sections. The resolution can be improved by changing the scanning methods and process.

119 Diagnostic utility of histone H3.3 G34W, G34R, and G34V mutant-specific antibodies for giant cell tumors of bone

Hidetaka Yamamoto[1], *Takeshi Iwasaki*[2], *Yuichi Yamada*[3], *Kenichi Kohashi*[4], *Yoshinao Oda*[1]. [1]Kyushu University, Fukuoka, [2]Kyushu University, [3]Kyushu University, Fukuoka-shi Fukuoka-, Japan, [4]Kyushu University, Fukuoka,

Background: Giant cell tumors of bone (GCTBs) are characterized by mononuclear stromal cells and osteoclast-like multinucleated giant cells; up to 95% have *H3F3A* gene mutation. The RANKL inhibitor denosumab, when used for the treatment of GCTB, leads to histological changes such as new bone formation and giant cell depletion.

Design: We assessed the diagnostic utility of immunohistochemical staining with the antibodies against histone H3.3 G34W, G34R and G34V mutant proteins for GCTB and other histologically similar bone and joint lesions.

Results: H3.3 G34W, G34R and G34V mutant protein expressions were detected in mononuclear stromal cells in 47/51 (92%), 1/51 (2%) and 3/51 (6%) cases of primary GCTBs, respectively, in a mutually exclusive manner. All recurrent/metastatic GCTBs (n=14), post-denosumab GCTBs (n=8) and secondary malignant GCTBs (n=2) were positive for H3.3 G34W. The immunohistochemical results were essentially correlated with the *H3F3A* genotype determined by mutation analysis. In post-denosumab GCTBs, H3.3 G34W expression was seen in spindle cells and immature bone-forming cells. H3.3 G34W, G34R and G34V were negative in 121/122 cases of non-GCTB, including chondroblastoma, osteosarcoma, primary aneurysmal bone cyst and other giant cell-rich lesions. The exception was a single case of undifferentiated high-grade pleomorphic sarcoma that was positive for H3.3 G34W, suggesting the possibility of sarcomatous overgrowth of primary malignant GCTB.

Conclusions: H3.3 G34W/R/V mutant-specific antibodies are useful surrogate markers for the *H3F3A* genotype and helpful for the diagnosis of GCTB and its variants. The expression of H3.3 G34W mutant protein in post-denosumab GCTB suggests that neoplastic stromal cells may persist even after the treatment and may play a role in new bone formation.

120 Comprehensive Detection of Known Fusion Genes in Sarcomas and Discovery of Novel Fusion Partners by a Clinical Targeted RNA Sequencing Assay

Guo Zhu[1], *Ryma Benayed*[2], *Caleb Ho*[1], *Kerry Mullaney*[2], *Purvil Sukhadia*[2], *Kelly Rios*[2], *Marc Ladanyi*[3], *Meera Hameed*[3]. [1]Memorial Sloan Kettering Cancer Center, New York, NY, [2]Memorial Sloan Kettering Cancer Center, [3]Memorial Sloan-Kettering CC, New York, NY

Background: Bone and soft tissue tumors constitute a heterogeneous group of both benign and malignant neoplasms with distinct clinical, histological and genetic characteristics. Integration of morphological, immunohistochemical and molecular methods is often necessary for a precise diagnosis and optimal clinical management.

Design: We have validated and implemented a clinical molecular diagnostic assay, MSK-Fusion Solid, for detection of gene fusions in solid tumors including sarcomas. It is a targeted RNA sequencing assay which utilizes Archer Anchored Multiplex PCR (AMP™) technology and next-generation sequencing. The assay allows targeted oncogenic fusion transcript detection without knowledge of the corresponding fusion partners or breakpoints in 64 specific genes known to be recurrently involved in rearrangements in solid tumors including sarcomas.

Results: From 1/2016 to 7/2017, 119 sarcomas from FFPE tumor material were submitted for Archer analysis and successfully passed all the sequencing quality control parameters. These sarcomas encompass 20 major tumor types arising from bone and soft tissue, including 113 soft tissue tumors and 6 osteosarcomas. Ewing and Ewing-like sarcomas, rhabdomyosarcoma and sarcoma-not otherwise specified (NOS) were the three most common tumor types. Recurrent or novel gene fusions were detected in 44% of cases (53/119). In the course of prospective clinical testing, we were able to identify the following novel events in this cohort. 1) Novel partner genes for known recurrent gene fusions, which include *TRPS1-PLAG1* in two soft tissue myoepithelial tumors and *VCP-TFE3* in a pancreatic PEComa. 2) A novel fusion, *SS18-POU5F1*, in a primitive round cell tumor with divergent differentiation. 3) A novel fusion, *EWSR1-NACC1,* in a spindle cell sarcoma-NOS. Moreover, potentially targetable kinase gene fusions involving *NTRK1*, *NTRK3*, *ROS1* and *BRAF* were identified in various tumor types.

Conclusions: This highly multiplexed, fusion partner-agnostic, molecular diagnostic assay for oncogenic fusions in solid tumors is a robust and efficient single test for detection of known fusions, and offers the potential to uncover unknown partner genes. Especially in sarcomas, where diagnostic difficulties remain and targetable drivers are rare, it is conceivable that new fusions can be discovered enhancing our diagnostic and therapeutic capabilities.